2013

EFFECTIVENESS OF STRAW BALE CHECK DAMS AT REDUCING POST-FIRE SEDIMENT YIELDS FROM EPHEMERAL CHANNEL CATCHMENTS

Keenan Storrar
The University of Montana

EFFECTIVENESS OF STRAW BALE CHECK DAMS AT REDUCING POST-FIRE SEDIMENT YIELDS FROM EPHEMERAL CHANNEL CATCHMENTS

By

KEENAN ALF TENBROECK STORRAR

Bachelor of Science, University of Montana, Missoula, Montana, 2008

Thesis

presented in partial fulfillment of the requirements
for the degree of

Master of Science
in Resource Conservation

The University of Montana
Missoula, MT

May, 2013

Approved by:

Sandy Ross, Dean of The Graduate School
Graduate School

Dr. Peter R. Robichaud, Chair
USDA, Forest Service
Rocky Mountain Research Station
Moscow, Idaho

Dr. Cara Nelson
Department of Ecosystem and Conservation Sciences

Dr. Andrew Wilcox
Department of Geosciences

Dr. Mike Patterson
Associate Dean, College of Forestry and Conservation

Storrar, Keenan A. T., M. S. Spring 2013 Resource Conservation

Effectiveness of Straw Bale Check Dams at Reducing Post-Fire Sediment Yields from Ephemeral Channel Catchments

Chairperson: Dr. Peter R. Robichaud

Increased sedimentation caused by post-fire flooding is a risk to people, homes, and buildings. The USDA Forest Service installs straw bale check dams in ephemeral channels to reduce sedimentation rates from small catchments. We set out to study if straw bale check dams effectively reduce sedimentation rates from five paired catchments following the 2010 Twitchell Canyon Fire in south central Utah. Each pair consisted of two adjacent catchments that had similar physical characteristics and areas, with catchment areas ranging from ~0.2 to 1.6 ha (~0.5 to 4.0 ac). For each pair we treated one catchment with four straw bale check dams per ha (two per ac) and left the other catchment untreated as a control. Sediment yields produced from catchments during 2011 and 2012 were measured as well as the mass of sediment trapped by individual straw bale check dam structures. We found straw bale check dams did not significantly reduce annual catchment sediment yields produced by 30-minute rainfall intensities (I_{30}) equal to or less than 14 mm hr^{-1} (0.5 in hr^{-1}), a 1-year return period event at the study area. The straw bale check dams were filled to sediment holding capacity early in the first post-fire year from sediment yields produced by 1- and 2-year I_{30} return period rain events, or by two rain events having less than 1-year I_{30} intensity return periods. Three of the five paired catchments did not capture the total 2011 annual sediment yields because sediment retention structures used to measure catchment yields were overwhelmed by sediment during large rain events, however reliable measurements indicate annual sediment yields of 19.53 to 25.71 Mg ha^{-1} [8.71 to 11.47 t ac^{-1}] passed over already full straw bale check dams. Straw bale check dams were non-functioning during the second post-fire year, allowing 3.74 to 13.12 Mg ha^{-1} [1.67 to 5.85 t ac^{-1}] of sediment to pass over structures. The mean mass of sediment trapped by individual straw bale check dams is 1.26 Mg (1.40 t). At a treatment rate of four straw bale check dams ha^{-1} (two ac^{-1}), they trapped 5.87 Mg ha^{-1} (2.62 t ac^{-1}) of sediment.

Acknowledgments

This project was funded by the USDA Forest Service Rocky Mountain Research Station and the Fishlake National Forest through a cooperative agreement with the University of Montana. I greatly appreciate being funded while I have researched this fascinating project.

I would like to thank all of the individuals who were involved in this project: my advisor the late Dr. Scott Woods, who initiated this project. His words of wisdom and advice have guided me through this project to its completion. Dr. Pete Robichaud for advising me on this project from the beginning to end, investing his personal time, providing field crews for data collection, and arranging for financial support to extend my time as a graduate student. Thanks to the Rocky Mountain Research Station personnel and field crew, including: Bob Brown for helping install and monitor the field site; Joe Wagenbrenner for helping at the field site and giving insight on data processing and analysis; Chris Bacon, Sierra Larson, Will Long, Cassie Byrne, Jesse Huntington, Olga Martyusheva, Tim Moran, and Carlos Silva for help in the field, and Dave Turner for his advice regarding my statistical analysis. Thanks to Adam Solt of the Fishlake National Forest for help in the field, first hand updates of conditions at the site, and enlisting over 40 Forest Service personnel to help measure and clean out over 200 t of sediment with shovels and buckets during the two years of data collection. Thanks to the University of Montana faculty and staff: Andrew Wilcox for advice in the early stages of this research and for the invaluable geomorphology class during my studies; Cara Nelson for advice in the planning stages and comments on this document; Dave Affleck for advise and additions to my R-code; Shonna Trowbridge for help with the Graduate School and College of Forestry policies; and Catherine Redfern for help with the budget. Thanks to Ann Storrar for help surveying many hours on the total station and collecting field data; Keif Storrar for help in the field; and the rest of my family for their continued support. Finally, I would like to thank Emma Schmidt for her love, support, and encouragement every step of the way during this project.

Table of Contents

I. Figures

II. Tables

1.0 Introduction

For over a century, wildfires have played a prominent and often challenging role in forest management in the Western United States. More homes are put at risk with the increasing size of wildfires and the encroachment of urban environments into forests susceptible to wildfire known as the wildland-urban interface. Now the effects of wildfire are no longer confined to uninhabited forested landscapes, but are increasingly a risk to human life, homes, roads, and structures (Baker, 2009). Large forest wildfire activity has increased in frequency and total area burned in the last two to three decades in the western United States (Westerling *et al*. 2006; Morgan *et al.* 2008). Wildfires have been growing in size because of longer fire seasons and more forest material has been made available for burning. Earlier spring snow melt has allowed fire ignition dates to be earlier in the season and drier, hotter summers have pushed fire containment dates to be later in the season. This has caused the average fire season length from 1987 to 2003 to be extended by 78 days compared to 1970 to 1986 (Westerling *et al*. 2006). Fires have also increased in size due to the buildup of forest biomass over large contiguous areas from forest management practices that include logging (Wilson and Dell, 1971) and fire suppression over the last century (Vaillant *et al*. 2009).

The wildland-urban interface in the West has experienced post-fire flooding and the increased sedimentation rates that have caused considerable damage to homes and infrastructure located even outside of burn perimeters (Gallup, 1975). After the 2010 Shultz Fire burned in the mountains above Flagstaff Arizona, a storm producing 45 mm (1.8 in) of rain in 45 minutes triggered a massive flood carrying sediment, rocks, and debris that ripped through neighborhoods sitting below the burned area, causing extensive damage to homes and businesses (Koestner *et al*. 2011). Land managers are tasked with mitigating flooding and increased sedimentation associated with post-fire environments using various treatments aimed at reducing these risks to people and structures (Napper, 2006).

Mitigation techniques to protect homes, roads, and structures from increased sediment yields are implemented on hillslopes, in small catchments, and in large watersheds. For instance land managers install straw bale check dams in ephemeral channels to mitigate undesired effects of increased sediment yields from small catchments. While these structures have been in use for over four decades (Foltz *et al.* 2009), previous studies have not shown if the treatment is successful at reducing a significant amount of ash and sediment from being transported out of burned catchments into higher order streams or onto alluvial fans (Ruby, 1997).

1.1 Post-fire landscape response to rainfall

Wildfire changes surface hydrology and sediment transport rates in the burned area (Canfield *et al*. 2005, Smith and Dragovich, 2008; Jackson and Roering, 2009; Malvar *et al*. 2011; Shakesby and Doerr, 2006). While many surface processes such as wind contribute to soil erosion, the process of soil erosion discussed in this paper will refer to the transportation of soil aggregates or soil particles by water (Wondzell and King, 2003), and is quantified as sediment yield, or the measure of the mass of sediment eroded past a given point per length of time (Moody and Martin, 2009).

In the post-fire environment, surface runoff and sediment yields are directly related to burn severity thus, there is increased runoff and sedimentation with increased burn severity (Shakesby and Doerr, 2006). Burn severity is a measure of the heat pulse that affects the soil and vegetation mortality rates (NWCG, 2006). The effects within high burn severity areas are high soil heating, high vegetation mortality, and the loss of surface and subsurface organic matter changing the hydrologic, microbial, and biogeochemical processes, which may take year to recover to pre-burn conditions (Lentile *et al*. 2006).

Rainfall amount and intensity are the primary drivers of sediment yields following a wildfire. Rainfall intensity is the maximum amount of rain to fall within a 10-minute (I_{10}), 30-minute (I_{30}), or 60-minute (I_{60}) period during a rainstorm, standardized to one hour (Janusz, 1986). There is a large variation in rainfall intensities across the West, with regional climate and local topography often being the strongest influencing factor. Moody and Martin (2009) divide the four climate zones of the Western US defined by Smith (1994) the Pacific, Sub-Pacific, Plains, and Arizona into four rainfall intensity boundaries (Low, Medium, High, and Extreme) according to the 2-year probability of receiving an event with a given 30-minute rainfall intensity ($I_{30}^{2\,yr}$). In an extensive review of past studies, they link annual post-fire sediment yields to rainfall intensity and show low sediment yields occur in regions with low rainfall intensities and high sediment yields occur in regions with high rainfall intensities. For instance, the Plains-Medium rainfall regime with an $I_{30}^{2\,yr}$ ranging from 19 to 36 mm hr^{-1} (0.8 to 1.4 in hr^{-1}) had a median sediment yield of 250 Mg ha^{-1} (112 t ac^{-1}), while in the Sub-Pacific-Low intensity rainfall regime with an $I_{30}^{2\,yr}$ range of 10 to 20 mm hr^{-1} (0.4 to 0.8 in hr^{-1}) the median sediment yield was 39 Mg ha^{-1} (17 t ac^{-1}) (Moody and Martin, 2009). Seasonal timing of sediment yields also vary by region depending on the climate. In the Colorado Rockies, high-intensity events correlate well to large post-fire sediment yields during the monsoon rains in mid to late summer, while precipitation in the form of snow or frontal rain events have been shown to produce little erosion (Benavides-Solorio and MacDonald, 2005). However, in southern California, heavy winter rains produce the maximum sediment yields, while sedimentation rates are at a minimum during the summer (Splitter, 1995; Moody and Martin, 2009).

1.2 Infiltration and overland flow

Wildfire reduces rainfall infiltration rates by altering soil and vegetation characteristics increasing surface runoff and sedimentation rates. When rainfall reaches the ground surface it either infiltrates into the soil profile or runs off as excess precipitation, entraining and transporting sediment at the surface. Infiltration rates determine the runoff amount and are largely determined by vegetation, soil texture, surface porosity, and soil water repellency, which can all be drastically altered in a post-fire environment (Brooks *et al. 2003*).

Wildfire reduces surface roughness causing increased surface runoff (Inbar *et al.* 1998; Malvar *et al.* 2011; Badía and Marti, 2008; Shakesby *et al.* 1993). High surface roughness in unburned forests is attributed to surface litter, duff, and shrubs that capture rainfall and slow the rate at which water drains off a hillslope. The slow drainage rate allows for water to infiltrate into the soil profile reducing surface runoff. The consumption of vegetation by fire reduces surface roughness causing water to quickly runoff from hillslopes and ephemeral channels (Shakesby and Doerr, 2006; Moody and Martin, 2001). In addition, fire combusts organic matter within the soil. This combustion reduces soil texture because the roots and fungi that holds soil aggregates together are broken apart, further reducing surface roughness (Wondzell and King, 2003).

Wildfire increases runoff by reducing surface porosity and soil structure. The breakdown of soil aggregates reduces soil structure and texture, seals surface pores, and smoothes and compacts the soil surface (Neary *et al*. 1999). A smooth and compact soil surface limits water infiltration, which adds to surface runoff (Meyer *et al*. 1992).

Water repellent soil resulting from wildfire reduces soil infiltration rates and increases runoff rates (Shakesby *et al*. 2000). Water beads up and sits on the surface of water repellent soils rather than soaking in (Wessel, 1988). Soil water repellency is formed by the condensation of volatilized organic compounds onto cool soil aggregates within the soil profile (DeBano, 2000). These volatilized organic compounds are produced during the combustion of surface litter and duff. The total amount and the type of organic matter consumed affect the spatial distribution (Pierson *et al*. 2008), depth, and severity of water repellency (DeBano, 2000). Combustion temperatures contribute to the depth of the water repellent layer that forms parallel to the soil surface (DeBano, 2000). The water repellent layer can be of varying thicknesses and may be present directly at the surface or at a depth of a few centimeters (~1 to 2 inches) (DeBano, 2000; Woods *et al*. 2007; Shakesby *et al*. 2000).

Soil water repellency strongly contributes to surface runoff at the beginning of rainstorms because it is inversely related to soil moisture (DeBano, 2000; Shakesby *et al*. 1993). In a rainfall simulation study Pierson *et al*. (2008) show a decrease in runoff over time as moisture was added to the soil profile and the severity of water repellency decreased. At a rainfall application rate of 85 mm hr^{-1} (3.3 in hr^{-1}) runoff peaked after 5.6 minutes with a minimum infiltration rate of 45 mm hr^{-1} (1.8 in hr^{-1}). After one hour of rainfall simulation, runoff had decreased to an infiltration rate of 57.6 mm h^{-1} (2.3 in hr^{-1}) (Pierson *et al*. 2008). The severity of water repellency decreased over time as water slowly infiltrated along preferential flow paths, adding moisture to the soil profile, and reducing the severity of the soil water repellency (Dekker and Ritsema, 1994).

Reduced soil infiltration from these wildfire effects leads to excess rainfall during high intensity rain events. Runoff has been shown to be significantly higher on burned plots than on unburned plots (45 % vs. 23 % respectively) in a rainfall simulation (Johansen *et al*. 2001).

1.3 Erosion

Runoff from excess rainfall is the principal driver of soil erosion following wildfire. The combustion of surface vegetation, litter, and duff exposes the mineral soil surface to rainfall and runoff causing significantly increased rates of soil erosion from hillslopes and channels (Brooks *et al.* 2003). Soil erosion is the process of soil particle detachment from the soil surface and the transport of the detached soil particles downslope resulting in a loss of soil material (Hausenbuiller, 1972). The rate of soil particle detachment is a function of the soil properties including soil texture, structure, organic matter and soil moisture (Hausenbuiller, 1972; Knapen and Poesen, 2010).There are two forms of soil erosion on hillslopes caused by flowing water. The first is water flowing in a thin uniform sheet across the surface that lacks preferential flow paths called interrill erosion. The second is by the concentration of water with increasing interrill flow depth and/or the topographic convergence of hillslopes forming channels called rills or gullies (Willgoose *et al*. 1992; Hausenbuiller, 1972) (Figure 1).

The two mechanisms that detach soil particles and aggregates from the soil surface are rainsplash and concentrated flow. Rainsplash is the primary detachment mechanism for interrill erosion (Knapen and Poesen, 2010). Rainsplash detachment is driven by rainfall intensity and the raindrop's kinetic energy (Hausenbuiller, 1972). Rainsplash detachment during interrill erosion is accelerated by the presence of water repellent soils. Water repellent soils experience high detachment rates by raindrops impacting and breaking apart large sediment laden water beads resting on the water repellent surface (Terry and Shakesby, 1993).

The second mechanism for soil detachment is concentrated flow. Concentrated flow both detaches and transports soil particles during rill erosion. Post-fire hillslope erosion is predominately from rill erosion, which causes up to 80 percent of the total sediment loss from hillslopes (Robichaud *et al.* 2010).

Soil particles are detached during concentrated flow by shear stress exerted from water onto the soil surface (Dingman, 2009). The threshold at which shear stress initiates particle motion at the soil surface is called the critical shear stress (Moody *et al*. 2005). Wildfire reduces critical shear stress by reducing vegetation cover and by soil heating, leading to increased sediment erosion. In a shallow channel flume study, Prosser and Slade (1994) found critical shear stress decreases in response to decreased vegetation. While Moody *et al*. (2005) shows critical shear stress is high (>2.0 N m^{-2} [0.04 lb ft^{-2}]) when soil is heated to moderate temperatures between 175^{o} and 275 ^{o}C (347 ^{o} and 527 ^{o}F), and reduced (0.5 to 0.8 N m^{-2} [0.01 to 0.02 lb ft^{-2}]) when soil is heated to very high temperatures >275 ^{o}C (527 ^{o}F).

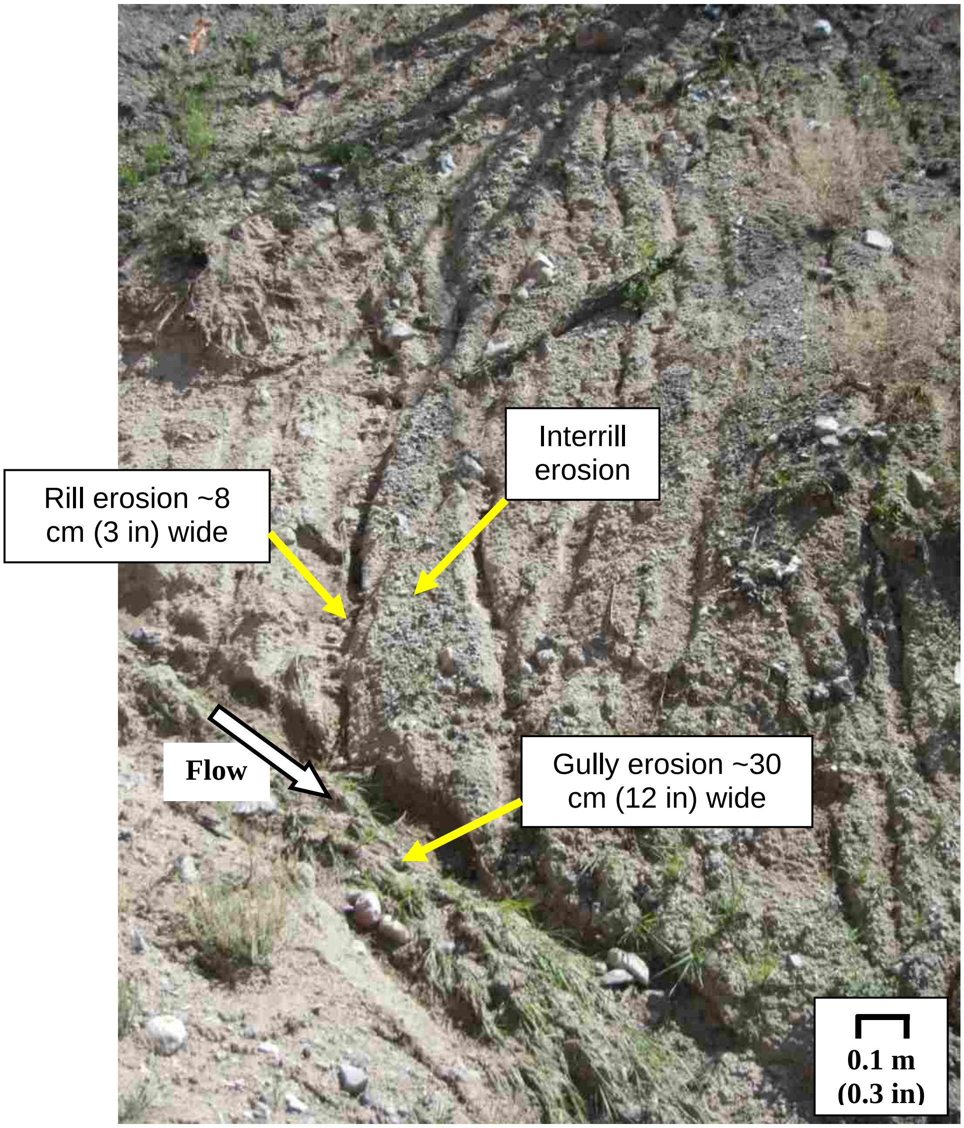

Figure 1. Hillslope interrill, rill, and gully erosion. Interrill erosion occurs as sheetwash overland flow, rill erosion is concentrated overland flow, and the concentration of flow from multiple rills forms gullies.

Post-fire soil erosion can be studied at a variety of scales. Shakesby and Doerr (2006) grouped the scales often studied in the literature by four methods: ground height changes, bounded plots, sediment traps, and slope transects. The methods to study erosion at these four scales include: point scale erosion pins (Smith and Dragovich, 2008), small hillslope plot sediment fences (Robichaud and Brown, 2002), large multi-hectare watersheds with sediment traps (Robichaud *et al*. 2008), and pre-/post-event surveys of channel cross-sections (Gabet and

Bookter, 2008; Keller *et al*. 1997). Soil erosion is not necessarily influenced by the same factors at these differing scales; therefore, care must be taken when directly comparing rates at different scales. In a review comparing many different scales, Scott et al. (1998) identified sediment yields as being inversely proportional to plot-areas. One contributing factor to this inverse relationship is with larger plot-areas the total surface roughness and infiltration capacity increase causing mobilized sediment to be re-deposited before it can be measured at larger scales (Shakesby and Doerr, 2006). At the smallest point scale using erosion pins (Smith and Dragovich, 2008), sediment is much more likely to be eroded away rather than deposited at the measurement location. This translates to very large sediment yield rates when scaled up to mass per unit area (Mg ha^{-1}, t ac^{-1}). In contrast, large scale sediment yields measured at watershed outlets are shown to be much lower than point erosion rates because re-deposition can occur prior to the sediment making it to the outlet, while hillslope fence plots fall in between these two extremes (Shakesby and Doerr, 2006).

1.4 Catchment erosion

Rill erosion on burned hillslopes increases runoff rates, runoff velocities, and sediment erosion rates as compared to natural or undisturbed hillslopes. Robichaud *et al.* (2010) studying rill erosion on natural forest soils vs. high burn severity soils shows significant increases in runoff rates (2.7 to 21 L min^{-1} [0.7 to 5.5 gal min^{-1}]), in runoff velocities (0.016 to 0.31 m s^{-1} [0.05 to 1 ft s^{-1}]), and in sediment flux rates (1.3×10^{-5} to 1.9×10^{-3} kg s^{-1} [2.9×10^{-5} to 4.2×10^{-3} lb s^{-1}]). On unburned hillslopes rills are disconnected from each other because high infiltration rates from vegetation slowing or stopping runoff reduces rill connectivity. These barriers shorten rill lengths, keeping them from linking up along the slope length. On hillslopes disturbed by wildfire, rills flow downhill for long lengths uninterrupted by barriers and can link up to form extensive rill networks. These highly efficient drainage networks start at or near the top of the hydrologic divide and continuously flow to the ephemeral channel at the base of hillslopes and out to the catchment outlet.

Sediment transported off hillslopes and into channels continues to work through the channel network both spatially and temporally (Moody and Martin, 2009). During large erosion events, hillslope erosion introduced to the channel can overwhelm the transport capacity of flow within the channel forcing sediment to deposit out, causing aggredation on the channel bed (Keller *et al*. 1997). However, if there is limited hillslope sediment supply to the channel, elevated flows may cause increased scour to the channel bed and banks (Canfield *et al.* 2005). The deposition and remobilization of sediment within channels may take place over a period of a few years or even hundreds of years (Moody and Martin, 2009; Willgoose *et al*. 1992; Keller *et al*. 1997; Legleiter *et al*. 2003; Inbar *et al*. 1998). Sediment yield amounts from ephemeral or low order channels vary widely and occur as suspended sediment all the way to debris flows (Meyer and Wells, 1997). Moody and Martin (2009) show large ranges in post-fire bedload sediment yields in channels of 14 to 300 Mg ha^{-1} (6.25 to 133.8 t ac^{-1}) with a mean of 240 Mg ha^{-1} (107 t ac^{-1}) in the first two years after a fire. Post-fire debris flows are unique from soil shear or slippage of one soil mass along a shear plane over a stationary soil mass (Hausenbuiller, 1972). In southern California, post-fire debris flows were shown to be correlated with short duration high intensity rain events (Kean *et al*. 2011). During these rain events overland flow entrains an increasing amount of sediment while working its way out the catchment through the progressive bulking of sediment laden runoff, forming a debris flow (Gabet and Bookter, 2008). Gabet and Bookter (2008) estimated progressively bulked debris flows in southwest Montana delivered as much as 574 to 3655 m^3 (750 to 4781 yds^3) of sediment from low order catchments to the valley floor.

1.5 Post-fire erosion mitigation

Sediment yields from ephemeral channels are a major concern to the USDA Forest Service Burned Area Emergency Response (BAER) teams who work to mitigate their destructive and dangerous effects by implementing channel treatments. One channel treatment commonly used is straw bale check dams (Robichaud *et al.* 2000). Straw bale check dams are made by tightly abutting straw bales end to end, keying each bale into the channel perpendicular to flow, and driving wooden stakes through each bale to secure it to the ground, forming a "U" shape structure across the channel (Napper, 2006). The bottoms of the straw bales on each end extend far enough up onto the channel banks to sit 25 to 30 cm (~10 to 12 in) higher than the straw bale in the center of the structure, directing flow over the center straw bale spillway (Napper, 2006). Energy dissipaters or rocks and/or anchored logs are placed directly at the down-channel base of the structure to reduce the effect of flow over the spillway scouring the channel bed. Straw bale check dams are designed to trap and store sediment mobilized within an ephemeral channel that is then released at a metered rate over a period of few years as the straw bales degrade (Tracy and Ruby, 1994; Napper, 2006). Mitigation targets may call for multiple structures to be installed along the longitudinal channel profile when taking into account catchment size, burn severity, and predicted sediment yields. The structures are spaced in the channel to maximize trap efficiencies by letting the trapped sediment from a lower dam extend enough up channel far enough to just touch the base of the next structure sitting higher in the channel (Napper, 2006).

Sediment trapped by straw bale check dams resembles the sediment trapped behind much larger concrete crib check dam structures, which serve the same purpose of trapping mobilized sediment in the channel (Napper, 2006). The trapped boulders, rocks, soil, and mud behind a concrete crib check dam is referred to as a debris cone with the point of the cone facing up-channel and base of the debris cone resting against or contacting the up-channel face of the structure (Gallup, 1975). A debris cone looks similar to pooled water behind the structure, however unlike the surface of water which is perpendicular to gravity or flat, the surface of a debris cone behind concrete crib check dams usually has a gradient of 0.7 of the original channel gradient (Gallup, 1975). Other channel structures aimed at reducing ephemeral sediment erosion include log check dams, loose rock check dams, and rock gabion check dams (Tracy and Ruby, 1994; Napper, 2006). In the Mediterranean, log debris dams (LDDs) were installed in a post-fire environment to reduce ephemeral channel sediment yields (Fox, 2011). These structures serve the same purpose as straw bale check dams of trapping and storing sediment mobilized in the channel. While debris cones have been studied for a few channel treatments, there is no clearly defined value of the amount of sediment trapped within the straw bale check dam debris cones. Only one observational study attempts to estimate the volume of sediment trapped by straw bale check dams, but the trapped sediment volumes were measured after the structures were fill to capacity giving only a rough estimate of trap volumes (Miles *et al*. 1989).

The sediment storage capacity of straw bale check dams, log debris dams, and concrete crib check dams is a function of the spillway height of the structure. These channel treatments have a wide range of spillway heights with the smallest structures log and straw bale check dams, having spillways of 0.20 to 0.40 m (0.6 to 1.2 ft), and larger concrete crib check dams having spillways as high as 8 m (26 ft) (Gallup, 1975). A straw bale check dam's spillway height is limited to the width of a straw bale resting on its side, ~45cm (18 in), minus the depth the straw bale is keyed into the channel bed, ~10cm (4 in), for a spillway height of ~35cm (14 in). Fox (2009) found gaps and holes within the log debris dams that had a mean structural spillway height of 105 cm (3.4 ft) captured sediment only to a mean height of 50 cm (1.6 ft) or a 50% reduction in the structural storage capacity. To reduce these negative effects of flow between straw bales and a reduction in straw bale check dam spillway height, excess loose straw, sticks, and rocks are tightly wedged in the gaps between abutting straw bales.

There is limited experimental knowledge on how to install straw bale check dams to effectively reduce sediment yields from burned catchments. At construction sites, straw bale check dams have been effective when the catchment area for one structure is < 0.4 ha (1 ac), the flow does not exceed 0.3 $m^3 s^{-1}$ (11 $ft^3 s^{-1}$), and the trapped sediment is removed when the structure fills beyond halfway of its sediment holding capacity (Goldman *et al.* 1986). Tracy and Ruby (1994) suggest straw bale check dams can be used in burned watersheds with an area of ~65 ha (160 ac) or less. Most notably these guidelines do not relate the amount sediment straw bale check dams will trap and prevent from exiting catchments and there are no studies showing straw bale check dams will capture a given amount of sediment when treated at a given rate per area.

Most often straw bale check dams are rated on an individual structure basis, such as a success or failure rating. This rating is based on how much sediment a straw bale check dam structure captures, but even suggestions and evaluations with this commonly used rating system range widely. Ruby (1997) suggests a treatment is unsuccessful in primary watersheds or small catchments if fine sediments and ashes are released into higher order channels. Following the 1991 Oakland Hills fire in California, 440 straw bale check dams were installed in channels and gullies (Collins and Johnston, 1997). The straw bale check dams failed if they had any of these following conditions after an erosion event: side cut or flow around structure, undercut, sediment trapped and then re-eroded, moved or displaced from original position, and unfilled. Three months post-installation of structures, 43% to 46% were considered functioning, and after 4.5 months 37% to 43% were considered functional, indicating an overall failure rate greater than 50% (Collins and Johnston, 1997). Following the 1987 South Fork Trinity River Fire 1300 straw bale check dams were installed (Miles *et al*. 1989). On average the straw bale check dams trapped 1.1 m^3 (41 ft^3) of sediment and had a failure rate of only 13% from piping underneath or between straw bales (Miles *et al*. 1989). Foltz (*et al.* 2009) synthesized interviews from 30 BAER team engineers/hydrologists, unpublished literature and relevant publications for a post-fire BAER road treatment handbook. The report evaluated straw bale check dams at 10 sites and found 'good to excellent' performance at 60% of sites, 'fair' at 30%, and 'poor' at 10%. The majority of these evaluations are lacking in that they do not relate how much sediment was transported past the individual structures even if the structures were considered functioning.

Increased sedimentation rates following wildfires have become a great risk to human life and property located in the wildland-urban interface. Increased peak flows and sediment yield rates in response to high intensity rain events have devastating effects beyond the perimeter of the burned areas. The use of straw bale check dams in post-fire ephemeral channels has been increasing over the past four decades (Foltz *et al.* 2009) to mitigate increased sedimentation rates from burned catchments. However, there is no quantitative information on the ability of straw bale check dams treated in ephemeral channels to reduce sediment yields from burned catchments.

1.6 Principle research objectives

1) Determine if there is a significant difference in sediment yields between catchments treated with straw bale check dams and untreated catchments taking into account rainfall intensities and hillslope erosion rates.

2) Quantify the mass of sediment trapped by straw bale check dams and the mass of sediment scoured in the channel below straw bale check dams and relate these amounts to channel gradient.

3) Relate the amount of sediment mobilized past straw bale check dams to the annual sediment yields from treated catchments to determine the trap efficiency of the treatment.

4) Determine if straw bale check dams help to stabilize and protect the channel from knickpoint migration.

2.0 Methods

2.1 Site description

This study was conducted within the burned area of the 2010 Twitchell Canyon Fire that burned 17,960 hectares (44,380 acres) at high elevations in the Tushar Mountains of south-central Utah, from 20 July to 16 October (UT-FIF, 2010). Dominant pre-fire vegetation at the study site included pinyon pine (*Pinus edulis*), juniper (*Juniperus osteosperma)*, and gamble oak shrub (*Quercus gambelii*), with perennial grasses/forbs and mountain big sagebrush (*Artemisia tridentata)* dominating the understory (UT-FIF, 2010). Soil types are highly erodible *Aridic Argiustolls* and *Aridic/Typic Haplustolls* (UT-FIF, 2010) (34 % sand, 65 % silt, < 1 % clay) derived from the Sevier River Formation parent material (Rowley *et al*. 2002), which is the only exposed bed rock unit at the study site. The Sevier River Formation unit, within the Mount Belknap Volcanics series, is 100 to 300 m (~330 to 980 ft) thick, has a west-east strike, and a shallow dip of 15° to the north, allowing for a surfically continuous exposure in the area (Rowley *et al*. 2002, Cunningham and Steven, 1979). Rowley (*et al*. 2002) describes the unit material as "gray, tan, yellow, white, pink, and light-green sandstone, pebbly to boulder conglomerate, mudstone, and siltstone of fluvial and locally lacustrine origin" interbedded with high-silica rhyolite, airfall tuff, and basalt (Cunningham and Steven, 1979). The fluvial and lacustrine or river and lake deposits do not reflect current topographic features and were probably laid down in basins that existed prior to basin and range faulting (Rowley *et al*. 2002). The interbedded extrusive igneous or volcanic rocks erupted from both the Mount Belknap caldera in the current Tushar Mountains, and the Red Hills caldera in the Antelope Range northwest of the Tushar Mountains 19 m.y.a. (Cunningham and Steven, 1979).

The average annual rainfall at the study site is 500 to 550 mm yr^{-1} (~20 to 22 in yr^{-1}) with the majority of precipitation occurring as snow (Utah State University, Climate Center, 2010). At the Kimberly Mine SNOTEL site located 4 to 4.5 km (2.5 to 2.8 mi) away and ~500 m (~1640 ft) higher in elevation (2783 m, 9130 ft), two thirds to four fifths of precipitation occurred as snow during the 2010-2011 and 2011-2012 water years (USDA, NRCS, http://www.wcc.nrcs.usda.gov, Kimberly Mine). The regional climate is influenced by the northernmost extent of the Arizona and New Mexico monsoon precipitation regime during the summer (Higgins *et al*. 1998). With precipitation brought up from southern Mexico beginning in early July and lasting into September, which ends the spring drought and tails off in the late summer (Higgins *et al*. 1997). Winter precipitation is from frontal systems out of the Pacific Northwest (UT-FIF, 2010). The point precipitation frequency estimate for the 10-minute rainfall intensity (I_{10}) return period with 90% confidence intervals at the site given by Bonnin *et al*. (2006) are a 1-year I_{10} of 37 (32-42) mm hr^{-1} [1.5 (1.3-1.7) in hr^{-1}], a 2-year I_{10} of 48 (42-55) mm hr^{-1} [1.9 (1.7-2.2) in hr^{-1}], and a 5-year I_{10} of 66 (58-76) mm hr^{-1}[2.6 (2.3-3.0) in hr^{-1}]. The point precipitation frequency estimate for the 30-minute rainfall intensity (I_{30}) return periods with 90% confidence intervals are a 1-year I_{30} of 20 (18-23) mm hr^{-1} [0.8 (0.7-0.9) in hr^{-1}], 2-year I_{30} of 26 (23-31) mm hr^{-1} [1.0 (0.9-1.2) in hr^{-1}], 5-year I_{30} of 37 (32-42) mm hr^{-1} [1.5 (1.3-1.7) in hr^{-1}] (Bonnin *et al.* 2006).

2.2 Paired catchments

We conducted our study in small ephemeral channel catchments. Ten ephemeral channel study catchments were paired, with each pair consisting of one treated and one untreated or control catchment. Catchments ranged in size from 0.2 to 1.6 ha (0.5 to 4.0 ac) (Figure 2).

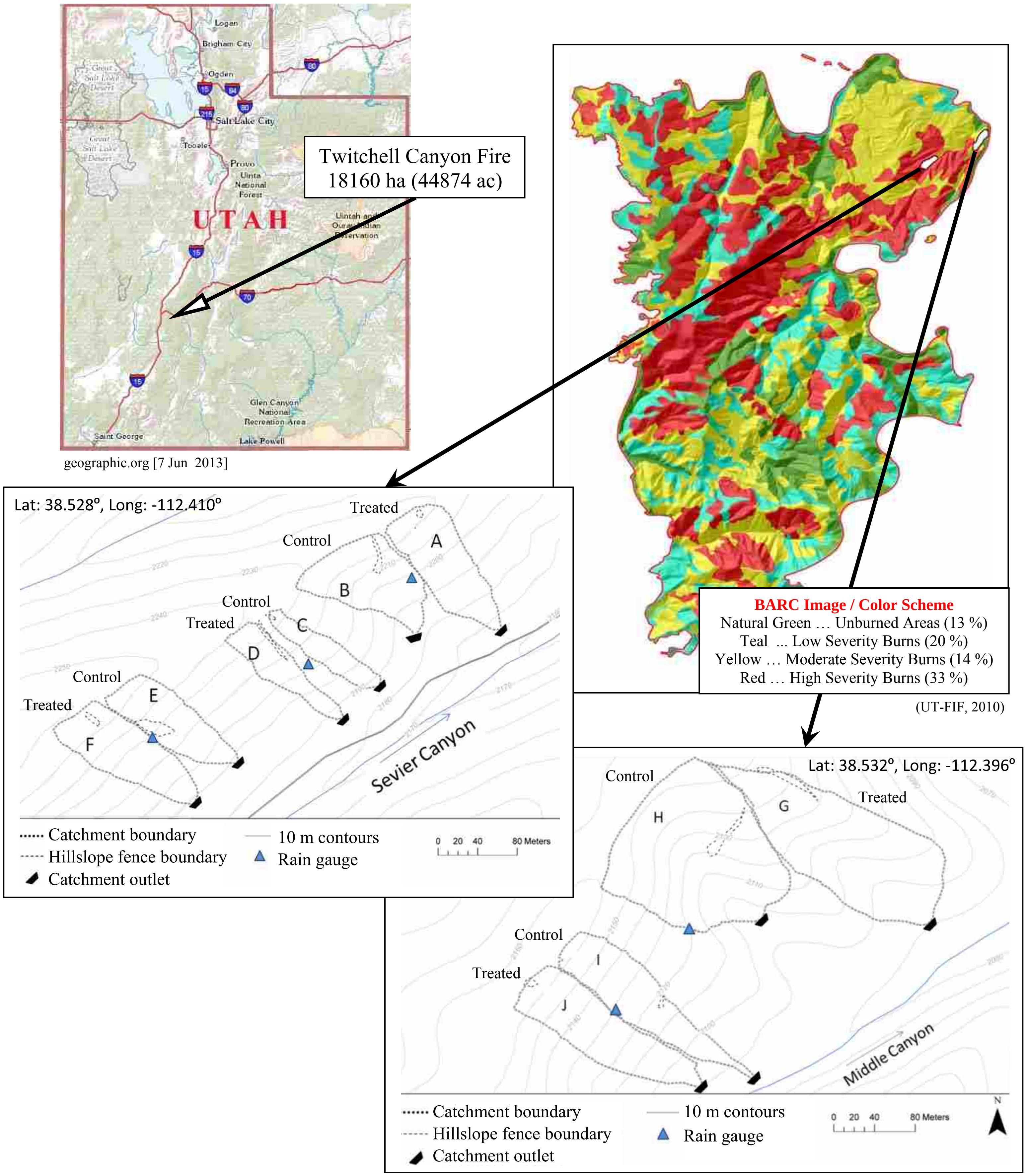

Figure 2. (Starting in top left of page with figure descriptions moving clockwise) 1. Twitchell Canyon Fire in south-central Utah. 2. Burned Area Reflectance Classification (BARC) map indicating burn severity, the study paired catchments are colored white and outlined in black. 3. Treated and control catchments within pair and the locations of hillslope plot boundaries, rain gauges, and catchment outlets.

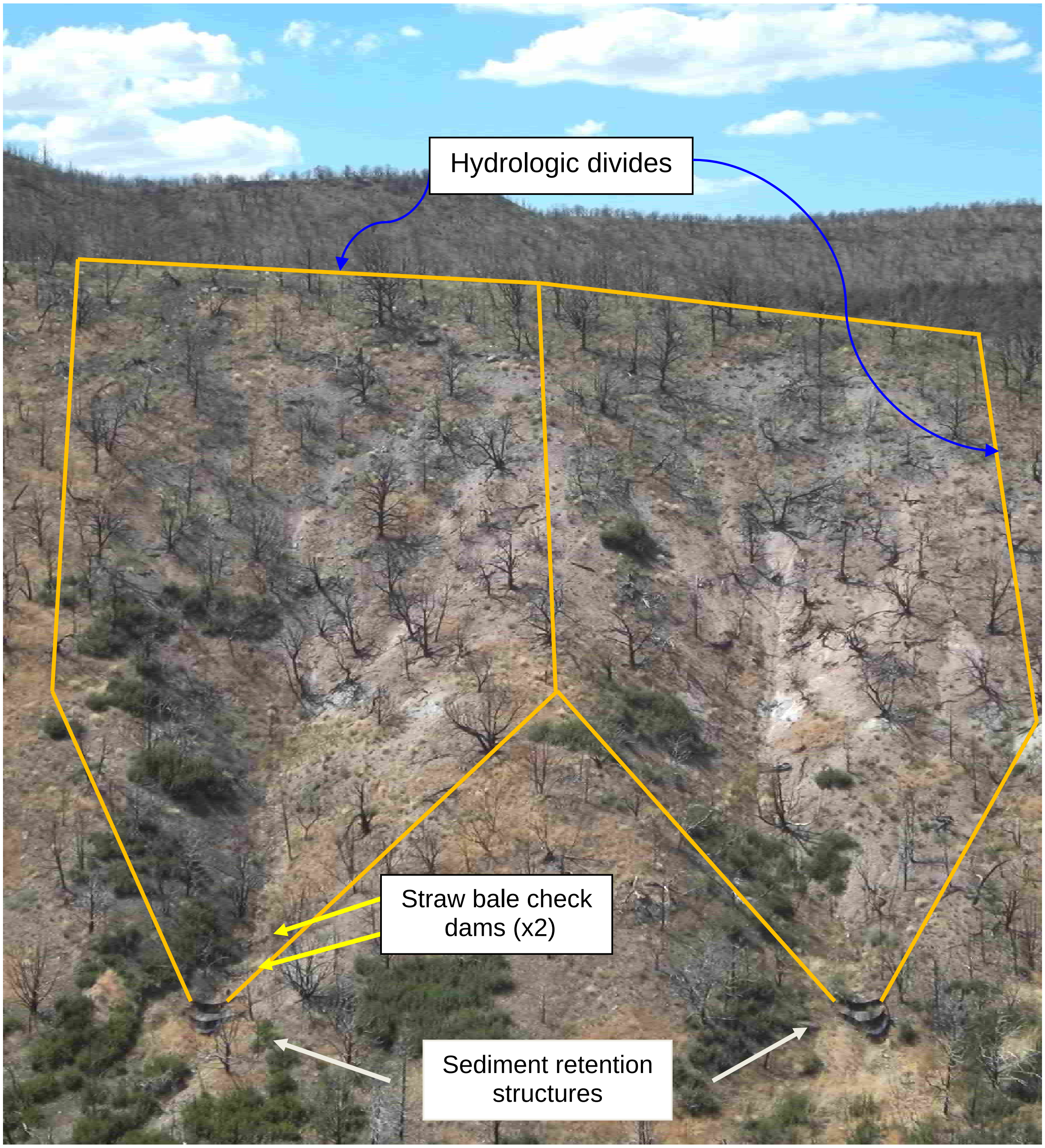

Figure 3. Paired catchment E-F, the treated catchment (0.6 ha, 1.4 ac) is photo left and the control catchment (0.4 ha, 1.1 ac) is photo right. The upper hydrologic divide along the ridge line bounds the top of the catchments, sediment retention structures bound the catchments at the base, and catchment sides are at the divergence of overland flow into the catchment or not into the catchment.

Adjacent paired catchments were similar in area, aspect, degree of channel incision, and hillslope and channel gradients, and were burned at high severity as defined in the 'Glossary of Wildland

Fire Terminology'. All above-ground organic matter, such as larger fuel and duff, were consumed resulting in high vegetation mortality, reduced ground cover, and high soil heating (Figure 3) (NWCG, 2006).

Study catchment pairs exhibited similar traits and characteristics. The study catchments are located between 2060 and 2250 m (6760 to 7380 ft) in elevation, and range in vertical scale (Willgoose *et al*. 1991) from ~50 to 80 m (~160 to 260 ft) measured from catchment outlet to the catchments highest hydrologic divide. The relief or vertical scale of catchments within each pair is roughly equal with vertical differences ranging from 3 to 10 m (~10 to 33 ft). Study catchments have steep headwalls and side slopes with an average gradient of 58 %, and a range of 41 to 78 %, that drain into ephemeral bedrock channels as steep as 50 % and as shallow as 23 %, with an average gradient of 29 % (Table 1).

Table 1. Catchment name and numbered pair, treatment, catchment area (ha [ac]), vertical scale of catchment (m [ft]) or the vertical height from the catchment outlet to the highest hydrologic divide, average channel slope (%) from the outlet up to the channel head, and channel length from the outlet to the channel head (m [ft]).

Catchment. Pair	Treatment	Catchment area (ha [ac])	Vertical scale (m [ft])	Mean channel gradient (%)	Channel length (m [ft])
A.1	Treated	0.5 [1.4]	56 [184]	23	85 [279]
B.1	Control	0.6 [1.4]	59 [194]	27	48 [157]
C.2	Control	0.2 [0.5]	53 [174]	47	52 [171]
D.2	Treated	0.3 [0.7]	57 [187]	49	37 [121]
E.3	Control	0.4 [1.1]	63 [207]	36	45 [148]
F.3	Treated	0.6 [1.4]	69 [226]	32	50 [164]
G.4	Treated	1.4 [3.3]	76 [249]	20	90 [295]
H.4	Control	1.6 [3.9]	21 [69]	30	125 [410]
I.5	Control	0.6 [1.5]	66 [217]	26	118 [387]
J.5	Treated	0.7 [1.7]	71 [233]	33	130 [427]

The bedrock ephemeral channels begin high in the drainages and form from the topographic convergence of hillslopes, rills, and gullies over a distance of 4 to 9 m (13 to 30 ft) before they are fully defined. Channel lengths range from 38 to 137 m (~125 to 450 ft) and drain at catchment outlets onto alluvial fans or into higher order ephemeral channels. In the largest paired catchment (1.4 ha and 1.6 ha [3.5 ac and 4.0 ac]), the channels are incised to bedrock 1 m

(~3 ft) deep for distances of 30 m (~100 ft) in colluvial deposits before the outlet. Paired catchments are located in two separate canyons, 1.2 km (0.75 mi) apart; with three pairs in Sevier Canyon and 2 pairs in Middle Canyon to the east. In Sevier Canyon, the pairs have a southeast aspect and are spaced over a distance of 400 m (~1300 ft), on a southwest to northeast dipping ridge. The pairs in Middle Canyon have a southeast aspect, are spaced 275 m (~900 ft) apart, and sit on a southwest to northeast dipping ridge.

2.3 Straw bale check dams

One catchment within each pair was randomly selected for treatment with straw bale check dams at the beginning of the first post-fire year. Each straw bale check dam was installed following BAER handbook guidelines (Napper, 2006), using three to five straw bales tightly abutted end to end and keyed or trenched 10 cm (~4 in) in to the channel bed and banks creating a U-shaped structure perpendicular to flow (Figure 4).

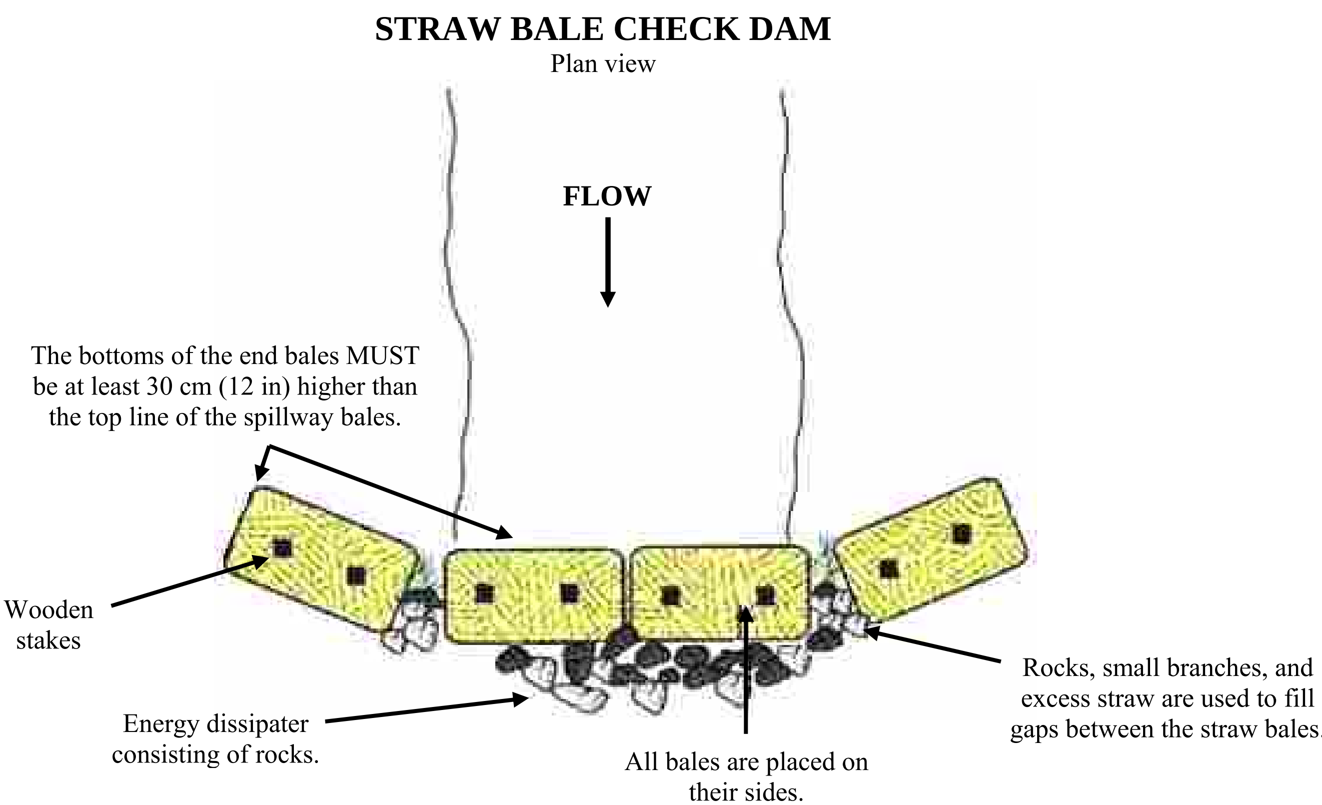

Figure 4. Plan view structural diagram of straw bale check dam structure modified from Napper (2006). Straw bale check dam structures open up-channel.

We followed standard installation procedures. Straw bales were 46 x 36 x 96 cm (18 x 14 x 38 in) in size, weighed ~18 kg (40 lb), and were secured by two to three wooden stakes (2.5 x 5 cm [1 x 2 in]) driven through each bale into the ground. The bottoms of the straw bales on the ends of the U-shaped structure sat higher than the top of the straw bale in the middle of the structure, this directed flow in the channel over the structural low point in the center creating a spillway (Napper, 2006) (Figure 5). The straw bale check dam structures were installed just upstream of catchment outlets (5 to 15 m [16 to 50 ft]) at a rate of 4 ha^{-1} (~2 ac^{-1}) and were generally spaced 4.5 m (15 ft) apart (Figure 6).

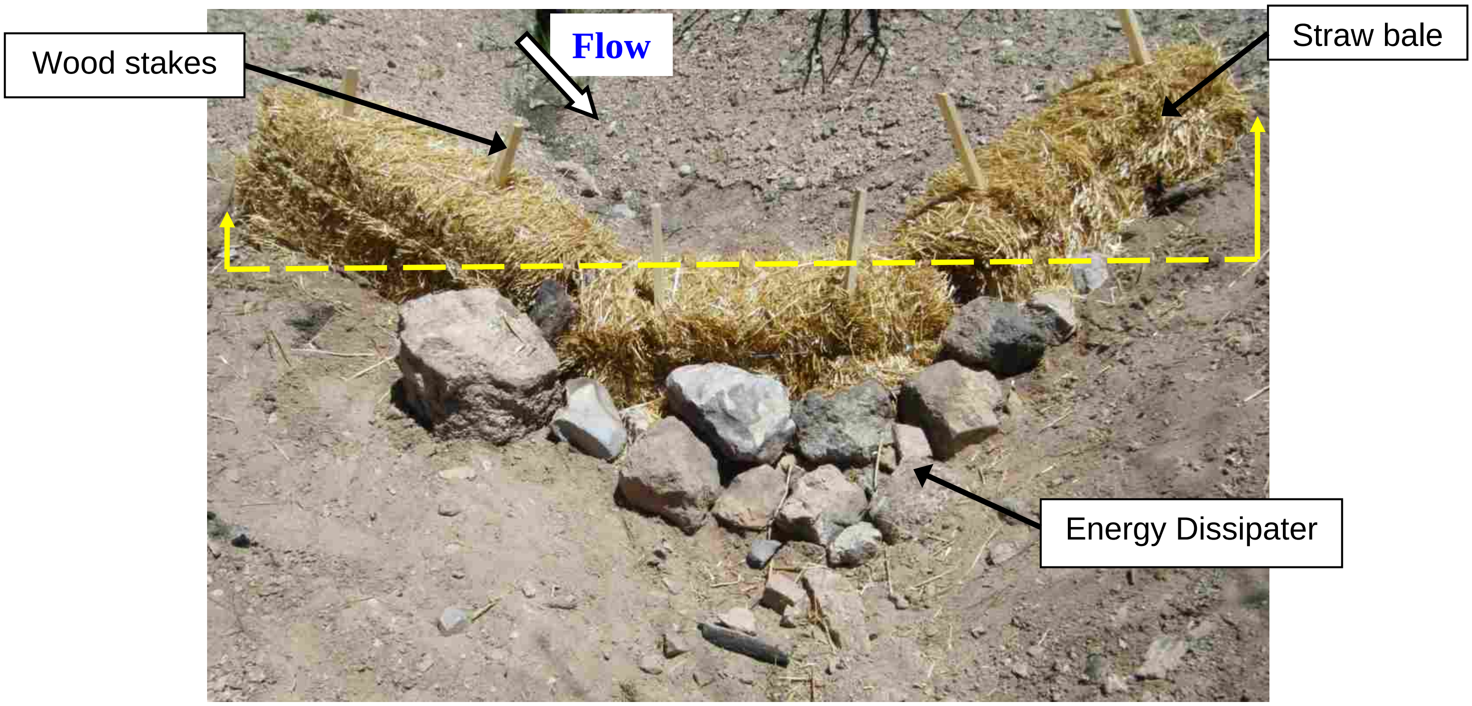

Figure 5. Down-channel face of a straw bale check dam at ground level looking up-channel. Straw bales are keyed into the bed and banks to create a U-shaped structure that spans the width of the channel. Bottoms of bookend straw bales (yellow arrows) sit vertically higher than top of the center spillway bale (yellow dashed line). Energy dissipator rocks sit against the structure on the down-channel side below the center spillway to help reduce scour to the channel-bed.

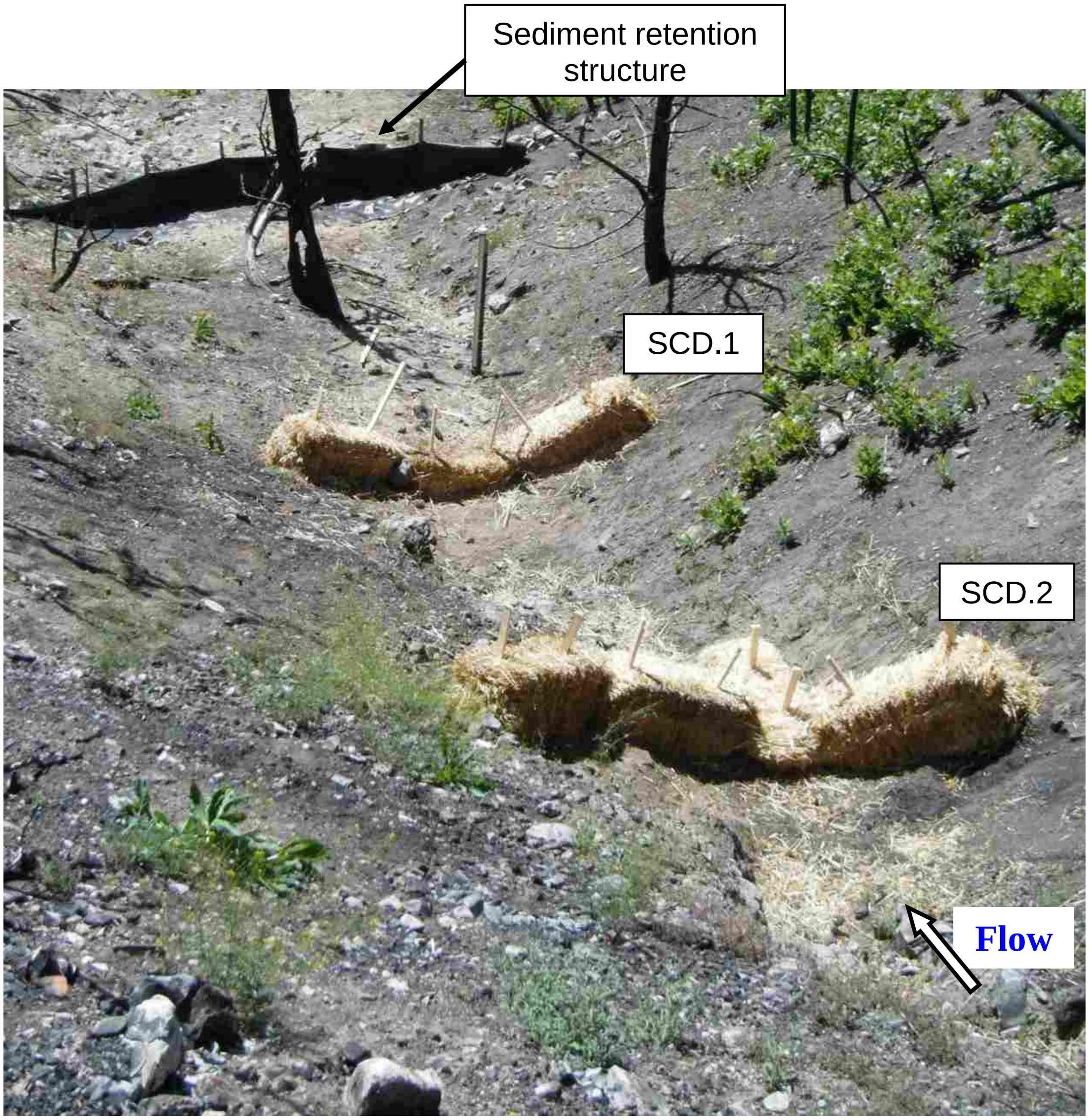

Figure 6. Channel treated with straw bale check dams (SCD). In a few instances the center spillway straw bales were positioned lengthwise or running parrallel with the channel when steep hillslopes and narrow channels prohibited the lengthwise placement of staw bales perpendicular to the channel as seen with SCD.2. Photo is looking down channel.

2.4 Measuring catchment sediment yields

The sediment yields were measured at catchment outlets. During the first and second post-fire years (2011 and 2012), the total bedload sediment yields eroded from catchments during each rain storm were captured in the ephemeral channel at the catchment outlets with reinforced sediment retention structures. The materials used to build the retention structures included standard framing lumber boards (10 x 4 x 305 cm [4 x 1.5 x 120 in]), wood stakes (5 x

5 x 120 cm [~2 x 2 x 50 in]), welded mesh wire 5 x 10 cm mesh openings [2 x 4 in], 14 gauge wire, and high tensile strength woven geotextile fabric (US Fabrics, Cincinnati, OH). Lumber framed structures spanning the channel widths were secured to the channel bed and banks with side walls extending out from the center spillway wall and angled slightly up-channel (Figure 7). The structures center spillway walls ranged in height from 90 to 150 cm (35 to 60 in) tall depending on the channels shape and depth in which the structure was installed. Welded wire and geotextile fabric were secured to the up-channel face of the lumber frames and cornered at the lumber frame-ground contact to extend up the channel bed 1 to 3 m (~3 to 10 ft).

Figure 7. Lumber framing of sediment retention structure secured into the channel bed and banks with the added strength of wire mesh attached to the up-channel face. Spillway wall is located in the center of the structure with side walls opening up-channel. Photo looks up-channel.

This reduced the chance of flow undercutting the structure and provided a base reference to help distinguish between captured eroded sediment and the original channel bed. Two sediment retention structures were built in tandem in each catchment's channel to capture total bedload sediment yield during a rain event, and in two channels an additional third structure was added halfway into the 2011 season after sediment yields overtopped the original two structures (Figure 8).

Figure 8. Tandem sediment retention structures in the channel. Geotextile woven fabric was secured to the up-channel face of the framed structures and extends up-channel attached with sod staples to the bed and banks. Tandem structures increased the maximum sediment storage capacity of sediment retention structures. Photo looks down-channel.

Sediment yields were measured using sediment retention structures. Retention structures in treated catchments were installed far enough below the lowest straw bale check dam to not affect check dam function, but close enough to minimize sediment introduction to the channel downstream of the check dam from hillslopes or channel bed scour. Sediment yields captured by retention structures were measured and removed from the retention structures using two different techniques depending on the captured sediment yield amount. Small sediment yields were weighed using plastic buckets (20 l, 5 gal) and sub-sampled into sealed airtight plastic bags before discarding the excess measured sediment below and off to the side of the structures. The sub-samples were taken back to the laboratory and oven dried over night at 105 ^{o}C to gravimetrically determine the soil water content, which was used to convert the wet mass of the field sediment yield to a final sediment yield dry mass (Cambardella *et al*. 1994). For large sediment yields the sediment was removed by hand or mini-excavator (Kubota, KX161, Torrance, CA) after surveying the trapped sediment with a surveyor's total station. The total station (Topcon, GTS-2110, Livermore, CA) took twenty-five to fifty point measurements of the location of a prism mounted survey rod, in planar horizontal (x, y) and vertical (z) space relative to the known position of a #4 rebar monument off to the side of the channel, while it crisscrossed back and forth across the surface of the captured sediment. The survey points were imported into surface topography software (Trimble Geomatics Office (TGO), Trimble Engineering and Construction, Dayton, OH) to build a surface using the finite element method, by connecting the surveyed points in a triangular network. Pre-event surfaces were built for all sediment retention structures using data of surveyed retention structures and the up-channel bed and banks catchment area prior to the first event. The volume of the captured sediment yields were determined by subtracting the pre-event surface from the post-event captured sediment yield surface. To convert captured volumes to mass, two to five core bulk density (g cm^{-3}) samples were taken within the captured sediment at depth intervals of 10 to 40 cm (~4 to 16 in), taking more samples for deposits with steep moisture gradients and fewer for drier deposits.

Final sediment analysis was done in a laboratory. The oven dried bulk density mass of sample cores were used convert the volume of measured sediment at the corresponding depths they were taken at to a final dry mass (Robichaud and Brown, 2002). Sediment yields were measured twice in two separate sediment retention structures using both the weighing bucket and survey measurement techniques. The percent difference, or relative uncertainty, associated with the surveying technique was determined by comparing it to the most accurate direct measurement of the total sediment mass by weighing buckets (Robichaud and Brown, 2002).

Absolute uncertainty (±Δ), which is the measured sediment mass multiplied by the relative uncertainty is given for all sediment yields measured with the surveying method.

2.5 Measuring rain events

We measured spring, summer, and fall rainfall events. Five tipping bucket rain gauges recorded rain event duration, intensity, and total precipitation monitored continuously for the duration of the monsoon seasons for both the first and second post-fire years, from 10 Jun 2011 to 8 Oct 2011 and 7 May 2012 to 26 Sep 2012. Four rain gauges are located on the adjoining ridge between paired catchments, and one rain gauge is located on the far western ridge of a paired catchment (Figure 9). Tipping-bucket rain gauges (8" Tipping Bucket Rain Gauge, RainWise, Bar Harbor, ME; HOBO Event Logger, Onset Computer Corporation, Bourne, MA) record volume (0.254 mm [1/100 in]) per time with a resolution of 0.5 seconds (Ciach, 2003). Rain data was standardized to tips per minute, and events were separated by the passing of a six hour time interval between consecutive tips. Total precipitation (mm) [in], duration (min), and 10-minute (I_{10}) and 30-minute (I_{30}) rainfall intensities were determined for each event and categorized according to their 10 minute intensities for 1, 2, and 5-year recurrence intervals (Bonnen *et al.* 2006).

Figure 9. Tipping bucket rain gauge (~20 cm [8 in] opening) set level to the ground and located roughly half way up catchment ridge (monitored catchment in background). The rain gauge was mounted to a plate of sheet metal attached to the top of a 10 cm (4 in) diameter PVC post. The hollow PVC post was buried 45 cm (~18 in) into the ground, filled to the brim with soil, and secured with three guy-wires spaced at 120^{o} that were attached to the post 140 cm (~55 in) from the ground surface and anchored at the ground with rebar to reduce systematic error of wind disturbance tipping the recording bucket.

2.6 Measuring hillslope sediment erosion

We measured hillslope erosion rates in each catchment. Hillslope erosion rates were measured during 2011 and 2012with one hillslope fence in each catchment, following the design by Robichaud and Brown (2002), and at two different randomly assigned contributing areas (m^2) [ft^2] within a paired catchment. Sediment fences were built with a 3 m (~10 ft) wide opening positioned perpendicular to the slopes fall line, by driving wood stakes (5 x 5 x 120 cm [2 x 2 x 50 in]) and securing geotextile woven fabric to the up-slope side, to capture the total sediment yielded from the contributing hillslope area. Small contributing area (m^2 [ft^2]) hillslope plot erosion rates were measured with a sediment fence near the uppermost hydrologic divide of catchments and large contributing area (m^2 [ft^2]) hillslope plot sediment delivery rates to the channel were measured with a sediment fence located at the hillslope base just above the defined channel. The catchment area of small hillslope fence plots ranged from 39 to 65 m^2 (420 to 700 ft^2), averaging 50 m^2 (540 ft^2), with an average slope length 16 m (53 ft) and gradient of 50 %, and the catchment area of large hillslope fence plots ranged from 42 to 204 m^2 (~450 to 2200 ft^2), averaged 130 m^2 (1400 ft^2) and had an average slope length of 46 m (151 ft) and gradient of 50 % (Table 2). Sediment yields collected in hillslope fences were removed by hand with buckets (20 *l*, 5 gal), weighed and sub-sampled into sealed airtight plastic bags after each event, discarding excess weighed material directly below the fence. In the laboratory, the water content was gravimetrically determined by oven drying sub-samples at 105 ˚C and used to convert the sediment yields to a dry mass (Cambardella *et al*. 1994).

Table 2. Hillslope fence name and pair, fence location on catchment hillslope (upslope, base of hillslope), contributing area of hillslope (m^2 [ft^2]) draining into fence, slope length (m [ft]) from the hydrologic divide to the hillslope fence, and slope (%) above the hillslope fence.

Hillslope fence.pair	Fence location	Contributing area (m^2 [ft^2])	Slope length (m [ft])	Slope (%)
A.1	upslope	29 [312]	11 [36]	53
B.1	base of hillslope	116 [1249]	43 [141]	62
C.2	upslope	22 [237]	11 [36]	61
D.2	base of hillslope	108 [1162]	55 [180]	43
F.3	upslope	64 [689]	21 [69]	43
E.3	base of hillslope	276 [2970]	44 [144]	58
G.4	upslope	227 [2981]	66 [217]	25
H.4	base of hillslope	224 [2411]	64 [210]	46
J.5	upslope	59 [635]	12 [39]	67
I.5	base of hillslope	27 [291]	12 [39]	39

2.7 Measuring straw bale check dam trap/scour volume and mass

Straw bale check dams were measured pre- and post-sediment yield events. Straw bale check dams were surveyed both up- and downstream of straw bale check dam influence using the same technique described earlier with a surveyor's total station set up over a # 4 rebar monument and a prism-mounted survey rod. The point location of the prism-mounted survey rod was recorded in planar horizontal (x, y) and vertical (z) space while it crisscrossed back and forth up the channel and over the structures, beginning below the scour zone influence of the lowest straw bale check dam and ending above the trap zone influence of the highest straw bale check dam in the channel; once at the time of installation 26 Jun 2011 and again at the end of the field season 10 Oct 2011.

We processed the survey data of straw bale check dams using computer software. The survey data was imported into the surface topography software program, TGO, and surfaces were built for the base or pre-erosion event 26 Jun 2011 survey and the post-erosion events survey on 10 Oct 2011. The volume of trapped sediment behind straw bale check dams was calculated by subtracting the pre-erosion events 26 Jun 2011 surface from the post-erosion events 10 Oct 2011 surface. The method was reversed to determine scour below straw bale check dams, by subtracting the post-erosion events 10 Oct 2011 surface from the pre-erosion event 26 Jun 2011 surface. Two bulk densities (g cm^{-3}, lb ft^{-3}) were taken within the trapped deposit behind each straw bale check dam at depths of 0-5 cm (0-2 in) and ranging from 25-30 cm (10-12 in) to 35-40 cm (14-16 in), and one bulk density was taken in the channel bed scour zone (if scour was present) below each straw bale check dam. Trapped sediment volumes were converted to dry mass (Mg m^{-3} [t ac^{-1}]) from the mean oven-dried bulk density of samples taken in the respective trapped deposit, and oven-dried bulk densities taken in the channel scour zone were used to convert scour volumes to dry to mass (Mg m^{-3} [t ac^{-1}]) (Robichaud *et al*. 2008).

2.8 Ground cover

Ground cover was measured in each catchment at the site. Ground cover was measured in the spring and fall of 2011 and the fall of 2012 to quantify burn severity and vegetative regrowth in each catchment along one 40 m (131 ft) channel transect and two 40 m (131 ft) hillslope transects, using five 1 x 1 m (3 x 3 ft) plots evenly spaced at 0, 10, 20, 30, and 40 m (~ 0, 33, 66, 98, 131 ft). The plots had 100 points located at the junctions of a 10 x 10 cm (4 x 4 in) grid and the cover that fell below each point was chosen from a set of five variables (mineral soil, vegetation, litter, woody debris, rock) (Robichaud and Brown, 2002).

2.9 Channel cross-sections

We measured channel stability over time with channel cross-sections. Three to five channel cross-sections per catchment were established to measure channel stability or the degradation or aggradation of the channel bed over time (Keller, 1990). In each catchment, monumented cross-sections perpendicular to flow and spaced every 30 m (~98 ft) were set using # 4 rebar monuments on the river left (RL) and river right (RR) sides of the channel (Harrelson *et al.* 1994), above the maximum potential flow discharge height. An initial survey of channel cross-sections was done at the time of site installation, 26 Jun 2011, with a Global Positioning System (GPS) survey device that wirelessly communicated point location in X, Y, Z space to a reference receiver set up over a known rebar monument in the area (www.GPS.gov, accessed 14 Oct 2012). However, the GPS survey point data was not recorded on an exact line between the cross-section rebar monuments, which caused large uncertainties in cross-section heights in the steep gradient channels. Thus, the initial survey data were not used here it was not possible to accurately compare the initial survey data, 26 Jun 2011, to the two following surveys on 27 Jul 2011 and 6 May 2012, which fell exactly on a straight line between the rebar monuments. Any change in bed height from 27 Jul 2011 to 6 May 2012 was attributed only to sediment erosion events during the 2011 summer and fall because no channel or hillslope erosion occurred between 10 Oct 2011 and 6 May 2012, during the 2011-2012 winter.

The channel cross-sections were surveyed following methods described by Harrelson *et al.* (1994) on 27 Jul 2011 and 6 May 2012, relating vertical heights relative to the top of the RL and RR rebar monuments to cross-channel distances between RL and RR rebar monuments. Horizontal distance, x (+/- 0.05 m [+/- 0.16 ft]), was measured with a cloth tape measure strung taut between the RL and RR rebar monuments, always pulling the tape from 0 m on RL to the RR monument. Horizontal distance points were chosen at varying spacing lengths to provide higher resolution (+/- 0.10 m [+/- 0.33 ft]) in the channel thalwag or active channel flow area and lower resolution (m +/- 0.50 m [+/- 1.64 ft]) at hillslope points unaffected by flow. A metric scale stadia rod held plum measured the vertical height, y (+/- 0.01 m [+/- 0.03 ft]), from ground level up to a self-leveling laser level beam (PLS^3 Point to Point Laser, Pacific Laser Systems, San Rafael, CA) projected at a known height over the tops of the RR and RL rebar monuments. Vertical heights were measured at the same horizontal distances along a cross-section profile in both surveys to better detect any change in channel bed elevation between surveys.

Areas were calculated for each cross-section profile for both survey dates. First the cross-section measurements were standardized to the RL and RR rebar monuments by subtracting the instrument height or the height difference between the laser beam and the rebar monument top that sat higher in elevation, from the field data measurements. The trapezoidal areas between adjacent horizontal measurements and their corresponding vertical measurements, working from RL to RR, were determined and summed to find the total cross-section area (Area by Coordinate Method, www.nrcs.usda.gov/technical/eng_spreads.html, accessed 20 Aug 2012).

2.10 Straw bale check dam analysis

Trap efficiency (% of sediment) of straw bale check dams (SCDs) was analyzed for the first and second post-fire years in treated catchments. This is the cumulative mass per unit area trapped by straw bale check dams in a catchment compared to the potential catchment sediment yield or the total amount of sediment that would have eroded in the absence of the straw bale check dams. Trap efficiency was calculated for 2011 with Equation 1. Trap efficiency was calculated for 2012 by adding only the 2012 total annual sediment yield to the denominator in Equation 1. I calculated trap efficient using:

$$SCD\ Trap\ efficiency\ (\%) = \left(\frac{\Sigma\ SCD\ trapped\ mass\ (Mg\ ha^{-1})}{SCD\ Trapped\ mass\ (Mg\ ha^{-1}) + Total\ catchment\ sediment\ yield\ (Mg\ ha^{-1})} \right)$$

(Equation 1)

where, SCD trapped mass (Mg ha^{-1} [t ac^{-1}]) is the sum of sediment mass trapped behind all the straw bale check dams in a catchment per unit area (Mg ha^{-1} [t ac^{-1}]), at four straw bale check dams ha^{-1} (two ac^{-1}), and total catchment sediment yield is the annual sediment yield (Mg ha^{-1} yr^{-1} [t ac^{-1} yr^{-1}]) from the treated catchment for 2011 for first year trap efficiency, and the cumulative sediment yield from the catchment during 2011 and 2012 for second year trap efficiency. This equation assumes, in the absence of the straw bale check dams, 100 % of sediment trapped by the structures would have been transported, captured, and measured in the sediment retention structure at the catchment base. In Sevier Canyon, where the annual sediment erosion rates were limited by sediment retention structure failure or overtopping during large erosion events, trap efficiency provides a conservative estimate of straw bale check dam effectiveness.

The paired catchment sediment yield ratio was determined with the equation:

$$2011\ Paired\ catchment\ ratio = \left(\frac{SCD\ Trapped\ Mass\ (Mg\ ha^{-1}) +\ Treated\ catchment\ sediment\ yield\ (Mg\ ha^{-1})}{Control\ catchment\ sediment\ yield\ (Mg\ ha^{-1})} \right)$$

(Equation 2)

Sediment retention structure failures or overtopping did not allow for paired catchment ratios to be calculated in Sevier Canyon, thus only two paired catchments from Middle Canyon were used in 2011. Given the straw bale check dams were full at the start of 2012 the paired catchment ratio for 2012 pairs was:

$$2012\ Paired\ catchment\ ratio = \left(\frac{Treated\ catchment\ sediment\ yield\ (Mg\ ha^{-1})}{Control\ catchment\ sediment\ yield\ (Mg\ ha^{-1})}\right)$$

(Equation 3)

2.11 Particle size distribution analysis

We analyzed soil texture eroded from hillslopes and at catchment outlets. Soil was repeatedly sampled for the five events in each of the four catchments in Middle Canyon in 2011. Sands, silts, and clays or sediment fines ≤ 6.0 mm (0.2 in) were sampled in hillslope fences and sediment retention basins in each catchment to characterize undispersed soil texture of hillslope erosion and catchment sediment yields (Gee and Bauder, 1986). Samples were prepared by mixing the air dried soil bulk sample on a mixing tray for 2 to 3 minutes until homogeneous. Large samples were cut down to the appropriate size of ~70 g (0.15 lbs) by halving the sample twice into four equally sized piles. A coin toss was used to randomly select two piles for further reduction through mixing and quartering to the desired sample size. Excess soil was discard. The final 70 g (0.15 lbs) sample was halved, using the final randomly selected half of the soil bulk sample for the particle size analysis, and the other half was deposited in a labeled and sealed plastic bag for % organic matter content analysis and as a backup sample. The sample was transferred to a 0.075 mm square mesh sieve sitting in a plastic basin. De-ionized water was added to the basin only high enough to just contact the base of the soil sample resting on the screen and left for 20 minutes, or enough time for the sample to fully saturate by drawing water up through it. The sample was then wet sieved with de-ionized water through thirteen square sieves sized (mm): 25.400, 19.000, 12.700, 6.300, 4.750, 3.350, 2.000, 1.680, 1.000, 0.425, 0.250, 0.150, and 0.075. The retained mass of soil in each sieve was transferred to small pre-weighed tins and oven dried at 105 ^{o}C (221 ^{o}F). The tin mass was subtracted from the mass of the dried retained mass and tin mass to determine the retained dry mass for the particular sieve size. The mass passing 0.075 mm (3 x 10^{-3} in) was transferred to a 2000 mL (0.53 gal) beaker, de-ionized water was added to bring the water level to 2000 mL (0.53 gal), and the sample was left to sit overnight standardized the temperature of the water. A vacuum pipette analysis was performed on the sample to determine the final mass of silt and clay (Gee and Bauder, 1986). The sample mass for each particle size was converted to percent finer starting with the largest sieve at 100% and progressing to the smallest measurement of 0.004 mm (2 x 10^{-4} in). The mean D_{50} grain size where 50 % of the mass was finer than the given grain diameter was linearly interpolated where it fell between two sieve sizes using the equation:

$$D_{50} = 10\text{^}(\log(A) - \log(B) \bullet \left[\frac{50-\%B}{\%A-\%B}\right] + \log(B))$$

(Equation 4)

where, A is the sieve size in mm larger than 50% finer, B is the sieve in mm smaller than 50% finer, %A is the percent finer than sieve A, and %B is the percent finer than sieve B. Log transformation adjusts for the exponential distribution of % finer particle size (www.swrcb.ca.gov, accessed 15 Feb 2013).

2.12 Percent organic matter content

We determined the amount of organic matter eroded in the sediment. Percent organic matter was determined for all samples taken in Middle Canyon in 2011 using the additional mixed and split sample from the particle size analysis. A sample of ~10 g (~0.02 lbs) was weighed in grams to two significant figures in a pre-weighed crucible and placed into a combustion furnace at 450 ^{o}C (840 ^{o}F) and left overnight. The crucible and sample were weighed after all organic matter was combusted within the sample and the percent organic matter content was gravimetrically determined by subtracting the crucible weight from pre- and post-combustion sample mass.

2.13 Statistical analysis

Sediment yields were repeatedly measured longitudinally through time at catchment outlets. Sediment yields were analyzed on an annual basis to determine significance of treatment effectiveness in Middle Canyon for 2011 and in Sevier and Middle Canyons for 2012 (Ramsey and Schafer, 2002). Paired catchment data from Sevier Canyon in 2011 were not analyzed for treatment effectiveness due to missing or incomplete data from all three pairs. In 2011, five repeated measures and in 2012 four repeated measures were sampled on the response variable of area normalized sediment yields at varying temporal lengths or unequally spaced number of days between events at catchment outlets. Sediment yield were skewed right and unequally distributed. Therefore, values were log-normalized, but first in order to log transform zero values 0.002 Mg ha^{-1} (half the smallest recorded erosion rate) was added to all sample values prior to transformation.

I constructed both generalized least squares and mixed effects models to analyze paired catchment sediment yield data. For both these models, treatment type (control or treated) and paired catchment were used as explanatory variables, and fixed effects covariates believed to influence sediment yields were included thus creating a full model. The area normalized sediment yield samples were grouped or nested by catchment allowing for within group variance and were autocorrelated with a continuous time covariate, the number of days since fire containment that the event occurred (R Core Team, 2012; Zuur, 2009). The full model was run while holding the fixed effects equal, using the Restricted Maximum Likelihood Estimation (REML) to allow for comparison between 1) a generalized linear fixed effect model with no random structure, 2) a random intercept mixed effect model, and 3) a random slope and intercept mixed effect model (Zuur, 2009). The optimal model was chosen as having the lowest Akaike Information Criteria (AIC) value which measures the fit and adds penalties for the number of terms in the model (Zuur, 2009; Ramsey and Schafer 2009). The best fitting full model with no random or a random structure was visually inspected for normality using quantile-quantile plots and for equal variance with residual verse fitted plots.

I dropped covariates from the full model if they were not significant and kept them if they were significant. Backward selection tested for significant fixed effect covariates within the full model using maximum likelihood (ML) estimation. Each fixed effect covariate was tested for significance ($p < 0.05$) in the progressively pared down full model when a non-significant fixed effect was dropped (Zuur, 2009). The covariates tested for significance in the full model for straw bale check dam treatment effectiveness included: total event rainfall (mm), 10-min rainfall intensity (I_{10}) (mm hr^{-1}, in hr^{-1}), 30-min rainfall intensity (I_{30}) (mm hr^{-1}, in hr^{-1}), upslope and base of hillslope log-normalized erosion rates (Mg ha^{-1}, t ac^{-1}), channel and hillslope gradient (%), antecedent soil moisture or the sum of total rainfall (mm, in) that fell during the ten days leading up to the sediment yielding event, basin shape a unit-less relationship between catchment area and channel length, the interaction of year and upslope and year and base of slope log-normalized erosion rates, and mineral soil cover in the channel, on the left hillslope, and the right hillslope. Only one of the three rainfall variables were included in the model at a time after inspection of a full model that included multiple rainfall covariates showed high correlation < -0.75, indicating a lack in independence. Mineral soil was transformed by the arcsine square root for a more normal distribution (Lloret, 1998). The final model was inspected for a low AIC value, normality, equal variance, and the final model residuals were plotted against each explanatory variable to check for equal distribution in spread.

Sediment yields were analyzed on a yearly basis to determine the final best fitting statistical model. When the first and second post-fire years of Middle Canyon data were grouped, the interaction of year and log-normalized upslope erosion rates, and the interaction of year and log-normalized base of hillslope erosion rates had a significant effect on the model. This showed hillslope erosion rates were different between the first and second post-fire years, thus it was deemed appropriate to test for treatment significance on a yearly basis. The repeated measure samples of sediment yields in Middle Canyon during 2011 were modeled with no random intercept component which had the lowest AIC = 66.54 (df = 11) compared to the random intercept (AIC = 68.54) and the random intercept and slope (AIC = 72.54) model structures. This model was also logical choice because it had only four catchment groups making it difficult to accurately model the random variance component of nested catchment groups. The I_{30} rainfall intensity fixed covariate was a better fit in the full model with an AIC = 51.59 rather than I_{10} rainfall intensity with an AIC = 81.42. Non-significant fixed effect covariates of channel and hillslope gradient (%), antecedent soil moisture, basin shape, base of hillslope log-erosion rates, and mineral soil cover in the channel and on the left and right hillslopes were dropped from the full model, which left only I_{30} and upslope fence log-normalized sediment erosion rates as the only significant fixed effect parameters. However, when extracting confidence intervals the optimization algorithms running applied to run the

REML were having estimates of covariance parameters that did not meet the requirement of positive definiteness at all iterative steps resulting in an error (West *et al*. 2007). This was a result of the model being overparameterized due to the small sample size therefore, the lesser significant fixed effect covariate, log-upslope erosion rate, was dropped to leave I_{30} as the only fixed effect covariate. For the second post-fire year a random intercept model structure was the best fitting and was used to test for significance of treatment effect with log-normalized sediment yield data from Middle Canyon and Sevier Canyon data.

I used this same statistical modeling procedure with hillslope erosion rates, particle size distributions, and organic matter content. I tested if there was a significant difference between upslope and base of hillslope fence log-normalized erosion rates. I tested to determine if there were differences in mean D_{50} % finer particle size and organic matter content, between: upslope sediment to base of hillslope sediment; sediment at catchment outlets to hillslope sediment; and treated catchment sediment to control catchment sediment in Middle Canyon for 2011 and from 2012 sediment samples from Middle Canyon that have been processed at the time of this writing.

I statistically analyzed trap volumes of straw bale check dams verses channel gradient, and the stability of the channels. I used a linear regression model to determine if channel gradient had a significant effect on the mass of sediment trapped by straw bale check dams. A paired t-test statistic tested for a significant difference in the repeated measure of mean cross-sectional areas by catchment between the 27 Jul 2011 and 7 May 2012 survey dates.

I statistically analyzed mineral soil exposure and ground cover to help quantify burn severity at the site. Prior to statistical analysis of the five ground cover variables, they were square-root or arcsine square-root transformed (Lloret, 1998). For Spring and Fall 2011 and Fall

2012 ground cover, I used Welch Two Sample t-tests to assess significant difference between left and right hillslope transects and hillslope to channel transects for the five cover types. Ground cover of left and right hillslope transects (looking down the channel) were grouped prior to testing for a significant difference between hillslope ground cover and channel ground cover. A paired t-test was used to test for significant difference between repeated measures of: 2011 Spring v. 2011 Fall "hillslope v. hillslope" and "channel v. channel"; 2011 Fall to 2012 Fall "hillslope v. hillslope" and "channel v. channel". Left and right (looking down channel) hillslope vegetation transects were significantly different in the Fall of 2012; these transects were individually tested against Fall 2011 left and right hillslope transects. Statistical significance occurred if $\alpha \leq 0.05$. I used the software R v.2.15 for all statistical analysis (R Core Team, 2012).

3.0 Results

3.1 Rain events

The area experienced roughly average rainfall during the two study years. The mean monthly rainfall at the Snotel site from 1981 – 2012 during the months of April through September is 274 mm (10.8 in), making the total rainfall during the 2011 monitoring period similar to the mean rainfall for the area. Rain gauges A-B (elev. 2190 m, 7185 ft), C-D (elev. 2197 m, 7208 ft), and E-F (elev. 2236 m, 7336 ft) in Sevier Canyon, were 250 m (820 ft) apart with E-F located higher in the drainage than A-B (Figure 2). Rain gauges G-H (elev. 2104 m, 6902 ft) and I-J (elev. 2133 m, 6998 ft) in Middle Canyon were 120 m (390 ft) apart with G-H to the northeast and lower in the drainage than I-J.

In 2011 all the rain gauges received more rainfall, but had fewer high intensity rain events compared to the same period of monitoring during the 2012 monsoon season. From 10 Jun to 8 Oct 2011 the five rain gauges received 41 to 49 rain events and recorded 189 to 240 mm (7.4 to 9.4 in) of total rainfall (Table 3). During the same time period in 2011, the nearby Snotel site 4 to 4.5 km (2.5 to 2.8 mi) and at elevation 2783 m (9130 ft) had 34 days with rainfall and recorded 277 mm (11 in) of precipitation. From the 7 May to 26 Sep 2012, 129 to 164 mm (5.1 to 6.4 in) of rainfall occurred during the 32 to 47 events across the gauges, while during the same period in 2012 the Snotel site recorded 246 mm (9.7 in) of precipitation.

Table 3. Paired catchment rain gauge, rain gauge elevation (m [ft]), monitored year, storm count, and total precipitation (mm, in) for the 5 paired catchment rain gauges. The continuously monitored periods through the 2011 and 2012 monsoon seasons are 10 Jun - 8 Oct 2011, and 7 May - 27 Sep 2012.

Paired catchment rain gauge	Elevation (m [ft])	Year	No. of rain events	Total rainfall (mm [in])
A-B	2190 [7185]	2011	41	240 [9.4]
		2012	35	150 [5.9]
C-D	2197 [7208]	2011	42	199 [7.8]
		2012	36	144 [5.7]
E-F	2236 [7336]	2011	49	237 [9.3]
		2012	47	164 [6.4]
G-H	2104 [6902]	2011	41	189 [7.4]
		2012	32	129 [5.1]
I-J	2133 [6998]	2011	45	194 [7.6]
		2012	32	134 [5.3]

In 2011 Sevier Canyon received more high intensity rainfall events and precipitation compared to Middle Canyon. Between the three gauges in Sevier Canyon, they received two 5-year I_{10} return period events with the highest intensity of 16 mm (0.6 in) total 59 mm hr^{-1} (2.3 in hr^{-1}), three 2-year I_{10} return period events, and two 1-year I_{10} return period events (Table 4). In addition to these large events equal to or greater than a 1-year return period intensity, a range of 41 to 49 events occurred at the three gauges during the season, with the vast majority of events having very low intensities and rainfall amounts (rain gauge E-F: Figure 10).

Table 4. Rainfall event date and post-fire year, monitored catchment pair, rainfall amount (mm, in), I_{10} rainfall intensity (mm hr^{-1}, in hr^{-1}) and return period, I_{30} rainfall intensity (mm hr^{-1}, in hr^{-1}) and return period. Sevier Canyon rain gauges: A-B, C-D, E-F. Middle Canyon rain gauges: G-H, I-J.

Event date {post-fire year}	Pair	Rainfall (mm)	I_{10} (mm hr^{-1}) [return period]*	I_{30} (mm hr^{-1}) [return period]*	Rainfall (in)	I_{10} (in hr^{-1}) [return period]*	I_{30} (in hr^{-1}) [return period]*
15 Jun 2011 {1}	A-B	14	43 [2]	28 [2]	0.6	1.7 [2]	1.1 [2]
8 Jul 2011 {1}	A-B	15	58 [5]	20 [1]	0.6	2.3 [5]	0.8 [1]
	C-D	14	55 [2]	20 [1]	0.6	2.2 [2]	0.8 [1]
	E-F	16	59 [5]	21 [1]	0.6	2.3 [5]	0.8 [1]
	G-H	11	27	13	0.4	1.1	0.5
	I-J	12	32 [1]	14	0.5	1.3 [1]	0.5
27 Jul 2011 {1}	A-B	8	18	10	0.3	0.7	0.4
	C-D	7	17	9	0.3	0.7	0.4
	E-F	8	18	10	0.3	0.7	0.4
	G-H	8	20	9	0.3	0.8	0.4
	I-J	8	18	9	0.3	0.7	0.3
3 Aug 2011 {1}	A-B	26	37 [1]	15	1.0	1.4 [1]	0.6
	C-D	22	32 [1]	13	0.9	1.3 [1]	0.5
	E-F	26	43 [2]	15	1.0	1.7 [2]	0.6
	G-H	17	17	12	0.7	0.7	0.5
	I-J	18	18	12	0.7	0.7	0.5
25 Aug 2011 {1}	A-B	10	32 [1]	19 [1]	0.4	1.3 [1]	0.7 [1]
	C-D	8	29	16	0.3	1.1	0.6
	E-F	9	27	17	0.4	1.1	0.7
	G-H	8	27	15	0.3	1.1	0.6
	I-J	8	27	15	0.3	1.1	0.6
6 Oct 2011 {1}	A-B	37	14	10	1.5	0.5	0.4
	C-D	21	11	10	0.8	0.4	0.4
	E-F	22	11	9	0.9	0.4	0.4
	G-H	10	15	12	0.4	0.6	0.5
	I-J	12	18	16	0.5	0.7	0.6
16 Jul 2012 {2}	A-B	15	47 [2]	23 [1]	0.6	1.9 [2]	0.9 [1]
	C-D	16	52 [2]	24 [2]	0.6	2.0 [2]	1.0 [2]
	E-F	15	52 [2]	24 [2]	0.6	2.0 [2]	1.0 [2]
	G-H	24	53 [2]	38 [5]	0.9	2.1 [2]	1.5 [5]
	I-J	26	61 [5]	41 [5]	1.0	2.4 [5]	1.6 [5]
31 Jul 2012 {2}	I-J	11	32 [1]	15	0.4	1.3 [1]	0.6
1 Aug 2012 {2}	A-B	6	37 [1]	13	0.3	1.4 [1]	0.5
	C-D	7	38 [1]	13	0.3	1.5 [1]	0.5
	E-F	7	40 [1]	14	0.3	1.6 [1]	0.5
	G-H	8	49 [2]	17	0.3	1.9 [2]	0.7
	I-J	8	44 [2]	16	0.3	1.7 [2]	0.6
14 Aug 2012 {2}	A-B	16	49 [2]	22 [1]	0.6	1.9 [2]	0.9 [1]
	C-D	13	40 [1]	19 [1]	0.5	1.6 [1]	0.7 [1]
	E-F	14	40 [1]	19 [1]	0.6	1.6 [1]	0.8 [1]
	G-H	6	23	10	0.2	0.9	0.4
	I-J	10	26	15	0.4	1.0	0.6
24 Aug 2012 {2}	A-B	7	37 [1]	13	0.3	1.5 [1]	0.5
	C-D	7	41 [1]	14	0.3	1.6 [1]	0.6
	E-F	8	44 [2]	15	0.3	1.7 [2]	0.6
10 Sep 2012 {2}	A-B	9	35 [1]	12	0.4	1.4 [1]	0.5
	C-D	9	35 [1]	12	0.4	1.4 [1]	0.5
	E-F	8	27	10	0.3	1.1	0.4
	G-H	11	35 [1]	13	0.4	1.4 [1]	0.5
	I-J	11	37 [1]	14	0.4	1.4 [1]	0.5

*I_{10} and I_{30} intensity return periods from: <http://hdsc.nws.noaa.gov/hdsc/pfds/pfds_map_cont.html?bkmrk=ut>
Lat: 38.526°, Long: -112.411° Accessed: 20 Jan 2013.

During the summers rainfall often occurred in short bursts precipitated from cumulous clouds. Short duration high intensity rain events were common for large events ≥1-year return periods, with most of the 2-year or 5-year I_{10} intensity return period events only registering as a 1-year or less I_{30} intensity return period (Table 4). Middle Canyon had a similar number of rain events as Sevier Canyon; in 2011 however, it had much lower intensity events with only one 1-year I_{10} intensity event and no events having an intensity of a 1-year I_{30} return period.

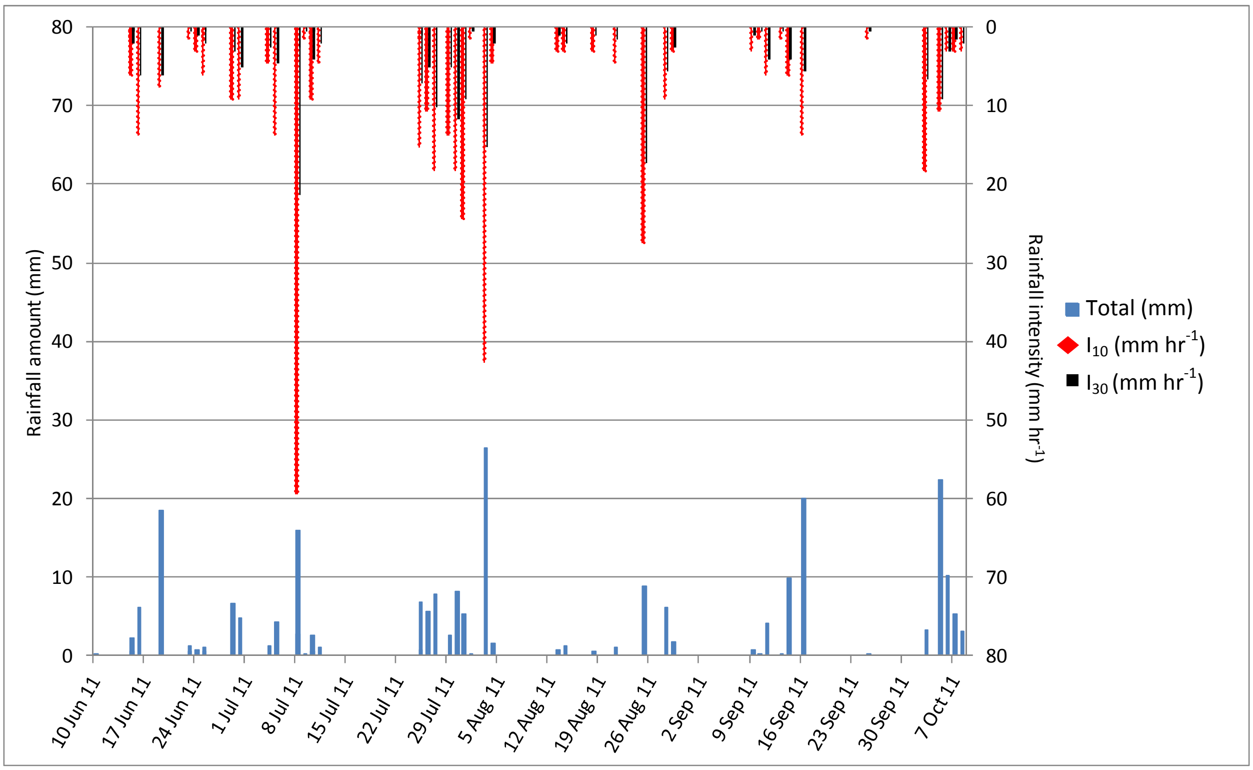

Figure 10. Rain events and corresponding 10-min (I_{10}) and 30-min (I_{30}) rainfall intensities from 10 Jun 2011 to 8 Oct 2011 for rain gauge E-F.

Sevier and Middle Canyons received less rainfall and fewer events during the 2012 monitoring season compared to the 2011 monitoring season (Table 3). However, both canyons received a greater number of events with intensities equal to or greater than a 1-year I_{10} return period (Table 4). Sevier Canyon received five 2-year I_{10} return period events, and nine 1-year I_{10} return period events, but unlike in 2011 it did not receive a 5-year I_{10} return period event (Figure

11). Middle Canyon received a far greater number of high intensity events in 2012 compared to 2011. The two pairs received a total of one 5-year I_{10} return period event with 26 mm (1.0 in) total and an intensity of 61 mm hr^{-1} (2.4 in hr^{-1}), three 2-year I_{10} return period events, and three 1-year I_{10} return period events. There were more I_{10} events that reached intensities equal to or greater than a 1-year return period than I_{30} events, and generally events had larger I_{10} return periods than I_{30} return periods. On 16 Jul 2012 the pair G-H received 24 mm (0.9 in) at an I_{30} of 38 mm hr^{-1} (1.5 in hr^{-1}) equivalent to a 5-year return period event with an I_{10} of 53 mm hr^{-1} (2.1 in hr^{-1}) equivalent to a 2-year I_{10} return period. This was the only event that had a larger I_{30} return period than an I_{10} return period during the two seasons of monitoring. Based on the events that produced sediment in the traps, an approximate threshold for detectable soil erosion was an I_{30} of 10 mm hr^{-1} (0.4 in hr^{-1}) or an I_{10} of 15 mm hr^{-1} (0.6 in hr^{-1}). The number of events exceeding the $I_{30} > 10$ mm hr^{-1} (0.4 in hr^{-1}) threshold ranged from eight to twelve events across the 5 rain gauges in 2011 and 2012.

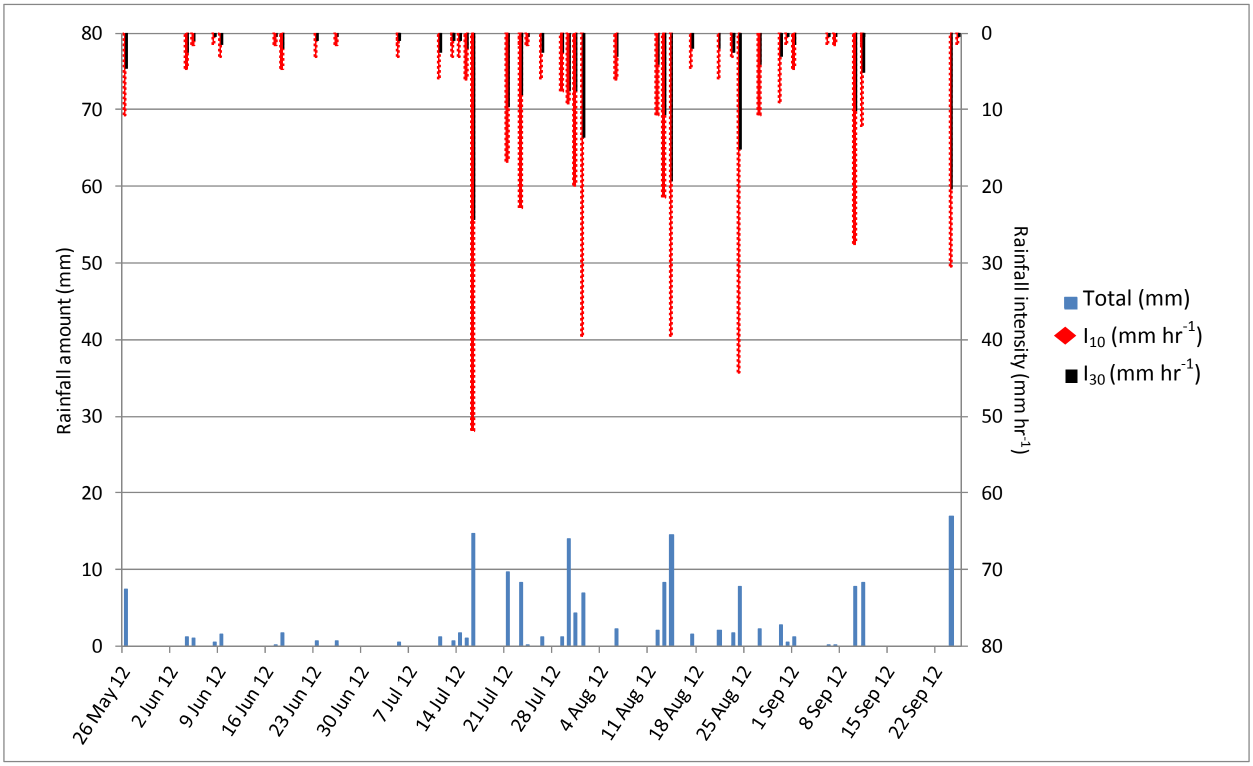

Figure 11. Rain events and corresponding 10-min (I_{10}) and 30-min (I_{30}) rainfall intensities from 7 May 2012 to 27 Sep 2012 for rain gauge E-F.

3.2 Paired catchment sediment yields

Large sediment yields from catchments were typical for 2011. The sediment retention structures were cleaned out five times during 2011 (Table 6 [a,b]). The cleanout in pair A-B on 26 Jul 2011 was the sum of two sediment yield events produced from a 2-year I_{30} return period event on 15 Jun and a 5-year I_{30} return period event on 8 Jul 2011. The I_{30} rainfall intensity was found to be the best predictor of sediment yields and I will refer to this intensity when addressing sediment yields. The rain event on 8 Jul 2011 caused sediment retention structures to be overwhelmed in 5 of the 10 catchments (all located in Sevier Canyon) causing sediment retention structures to fail or fill to the maximum storage capacity and be overtopped by sediment mobilized in the channel (Figure 12).

Figure 12. Sediment overwhelmed the upper sediment retention structure and caused the lower sediment retention structure to fail in catchment F from a high sediment yielding 16 mm (0.6 in) 1-year I_{30} 21 mm hr^{-1} (0.8 in hr^{-1}) return period event on 8 Jul 2011. Overwhelmed and failed fences occurred only in Sevier Canyon due to the high sediment erosion rates during 2011. The reliable sediment yield is the measurement of sediment in the upper fence shown here, and is a conservative estimate of the true sediment yield from the catchment during the rain event.

The second major sediment yield event on 3 Aug 2011 overwhelmed sediment retention structures in 3 of the 10 catchments, all of which were again located in Sevier Canyon. These two very large events accounted for 88 to 97 % of the reliable sediment yields from the six catchments in Sevier Canyon in 2011. The sediment yields from the other three events in 2011 that accounted for 3 to 12 % of the annual yield were small and did not overwhelm the sediment retention structures. Reliable sediment yields measured in overwhelmed sediment retention structures are conservative estimates limited by the size of sediment retention structure rather than the total sediment yield from the event. The sediment yields measured using the surveying technique had a relative uncertainty of ± 4% compared to the direct measurement of sediment yields by weighing buckets.

Table 5 a.) metric and b.) customary. Annual sediment erosion rates in 2011 and 2012 from treated and control catchment pairs.

a.

Catchment pair	2011 Mg ha^{-1} yr^{-1} (±Δ) Treated	2011 Mg ha^{-1} yr^{-1} (±Δ) Control	2012 Mg ha^{-1} yr^{-1} (±Δ) Treated	2012 Mg ha^{-1} yr^{-1} (±Δ) Control
A-B	19.53*	33.49 (±1.4)	13.12 (±0.6)	6.21 (±0.2)
C-D	20.62*	--†	6.80 (±0.3)	10.23 (±0.4)
E-F	25.71*	--†	11.22 (±0.4)	34.18 (±1.4)
G-H	4.33 (±0.1)	12.93 (±0.5)	3.74 (±0.1)	13.11 (±0.6)
I-J	3.54	19.27 (±0.5)	11.99 (±0.6)	17.14 (±0.5)

b.

Catchment pair	2011 t ac^{-1} yr^{-1} (±Δ) Treated	2011 t ac^{-1} yr^{-1} (±Δ) Control	2012 t ac^{-1} yr^{-1} (±Δ) Treated	2012 t ac^{-1} yr^{-1} (±Δ) Control
A-B	8.71*	14.94 (±0.6)	5.85 (±0.2)	2.77 (±0.1)
C-D	9.20*	--†	3.03 (±0.1)	4.56 (±0.2)
E-F	11.47*	--†	5.01 (±0.2)	15.25 (±0.6)
G-H	1.93 (±0.1)	5.77 (±0.2)	1.67 (±0.1)	5.85 (±0.2)
I-J	1.58	8.60 (±0.2)	5.35 (±0.2)	7.64 (±0.3)

* Total sediment yields were not captured during one or more rain events due to overtopping or partial failure of sediment retention structure. Yields measured when sediment retention structure was overwhelmed provides a conservative estimate of erosion rates. Absolute uncertainties not show for conservative sediment yield estimates.
† Annual sediment yield is not shown due to sediment retention structures total failure during a storm.
±Δ is absolute uncertainty associated with sediment yields measured using the surveying technique.

During 2011 Sevier Canyon experienced much greater sedimentation rates than Middle Canyon. In Sevier Canyon, we captured the total annual sediment only in control catchment B, which had an annual sediment yield of 33.49 (±1.4) Mg ha^{-1} yr^{-1} [14.94 (±0.6) t ac^{-1} yr^{-1}] (Table 5 a, b). The sediment retention structures in Sevier Canyon experienced partial or full failures during large events, making direct comparison of sediment yields from control and treated catchments difficult. Conservative annual sediment yields from the overwhelmed structures in catchments treated with 4 straw bale check dams ha^{-1} (2 ac^{-1}) were 19.53 Mg ha^{-1} yr^{-1} [8.71 t ac^{-1} yr^{-1}], 20.62 Mg ha^{-1} yr^{-1} [9.20 t ac^{-1} yr^{-1}], and 25.71 Mg ha^{-1} yr^{-1} [11.47 t ac^{-1} yr^{-1}] for catchments A, D, and F, respectively.

Table 6. Event date and corresponding paired catchment area normalized sediment yield **a.)** Mg ha^{-1}, **b.)** t ac^{-1}. The 8 Jul 2011 event overwhelmed or caused sediment retention structures to fail in five of the ten catchments, the other five held the total sediment yields. The 3 Aug 2011 event overwhelmed sediment retention structures in three of the ten catchments. Sediment yields for treated and control catchments A.1, C-D.2, E-F.3 are from reliable sediment yield data that is limited by retention structure storage capacity rather than true sediment yield. In Middle Canyon during 2011 is no significant difference between treated and control catchment sediment yields. In Sevier and Middle Canyons in 2012 there is no significant difference between treated and control catchment sediment yields.

a.

	Sevier Canyon						Middle Canyon			
Catchment pair	A	B	C	D	E	F	G	H	I	J
	Treated	Control	Control	Treated	Control	Treated	Treated	Control	Control	Treated
Event date [post-fire year]	Mg ha^{-1} (±Δ)		Mg ha^{-1} (±Δ)		Mg ha^{-1} (±Δ)		Mg ha^{-1} (±Δ)		Mg ha^{-1} (±Δ)	
8 Jul 2011 [1]	7.50*†	25.29 (±1.1)	Failed*	11.70*	Failed*	11.33*	2.55 (±0.1)	6.61 (±0.3)	11.39 (±0.5)	0.40
27 Jul 2011 [1]	0.08	0.02	0.02	0.04	0.03	0.09	0.01	0.00	0.00	0.01
3 Aug 2011 [1]	9.61*	7.30 (±0.3)	9.45	8.18	12.94*	12.97*	0.55	4.23 (±0.2)	5.45	1.43
25 Aug 2011 [1]	0.28	0.22	0.11	0.20	0.08	0.05	0.52	1.16	0.53	0.54
6 Oct 2011 [1]	2.06	0.66	1.03	0.50	1.16	1.27	0.70	0.93	1.90	1.16
16 Jul 2012 [2]	0.02	0.01	0.22	0.02	0.06	0.04	0.00	0.09	2.26	1.09
1 Aug 2012 [2]	1.51 (±0.1)	0.10	1.29	0.37	16.78 (±0.7)	1.40	3.17 (±0.1)	11.14 (±0.5)	12.38 (±0.5)	8.52 (±0.4)
14 Aug 2012 [2]	10.54 (±0.5)	5.72 (±0.2)	8.28 (±0.4)	6.04 (±0.3)	16.83 (±0.7)	9.29 (±0.4)	0.01	0.07	0.31	0.18
10 Sep 2012 [2]	1.05	0.38	0.43	0.38	0.51	0.49	0.56	1.81 (±0.1)	2.19 (±0.1)	2.20 (±0.1)

b.

	Sevier Canyon						Middle Canyon			
Catchment pair	A	B	C	D	E	F	G	H	I	J
	Treated	Control	Control	Treated	Control	Treated	Treated	Control	Control	Treated
Event date [post-fire year]	t ac^{-1} (±Δ)		t ac^{-1} (±Δ)		t ac^{-1} (±Δ)		t ac^{-1} (±Δ)		t ac^{-1} (±Δ)	
8 Jul 2011 [1]	3.34*†	11.28 (±0.5)	Failed*	5.22	Failed*	5.05*	1.14 (±0.1)	2.95 (±0.1)	5.08 (±0.2)	0.18
27 Jul 2011 [1]	0.04	0.01	0.01	0.02	0.01	0.04	0.01	0.01	0.00	0.00
3 Aug 2011 [1]	4.29*	3.25 (±0.1)	4.22	3.65	5.77*	5.78*	0.25	1.89 (±0.1)	2.43	0.64
25 Aug 2011 [1]	0.12	0.10	0.05	0.09	0.03	0.02	0.23	0.52	0.24	0.24
6 Oct 2011 [1]	0.92	0.29	0.46	0.22	0.52	0.57	0.31	0.41	0.85	0.52
16 Jul 2012 [2]	0.01	0.01	0.10	0.01	0.03	0.02	0.00	0.04	1.01	0.49
1 Aug 2012 [2]	0.68	0.04	0.58	0.17	7.49 (±0.3)	0.62	1.41 (±0.1)	4.97 (±0.2)	5.52 (±0.2)	3.80 (±0.2)
14 Aug 2012 [2]	4.70 (±0.2)	2.55 (±0.1)	3.69 (±0.2)	2.69 (±0.1)	7.51 (±0.3)	4.14 (±0.2)	0.00	0.03	0.14	0.08
10 Sep 2012 [2]	0.47	0.17	0.19	0.17	0.23	0.22	0.25	0.81	0.97	0.98

±Δ is absolute uncertainty of sediment yields measured using the survey technique; (±) bracket not shown if absolute uncertainty is < 0.05 or significant figure is equal to ±0.

*Did not capture total sediment yield from event; either one silt fence failed and one silt fence held to give a conservative value, or both sediment fences "Failed" and no sediment was captured. If the survey technique was used to measure these sediment yields the error is not given.

†Area normalized sediment yield is sediment accumulation from a 2-year I_{30} return period event on 15 Jun 2011 and a 1-year I_{30} return period event on 8 Jul 2011 because no cleanout of sediment retention structures occurred between the two dates.

The 2011 sediment yields in Middle Canyon's paired catchments G-H and I-J were much less than those in Sevier Canyon, allowing the sediment retention structures to capture the total annual sediment yield (Figure 13). In Middle Canyon the mean annual sediment yield from catchments treated with 4 straw bale check dams ha^{-1} (2 SCDs ac^{-1}) was 3.93 (±0.1) Mg ha^{-1} [1.75 t ac^{-1} yr^{-1}] and 16.10 (±0.5) Mg ha^{-1} [7.18 (±0.2) t ac^{-1} yr^{-1}] from control catchments or a 76 (±4) % reduction in sediment yield rates. Middle Canyon pairs G-H and I-J had a mean treated:control paired catchment ratio of 0.51 (±0.02): 1 (Table 9).

Figure 13. Total sediment yield captured by sediment retention structures in catchment I.5 from an event on 8 July 2011. Lower sediment yields in Middle Canyon allowed total annual sediment yields to be captured during the 2011 monitored period.

In Middle Canyon during 2011 there is no significant difference in sediment yields between catchments treated with straw bale check dams and those left untreated with a t-statistic -1.296 (df = 18, p = 0.216). The modeled slope for a treated catchment was -1.00 with 95% confidence intervals of -2.665 to 0.657. The I_{30} return period is a significant fixed effect covariate t = 2.79 (p = 0.015), having a slope of 0.513 and 95% confidence intervals of 0.119 to 0.908 (Table 7a.). The paired catchment ratios in Middle Canyon during 2011 were 0.36 (±0.01) to 0.67 (±0.03) with a mean of 0.51 (±0.02) (Table 9).

Table 7. Significance of straw bale check dam treatment in paired catchments using: a) a generalized least squares model for 2011 Middle Canyon catchment sediment yields, b) a random intercept model for 2012 Middle Canyon and Sevier Canyon catchment sediment yields.

a. 2011 Middle Canyon catchment sediment yields
Generalized least squares model

Variable	Slope value	Standard error	t-value	p-value	95 % Confidence Intervals lower	upper
Intercept	-1.314	4.257	-0.309	0.762	-10.446	7.817
pair	-1.121	0.779	-1.439	0.172	-2.793	0.550
treatment: Treated	-1.004	0.774	-1.297	0.216	-2.665	0.657
I_{30}	0.513	0.184	2.790	0.015	0.119	0.908

Degrees of freedom = 18
Residual standard error = 1.448

b. 2012 Middle Canyon and Sevier Canyon catchment sediment yields
Random intercept model

Variable	Slope value	Standard error	degrees of freedom	t-value	p-value	95 % Confidence Intervals lower	upper
(Intercept)	0.392	0.808	28	0.485	0.632	-1.264	2.047
pair	0.213	0.196	7	1.088	0.313	-0.250	0.676
treatment: Treated	-0.565	0.549	7	-1.029	0.338	-1.862	0.732
I_{30}	-0.098	0.025	28	-3.858	0.001	-0.150	0.046
log(upslope erosion)	2.390	0.284	28	8.410	0.000	1.808	2.972

No sediment retention structures failed or overtopped during 2012, allowing accurate measurement of annual sediment yields in all ten catchments. The sediment retention structures were cleaned out four times during the 2012 summer monsoon season. Two of the four events in Sevier Canyon accounted for 92 to 98% of the total 2012 annual sediment yields from the six catchments. The 2012 annual sediment yields from Sevier Canyon treated catchments ranged from 6.80 (±0.3) to 13.12 (±0.6) Mg ha^{-1} [3.03 (±0.1) to 5.85 (±0.2) t ac^{-1}] (Table 5 [a,b]), and the range of annual sediment yields from control catchments was 6.21 (±0.2) to 34.80 (±1.4) Mg ha^{-1} [2.77 (±0.1) to 15.25 (±0.6) t ac^{-1}]. The largest sediment yields occurred during the 14 Aug 2012 rain event, but control catchment E also had a significant sediment yield during the 1 Aug 2012 event (Table 6 [a,b]).

In Middle Canyon during 2012, both the control catchments in pairs G-H and I-J had larger annual sediment yields than treated catchments within the pairs. In paired catchment G-H, treated catchment G had an annual sediment yield of 3.74 (±0.1) Mg ha^{-1} [1.67 (±0.1) t ac^{-1}] (Table 5 [a,b]), and the control catchment H had an annual sediment yield of 13.3 (±0.6) Mg ha^{-1} [5.85 (±0.2) t ac^{-1}]. The 2012 sediment yields from paired catchment I-J were 11.99 (±0.6) Mg ha^{-1} [5.35 (±0.2) t ac^{-1}] in treated catchment J and 17.14 (±0.5) Mg ha^{-1} [7.64 (±0.3) t ac^{-1}] in control catchment I. The event on 16 Jul 2012 had a 5-year return period I_{30} intensity in pairs G-H and I-J and produced 0 to 13 % of the annual 2012 sediment yields in the four Middle Canyon catchments. While the 31 Jul 2012 event in I-J and the 1 Aug 2012 event in G-H and I-J with I_{30} intensities less than a 1-year return period produced 71 to 85% of the total 2012 annual sediment yield.

There was no significant difference $t = -1.029$ ($df = 7$, $p = 0.338$) in sediment yields between treated and control catchments in Sevier and Middle Canyons during the second-post fire year in 2012 (Table 7b.). The modeled slope of treated catchment sediment yields is -0.565 compared to control catchment yields with 95% confidence intervals of -1.862 to 0.732. The I_{30} rainfall intensity is a significant covariate t = -3.858 ($p < 0.001$), with a modeled slope of -0.098 and 95% confidence intervals of -0.150 to -0.046. Log-upslope hillslope erosion is also a significant covariate t = 8.410 (p = 0.000), with a modeled slope of 2.390 and 95% confidence intervals of 1.81 to 2.97. The 2012 paired catchment ratios for the five pairs in Sevier and Middle Canyons ranged from 0.29 (±0.01):1 to 2.11 (±0.01):1 with a mean of 0.82 (±0.2):1, and a median of 0.67 (±0.1):1 (Table 9).

3.3 Hillslope erosion

In 2011 the annual hillslope erosion rates were generally higher than control catchment sediment yield rates (Table 7). The majority (92 %) of annual erosion rates were from cleanouts early in the season from the 8 Jul and 3 Aug events (Table 8). On one occasion in 2011, the erosion rates in paired catchment A-B were the sum of eroded sediment yields from two large rain events with intensities equal to or greater than a 1-year I_{10} return period intensities.

Table 8. Annual hillslope erosion rates (Mg ha^{-1} yr^{-1} [t ac^{-1} yr^{-1}]) for 2011 and 2012, from upslope and base of hillslope fences by catchment pair.

		2011 (Mg ha^{-1} yr^{-1} [t ac^{-1} yr^{-1}])		2012 (Mg ha^{-1} yr^{-1} [t ac^{-1} yr^{-1}])	
	Hillslope fence pair	Upslope	Base of hillslope	Upslope	Base of hillslope
Sevier	A-B	103.1 [46.0]	120.1 [53.6]*	25.2 [11.2]	47.3 [21.1]
Canyon	C-D	22.2 [9.9]	25.6 [11.4]	14.2 [6.3]	9.9 [4.4]
	E-F	32.2 [14.4]	61.9 [27.6]*	11.0 [4.9]	44.8 [20.0]
Middle	G-H	7.2 [3.2]	0.1 [0.1]	6.8 [3.0]	0.5 [0.2]
Canyon	I-J	35.8 [16.0]	24.7 [11.0]	77.6 [34.6]	19.1 [8.5]

* Hillslope fence was overwhelmed by sediment erosion during one or more rain events. The erosion rate displayed is a conservative estimate of the true erosion rate.

Overall hillslope fences captured the very high erosion rates during 2011, with only a couple fences being overwhelmed on a few occasions. The fences at the base of hillslopes in catchments B and E were overwhelmed by sediment during the 8 Jul 2011 rain event, and hillslope fence E was overwhelmed again during the 3 Aug 2011 event. The reliable erosion rates from these cleanouts are conservative values that reflect the maximum storage capacity of the hillslope fence rather than the true hillslope erosion rate. Rocks and debris were detached by animal movement above hillslope fences A and J and deposited in the sediment fences before the last cleanout in Oct 2011. This sediment was not measured; however the annual hillslope erosion rates were probably not too affected by this because the amount of sediment (< 6 kg [13 lb]) discarded from the fences was only ~2 to 3 % of the total annual erosion rate. I_{10} rainfall intensity was the best predictor of hillslope erosion and I will refer to this intensity when discussing hillslope erosion rates.

Table 9. Hillslope erosion rates (Mg ha^{-1} [t ac^{-1}]) in Middle and Sevier Canyons, with catchment pair, event date and post-fire year, and fence location.

	Sevier Canyon						Middle Canyon			
Catchment pair	A	B	C	D	E	F	G	H	I	J
Fence location	upslope	base of slope	upslope	base of slope	upslope	base of slope	upslope	base of slope	upslope	base of slope
Event date {post-fire year}	(Mg ha^{-1} [t ac^{-1}])		(Mg ha^{-1} [t ac^{-1}])		(Mg ha^{-1} [t ac^{-1}])		(Mg ha^{-1} [t ac^{-1}])		(Mg ha^{-1} [t ac^{-1}])	
8 Jul 2011 {1}	87.6 [39.1]	84.3 [37.6]*	12.7 [5.7]	18.3 [8.2]	31.1 [13.9]*	22.9 [10.3]	5.1 [2.3]	0	12.1 [5.4]	23 [10.3]
27 Jul 2011 {1}	2.4 [1.1]	0.6 [0.3]	2.0 [0.9]	0.6 [0.3]	0.2 [0.1]	0.7 [0.4]	0.1 [0.1]	n/a	2.9 [1.3]	0.9 [0.4]
3 Aug 2011 {1}	12.4 [5.5]	33.1 [14.8]	6.1 [2.7]	6.1 [2.7]	24.8 [11.1]*	7.9 [3.5]	0.9 [0.4]	0	4.3 [1.9]	7.5 [3.4]
25 Aug 2011 {1}	0.6 [0.3]	0	0.8 [0.4]	0.1 [0.1]	0.1 [0.1]	0.1 [0.1]	0.5 [0.3]	0	4.3 [1.9]	4.2 [1.9]
6 Oct 2011 {1}	n/a	1.7 [0.8]	0.4 [0.2]	0.3 [2.4]	5.3 [2.4]	0.2 [0.1]	0.2 [0.1]	0	0.9 [0.4]	n/a
16 Jul 2012 {2}	n/a	3.4 [1.5]	1.1 [0.5]	0.3 [0.2]	0	n/a	0.1 [0.1]	0	11.4 [5.1]	25.5 [11.4]
1 Aug 2012 {2}	2.0 [0.9]	4.4 [2.0]	2.3 [1.1]	0.7 [0.3]	20.6 [9.2]	3.2 [1.5]	5.9 [2.7]	0.2 [0.1]	4.4 [2.0]	42.7 [19.1]
14 Aug 2012 {2}	22.6 [10.1]	38.6 [17.2]	9.5 [4.3]	8.1 [3.7]	23.7 [10.6]	7.4 [3.3]	0	0	0.3 [0.2]	0.3 [0.1]
10 Sep 2012 {2}	0.4 [0.2]	0.8 [0.4]	1.0 [0.5]	0.6 [0.3]	0.1 [0.1]	0.2 [0.1]	0.5 [0.3]	0.1 [0]	2.7 [1.2]	8.8 [3.9]

*Hillslope fence overwhelmed by sediment erosion during event.
n/a: animal disturbance introduced sediment into the fence it was not measured here.

The early season 8 Jul 2012 and 3 Aug 2012 events accounted for 95 % of the annual erosion rate in Sevier Canyon for upslope fences A, C, and F and the slope length fences B, D, and E (Table 8). The 2011 mean annual upslope erosion rate in Sevier Canyon was 52.6 Mg ha^{-1} [23.5 t ac^{-1}] with a range of 22.2 to 103.1 Mg ha^{-1} [9.9 to 46.0 t ac^{-1}] and the mean annual hillslope erosion rate for fences at the base of hillslopes was 69.2 Mg ha^{-1} [30.9 t ac^{-1}] with a range of 25.6 to 120.1 Mg ha^{-1} [11.4 to 56.3 t ac^{-1}].

In Middle Canyon the 2011 annual hilllslope erosion rates were much less than in Sevier Canyon, allowing hillslope fences to capture the total erosion during each event (Figure 14). In Middle Canyon the erosion rates varied widely for upslope fences of 7.2 and 35.8 Mg ha^{-1} [3.2 and 16.0 t ac^{-1}] and for base of hillslope fences of 0.1 and 24.7 Mg ha^{-1} [0.1 and 11.0 t ac^{-1}]. The first cleanout on 26 Jul 2011 accounted for 65 % of annual erosion in upslope fences and 49 % of annual erosion for base of hillslope fences. Mean hillslope erosion rates were higher than catchment sediment yields in Middle Canyon. The representative mean annual hillslope erosion rate of the combined four upslope and base of hillslope fences was 17.0 Mg ha^{-1} [7.6 t ac^{-1}], or 5 % higher than the representative mean annual sediment yields from control catchments H and I of 16.1 Mg ha^{-1} [7.2 t ac^{-1}].

Figure 14. Hillslope fence G captured total sediment yield from an 11 mm (0.4 in) 27 mm hr^{-1} (1.1 in hr^{-1}) rain event on 8 Jul 2011 that was less than a 1-year I_{10} recurrence interval event.

A random intercept mixed effect model was the best fitting random component for log-normalized hillslope erosion rates during 2011. Log-normalized hillslope erosion rates for upslope fences and base of hillslope fences for Sevier and Middle Canyons are not significantly different $t = 0.626$ ($df = 7$, $p = 0.55$). The fixed effect covariate I_{10} return period rainfall intensity fit the full model better than the I_{30} return period rainfall intensity ($df = 8$; I_{10} AIC = 172.12; I_{30} AIC = 190.83). Ten-minute intensity is a significant covariate $t = 6.58$ ($df = 35$, $p < 0.001$), and antecedent soil moisture is also a significant fixed effect covariate $t = 4.34$ ($df = 35$, $p < 0.001$). The modeled slope for the upper fence is 0.672 (95% CI; lower = -1.86, upper = 3.21). Ten-minute rainfall intensity has a slope of 0.08 (95% CI; lower = 0.05, upper = 0.10), and antecedent moisture has a slope of 0.06 (95% CI; lower = 0.03, upper = 0.09).

Annual hilllslope erosion rates in 2012 were generally less than 2011 rates for all hillslope fences, except for upslope fence J in Middle Canyon (Table 8). Upslope hillslope fences in Sevier Canyon had annual erosion rates range from 11.0 to 25.2 Mg ha^{-1} [4.9 to 11.2 t ac^{-1}], and base of hillslope fences had erosion rates range from 9.9 to 47.3 Mg ha^{-1} [4.4 to 21.1 t ac^{-1}]. Excluding hillslope fence E, 67 to 86 % of annual hillslope erosion in the five Sevier Canyon fences occurred during the 14 Aug 2012 event. The events on 1 Aug 2012 and 12 Aug 2012 in base of hillslope fence E accounted for 99 % of the annual hillslope erosion.

In 2012 Middle Canyon had a large range for annual upslope fence erosion rates. The two upslope fences measured 6.8 and 77.6 Mg ha^{-1} [3.0 to 34.6 t ac^{-1}] of sediment erosion, while the range for base of hillslope fences was 0.5 to 19.1 Mg ha^{-1} [0.2 to 8.5 t ac^{-1}]. The 16 Jul 2012 and 1 Aug 2012 events contributed 66 to 90 % to the annual sediment erosion rates. 2011 and 2012 hillslope sediment erosion rates vs. I_{10} rainfall intensities shows erosion rates increase with higher intensity events (Figure 15).

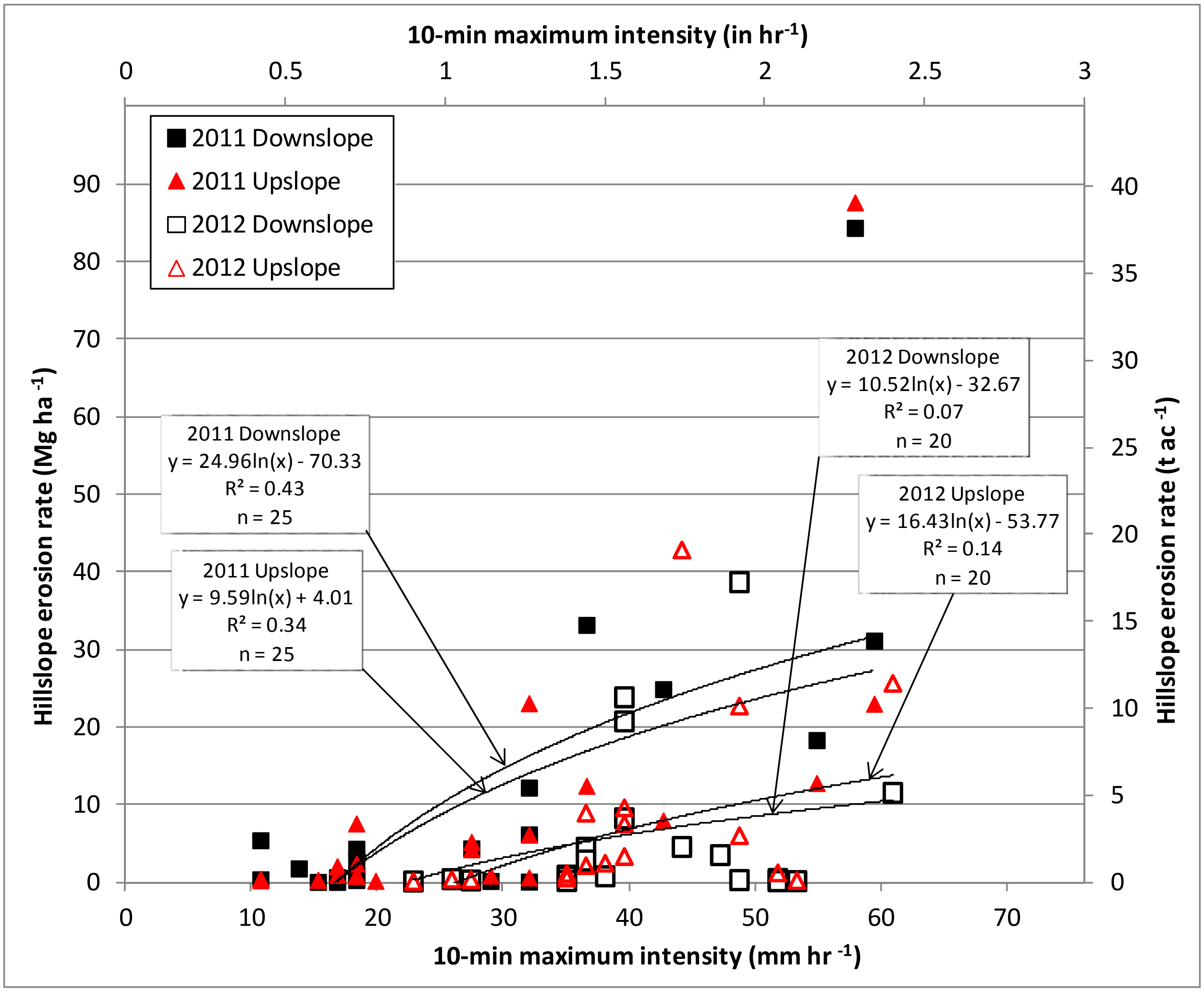

Figure 15. The relationship between 10-min maximum rainfall intensity (mm hr^{-1}, in hr^{-1}) and base of hillslope (downslope; squares) and upslope (triangles) erosion rates by year (2011 closed symbols, 2012 open symbols).

A random intercept mixed effects model was the most appropriate random structure for 2012 log-normalized upslope and base of hillslope erosion rates. There is no significant difference t = 0.650 (df = 7, p = 0.537) in hillslope erosion rates for upslope and base of hillslope erosion rates for Sevier and Middle Canyons during 2012. I_{10} rainfall intensity was a better fitting covariate than I_{30} rainfall intensity (I_{10}, AIC = 159.93, I_{30}, AIC = 164.73). The I_{10} rainfall intensity is a significant covariate in the model t = 2.86 (df = 26, p = 0.008), and antecedent soil moisture is also a significant covariate t= 2.29 (df = 26, p = 0.03). The modeled slope for the upper hillslope fence is 0.475 (95% CI: lower = -1.14, upper = 2.06). The modeled slope for the covariate I_{10} is 0.08 (95% CI; lower = 0.03, upper = 0.13), and the modeled slope for antecedent soil moisture is 0.037 (95% CI; lower = 0.006, upper = 0.068).

Upslope and base of hillslope erosion rates were grouped by year because of the lack of significance between fence plots and are tested for a significant difference by year. There is a significant difference $t = -2.90$ ($df = 72$, $p = 0.005$) between log-normalized hillslope erosion rates in 2011 compared to 2012. Ten minute intensity rainfall is a better fit in the model than I_{30} (I_{10}, AIC = 311.20, I_{30}, AIC = 336.31). The I_{10} rainfall intensity is a significant fixed effect covariate $t = 6.91$ ($df = 72$, $p < 0.001$), and antecedent soil moisture is a significant fixed effect $t = 4.53$ ($df = 72$, $p < 0.001$) in the model. The modeled slope for the response year is -0.89 (95% CI; lower = -1.51, upper = -0.28). The modeled slope for I_{10} rainfall intensity is 0.078 (95% CI; lower = 0.06, upper = 0.10), and the modeled slope for antecedent soil moisture is 0.04 (95% CI; lower = 0.03, upper = 0.06).

3.4 Straw bale check dams

All catchments were treated at a rate of 4 straw bale check dams per ha^{-1} (2 ac^{-1}) at the beginning of 2011 and were filled with sediment early in the year. Catchments A, D, and F in Sevier Canyon had areas of ~0.3 to 0.6 ha (~0.7 to 1.4 ac) were treated with two straw bale check dams per catchment. In Middle Canyon, treated catchment G with an area of ~1.4 ha (~3.3 ac) had six straw bale check dams and catchment J with an area of ~0.7 ha (~1.7 ac) was treated with three straw bale check dams. All the straw bale check dams in Sevier Canyon filled to sediment holding capacity or the height of trapped sediment behind the straw bale check dam was equal to the spillway height and overtopped during the 2-year and 1-year I_{30} intensity return period event on 15 Jun 2011 and 8 Jul 2011 in catchment A respectively. The SCDs filled to capacity during the 1-year I_{30} intensity return period event on 8 Jul 2011 in catchments D and F (Figure 16).

Figure 16. Channel F treated with 2 straw bale check dams that filled to capacity and were overwhelmed by a 16 mm (0.6 in), 21 mm hr^{-1} (0.8 in hr^{-1}) I_{30} intensity 1-year return period event. The majority of sediment trapped by straw bale check dams was a sandy loam, but large woody debris and cobble mobilized by overland flow were also trapped. Photo looks down channel.

The 8 Jul 2011 event was less than a 1-year I_{30} intensity return period in Middle Canyon and it filled the majority of straw bale check dams to their maximum sediment holding capacity. In catchment G the event filled three of the six straw bale check dams to their sediment holding capacity (Figure 17), and in catchment J the event filled two of the three straw bale check dams to maximum sediment holding capacity.

Figure 17. Straw bale check dam in catchment G filled to capacity during a 11 mm (0.4 in), 13 mm hr^{-1} (0.5 in hr^{-1}) I_{30} intensity rain event on 8 Jul 2011, which is less than a 1-year return period I_{30} intensity event. Spillway rocks to reduce scour were undisturbed by flow. Photo looks up-channel.

Even though structures were left empty after a sediment event had occurred, very fine silt and clay sediment was still transported out of the catchment. In catchment G, the sediment retention structure captured 2.55 (±0.1) Mg ha^{-1} [1.14 (± 0.1) t ac^{-1}] of sediment that was transported past three empty or partially full SCDs that sat lowest in the channel, closest to the catchment outlet (Figure 18). In catchment J, the sediment retention structure captured 0.40 Mg ha^{-1} [0.18 t ac^{-1}] of sediment that was transported past an empty SCD sitting the lowest in the channel and closest to the catchment outlet. These remaining partially full structures in treated catchments G and J were filled to their maximum sediment holding capacity during the 3 Aug 2011 event that had less than a 1-year I_{30} return period intensity.

Figure 18. In treated catchment G, this sediment retention sturcture captured 2.55 Mg of sediment that was transported past three empty or partially full straw bale check dams that sat lowest in the channel closest to the catchment outlet, during the 8 Jul 2011 storm.

All straw bale check dams trapped a net positive amount of sediment because no structures failed or were displaced from where they were installed. The mean volume of sediment trapped by straw bale check dams was 1.00 m^3 (35.2 ft^3) with a range of 0.29 to 2.22 m^3 (10.4 to 78.5 ft^3) (Table 9). The mean mass of sediment trapped by the straw bale check dams was 1.27 Mg (1.40 t) per structure with a range of 0.35 to 3.16 Mg (0.38 to 3.48 t) with an average bulk density of 9.86 Mg m^{-3} (616 lbs ft^3) (Figure 19). The mean mass of sediment trapped per catchment-area at a treatment rate of four straw bale check dams ha^{-1} (2 SCDs ac^{-1}) was 5.87 Mg ha^{-1} (2.62 t ac^{-1}) with a range of 3.40 to 10.48 Mg ha^{-1} (1.52 to 4.68 t ac^{-1}).

a)

b)

Figure 19. a) empty straw bale check dam at time of installation. **b)** same straw bale check dam filled to maximum sediment holding capacity with the height of trapped sediment equal to the spillway height. The volume of sediment trapped by this straw bale check dam was 0.64 m^3 (22.7 ft^3) or a trapped mass of 0.79 Mg (0.87 t). Below the spillway 0.04 m^3 (1.4ft^3) of sediment was scoured by flow or 0.05 Mg (0.05 t) of scoured mass.

Table 10. Straw bale check dam (SCD) name and catchment pair grouped by canyon, the channel gradient (%), volume (m^3 [ft^3]) and mass (average bulk density of 0.986 Mg m^{-3}) (Mg [t]) of sediment trapped behind individual straw bale check dams filled to capacity, mass of sediment trapped by straw bale check dams filled to capacity per unit-area when treated at a rate of four ha^{-1} (two ac^{-1}), volume (m^3 [ft^3]) and mass (average channel bulk density of 1.208 Mg m^{-3}) (Mg [t]) of sediment scoured below the spillway at the base of individual straw bale check dams filled to capacity, the net sediment storage effect of straw bale check dams filled to capacity (Mg [t]), and the mass sediment stored by straw bale check dams filled to capacity per unit area (Mg ha^{-1} [t ac^{-1}]) when treated at the rate of four straw bale check dams ha^{-1} (two straw bale check dams ac^{-1}), straw bale check dam trap efficiencies in 2011 and in 2012 (Equation 1), and 2011 paired catchment ratio (Equation 2) and 2012 paired catchment ratio (Equation 3).

	Catchment and straw bale check dam number	Channel gradient	Total volume of sediment trapped by SCD (m^3 [ft^3])	Total mass of sediment trapped by SCD (Mg [t])	Total mass of sediment trapped per unit-area (Mg ha^{-1} [t ac^{-1}])	Total volume of channel-bed scoured below SCD spillway (m^3 [ft^3])	Total mass of channel-bed scoured below SCD spillway (Mg [t])	Total mass of sediment scoured below SCD per unit-area (Mg ha^{-1} [t ac^{-1}])	Net effect of SCD on sediment: Trapped mass - scoured mass (Mg [t])	Net effect of SCD on sediment per unit-area: Trapped mass - scoured mass (Mg ha^{-1} [t ac^{-1}])	2011 Trap efficiency	2012 Trap efficiency	Treated:Control 2011 paired catchment ratio (±Δ)	Treated:Control 2012 paired catchment ratio (±Δ)
Sevier Canyon	A1	17%	2.10 [74.3]	2.57 [2.84]	10.48 [4.68]	0.08 [2.9]	0.10 [0.11]	0.39 [0.17]	2.48 [2.73]	10.09 [4.50]	35%*	24%*	--	2.11 (±0.16)
	A2		2.22 [78.5]	3.16 [3.48]		0.10 [3.6]	0.11 [0.12]		3.05 [3.36]					
	D1	49%	0.35 [12.4]	0.51 [0.57]	3.45 [1.54]	0.01 [0.3]	0.01 [0.01]	0.51 [0.23]	0.50 [0.55]	2.94 [1.31]	14%*	11%*	--	0.67 (±0.06)
	D2		0.29 [10.4]	0.43 [0.47]		0.09 [3.2]	0.13 [0.14]		0.30 [0.33]					
	F1	32%	1.67 [59.1]	2.52 [2.78]	7.73 [3.54]	0.05 [1.8]	0.06 [0.07]	0.23 [0.10]	2.46 [2.71]	7.50 [3.35]	23%*	17%*	--	0.33 (±0.03)
	F2		1.19 [42.0]	1.74 [1.91]		0.06 [2.1]	0.07 [0.07]		1.67 [1.84]					
Middle Canyon	G1	15%	0.56 [19.9]	0.47 [0.51]	4.31 [1.92]	0.07 [2.5]	0.09 [0.09]	0.06 [0.03]	0.38 [0.42]	4.24 [1.89]	50%	35%	0.67 (±0.03)	0.29 (±0.02)
	G2		1.59 [56.1]	1.71 [1.88]		n/a	n/a		1.71 [1.88]					
	G3		0.40 [14.1]	0.35 [0.38]		n/a	n/a		0.35 [0.38]					
	G4		1.37 [48.5]	1.66 [1.83]		n/a	n/a		1.66 [1.83]					
	G5		0.91 [32.0]	1.21 [1.33]		n/a	n/a		1.21 [1.33]					
	G6		0.32 [11.2]	0.43 [0.48]		n/a	n/a		0.43 [0.48]					
	J1	23%	0.44 [15.4]	0.49 [0.54]	3.40 [1.52]	0.03 [1.1]	0.04 [0.04]	0.17 [0.08]	0.45 [0.50]	3.23 [1.44]	49%	18%	0.36 (±0.01)	0.70 (±0.05)
	J2		0.90 [31.8]	1.00 [1.11]		0.02 [0.8]	0.03 [0.04]		0.97 [1.07]					
	J3		0.64 [22.7]	0.79 [0.87]		0.04 [1.4]	0.05 [0.05]		0.75 [0.82]					
	Mean	24%	1.00 [35.2]	1.27 [1.40]	5.87 [2.62]	0.06 [2.0]	0.07 [0.07]	0.27 [0.12]	1.22 [1.32]	5.60 [2.50]	--	--	--	--
	Median	--	0.90 [31.8]	1.00 [1.11]	4.31 [1.92]	0.06 [2.0]	0.06 [0.07]	0.23 [0.10]	0.97 [1.04]	4.24 [1.82]	--	--	--	--

* Trap efficiency given for reliable sediment yield data, however the true efficiencies are lower than the percentages shown, with catchments D and F closer to the true value.
(±Δ) absolute uncertainty associated with paired catchment ratios is from sediment yields measured using the survey method.

The trapped sediment debris cones were similar in appearance behind all the straw bale check dams. The mean height of trapped sediment measured near the base of the up-channel face of a straw bale check dam to the surface of the sediment deposit was 0.32 m (1.0 ft), with a median of 0.26 m (0.9 ft) and a range of 0.16 to 0.80 m (0.5 to 2.6 ft). Channel gradient did not have a significant effect $t = -1.177$ ($df = 12$, $p = 0.262$) on the log-normalized mass of sediment trapped by straw bale check dams (Figure 20), with a modeled slope of -1.952 (95% CI; lower = -5.565, upper = 1.661).

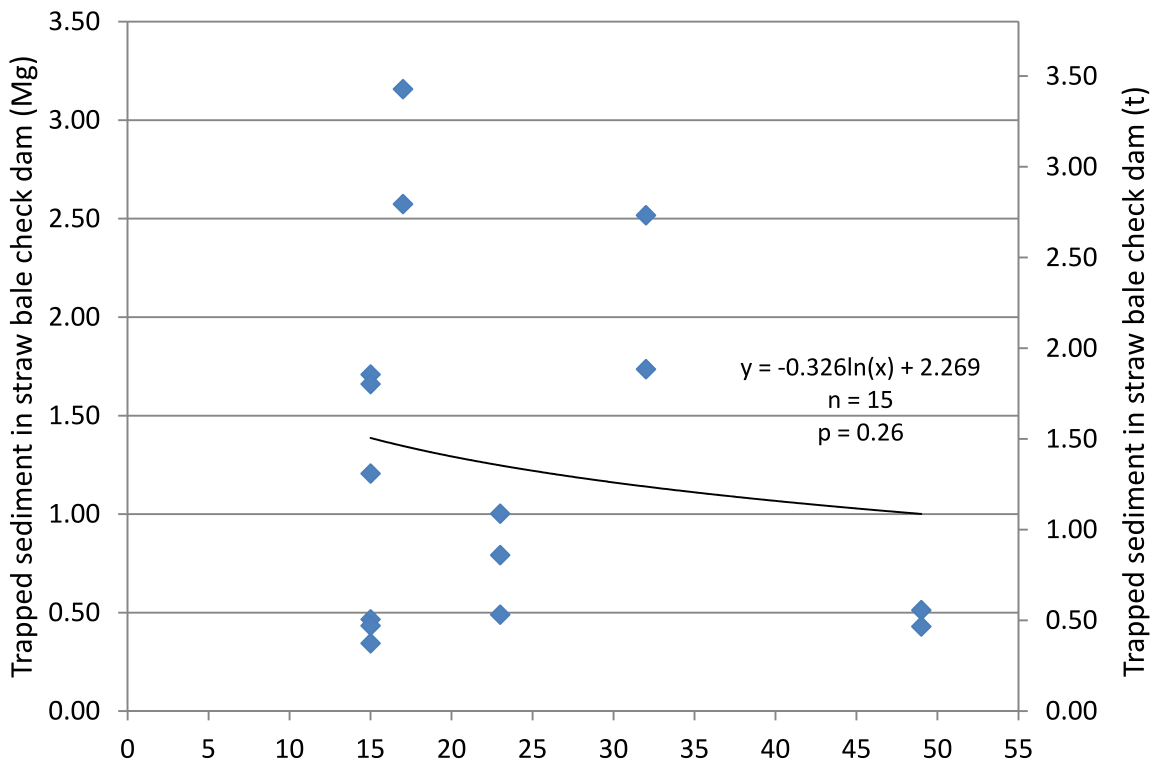

Figure 20. Channel gradient (%) effect on the mass (Mg, t) trapped by straw bale check dams filled to sediment holding capacity or the height of trapped sediment behind a straw bale check dam is equal to the spillway height.

There was very little scour below the spillway of straw bale check dams. The mean volume of down-channel scour below the structural spillway of straw bale check dams was 0.06 m^3 (2.0 ft^3), with a range of 0 to 0.10 m^3 (0 to 3.6 ft^3). The mean mass of down-channel bed scoured was 0.07 Mg (0.07 t) with a range of 0 to 0.13 Mg (0 to 0.14 t). The area normalized mean mass of channel-bed scoured due to the influence of 4 straw bale check dams ha^{-1} (2 ac^{-1}) was 0.27 Mg ha^{-1} (0.12 t ac^{-1}) with a range of 0.06 to 0.51 Mg ha^{-1} (0.03 to 0.23 t ac^{-1}). Gradient did not significantly influence $t = 0.98$ ($df = 12$, $p = 0.35$) the mass of sediment scoured below straw bale check dams. The modeled slope was 0.10 (95% CI; -0.13, 0.33).

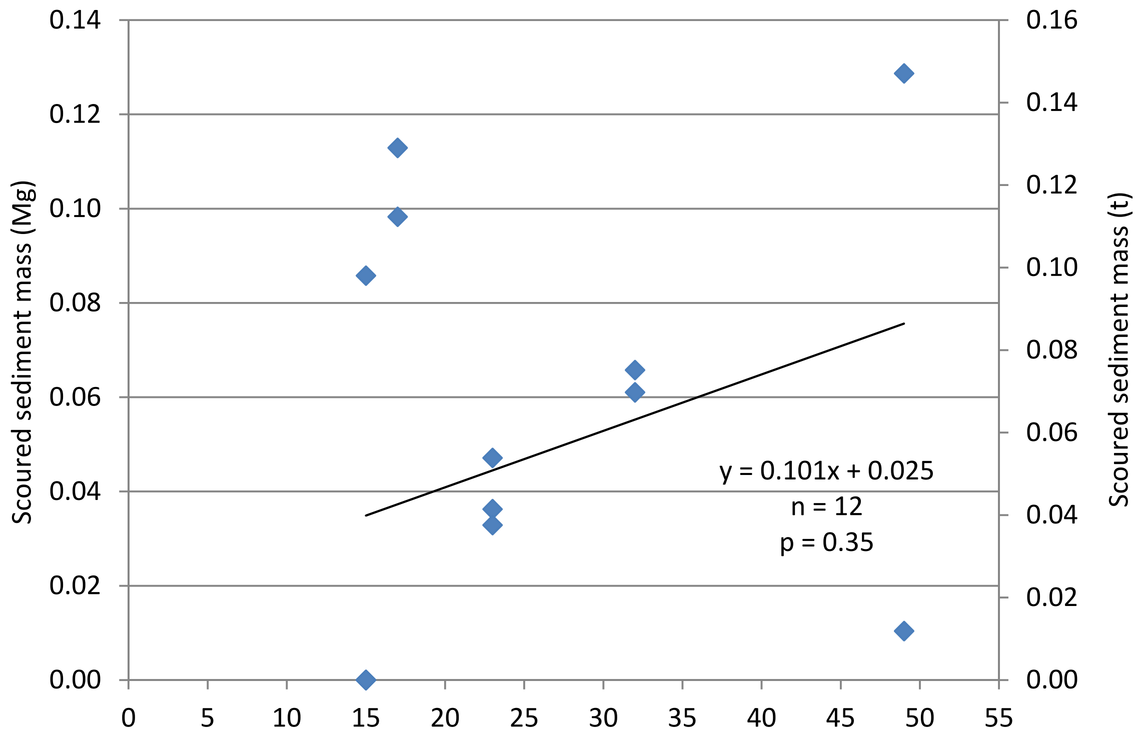

Figure 21. Channel gradient (%) effect on the mass (Mg, t) of sediment scoured below straw bale check dams.

Straw bale check dams stored a net positive sediment mass per treated catchment with a mean of 5.60 Mg ha^{-1} (2.50 t ac^{-1}) and a range of 2.94 to 10.09 Mg ha^{-1} (1.31 to 4.50 t ac^{-1}). Straw bale check dam trap efficiencies for 2011 are shown for Sevier Canyon, however their values reflect only reliable sediment yield data from structures that were overwhelmed by sediment during large erosion events. Catchments D and F with efficiencies of 14 and 23%, respectively, reflect values closer to the true efficiency of straw bale check dams in Sevier

Canyon because the sediment retention structures captured larger sediment yields before being overwhelmed compared to catchment A with a trap efficiency of 35% (Table 9). Middle Canyon had trap efficiencies of 50% for catchment G and 49% for catchment J. Trap efficiencies decreased in 2012 and had a range of 11 to 35%. Trap efficiencies are a function of the total amount of sediment eroded from the catchment with high efficiencies when small amounts of sediment are eroded from the treated catchment and low efficiencies when large amounts of sediment are eroded from the treated catchment (Figure 21). The efficiency of a straw bale check dam will go to 0 % if the straw bale fully biodegrades and the stored trapped sediment behind the bale is remobilized further down channel, which can take place over three or more years.

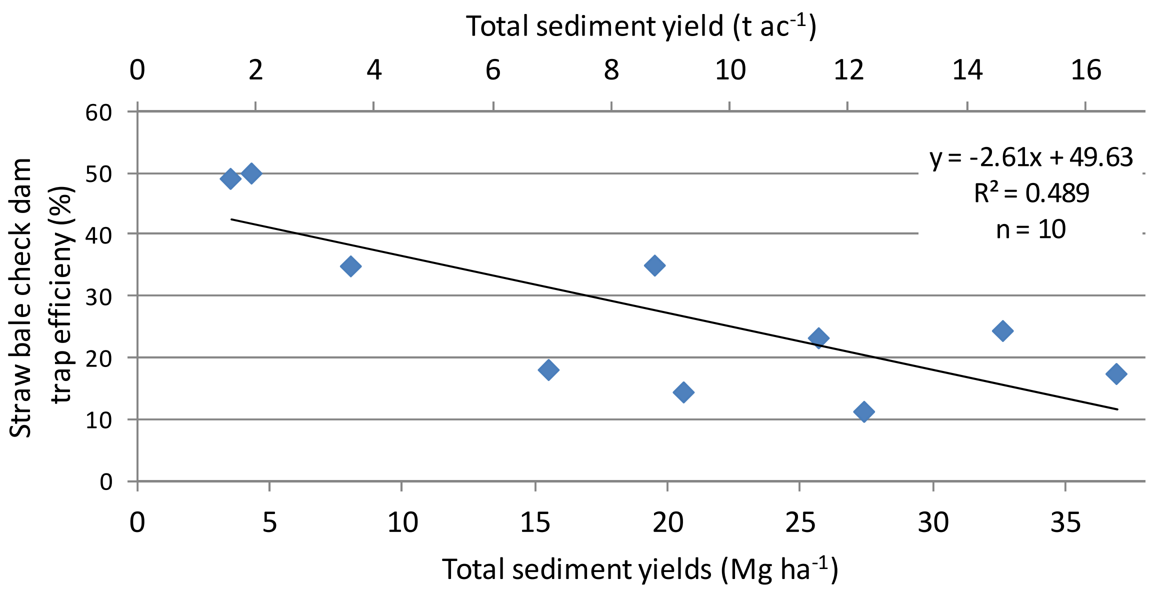

Figure 22. Straw bale check dam trap efficiency (%) and total sediment yield for treated catchments during 2011 and 2012.

3.5 Ground Cover

Hillslopes and channels had similar distributions of cover or exposure among the five ground cover types. There was little change for both the hillslope and channel cover from spring to fall in 2011 (Figure 22). Mineral soil covered the largest area on hillslopes with 53 % in the spring (S) and 56 % in the fall (F). The remaining ground cover for spring and fall hillslopes were rock cover (S-29 %, F-19 %), vegetation (S-10 %, F-18 %), woody debris (S-5 %, F-4 %), and litter (S-2 %, F-3 %). The percentages of ground cover in channels from spring to fall were, mineral soil (S-37 %, F-42 %), rock cover (S-38 %, F-27 %), vegetation cover (S-16 %, F-26 %), and woody debris and litter collectively accounted for very little coverage (S-10 %, F-6%). Vegetation is considered the most important ground cover variable with regard to erosion rates because litter was not present in the first post-fire year and had minimal effect on erosion during the second post-fire year. The significance of exposed mineral soil and vegetation cover is reported here, for additional inquiry of significance of the three other cover variables see Table 10. In the spring of 2011 there is a significant difference ($t = 2.92$, $p = 0.007$) between mineral soil cover on the hillslope and in the channel, this was also true in the fall of 2011 ($t = 3.09$, $p = 0.006$) (Table 10). There is a significant difference ($t = -3.81$, $p = 0.001$) in vegetation cover between the spring and fall of 2011.

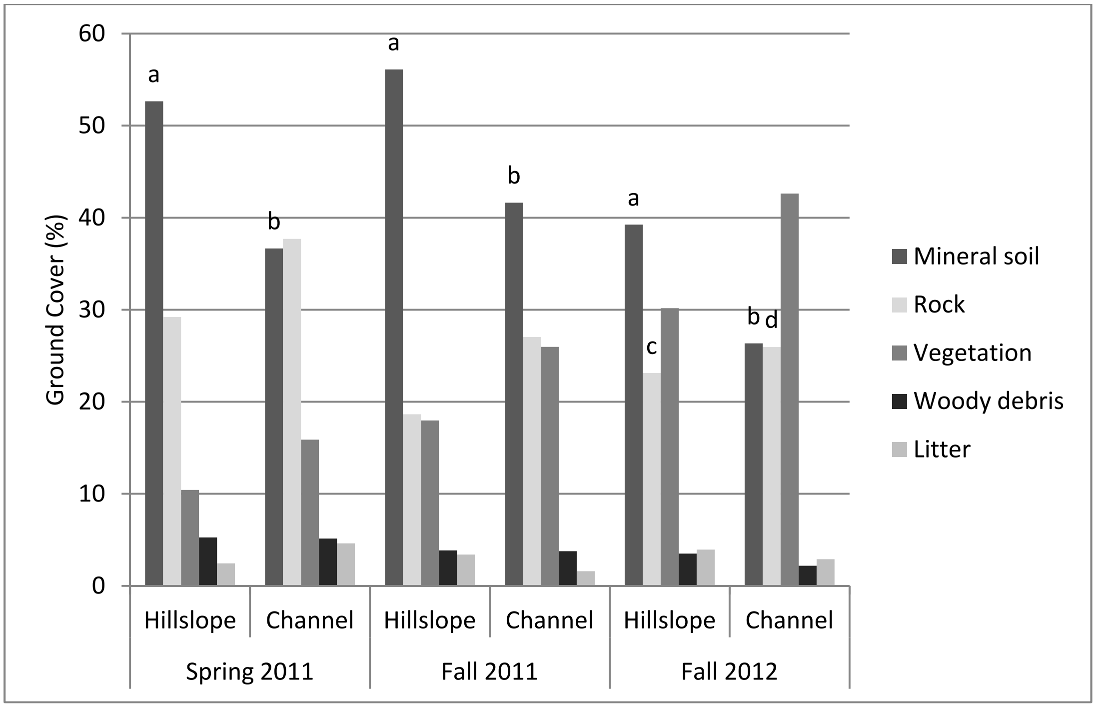

Figure 23. Percent ground cover of the five variables: mineral soil, rock, vegetation, woody debris and litter, shown for spring and fall of 2011 and fall of 2012. Labels a and b indicate mineral soil exposure on hillslopes is significantly than channels. Labels c and d indicate a significant difference in vegetation soil cover between hillslope and channel when.

Most of the ground cover or exposure variables remained unchanged from the fall of 2011 to the fall of 2012. The largest shift in hillslope cover from fall 2011 to fall 2012 was an increase in the percentage of area covered by vegetation (18 to 30%), and a decrease in mineral soil exposed (56 to 39%). The other cover variables were relatively equal between fall 2011 and fall 2012, with slightly more rock cover (19 to 23%) and woody debris and litter had no change in cover. The shift in ground cover in the channels was similar to the hillslopes from the fall of 2011 to the fall of 2012, with the vegetation cover having the largest increase (26 to 43%) and the largest decrease was mineral soil exposed (42 to 26%). The percent cover of rock, litter, and woody debris all changed 4% or less from fall 2011 to fall 2012. There is a significant difference ($t = 2.89$, $p = 0.009$) in fall 2012 mineral soil exposed between the hillslope and the channel (Table 10). There is a significant difference ($t = 4.32$, $p < 0.001$) between mineral soil exposure on the hillslope between 2011 and 2012, and also in the channels between 2011 and 2012 ($t = 5.21$, $p = 0.001$). Vegetation varied greatly by aspect and year. There is a significant difference ($t = -2.15$, $p = 0.045$) in vegetation cover between the Southeast and Southwest aspect slopes cover in the fall of 2012. Hillslope aspects are not grouped when compared between 2011 and 2012 because of this difference. However, 2012 vegetation hillslope cover is grouped when compared against 2012 channel cover because it is considered a representative sample of vegetation on the hillslopes. There was a significant difference between vegetation cover on Southeast aspects ($t= -3.04$, $p = 0.01$) and Southwest aspects ($t = -5.32$, $p < 0.001$) between 2011 and 2012. Vegetation cover on the hillslopes is significantly different ($t = -2.20$, $p = 0.047$) from the channels in 2012. Finally, there is a significant difference ($t = -4.04$, $p = 0.003$) between vegetation cover in the channels from 2011 and 2012.

Table 11. Test for significance difference in ground cover between SE (Southeast) and SW (Southwest) hillslope aspects, and channels: Spring and Fall of 2011 and Fall 2011 and Fall 2012.

Mineral soil	Sample date	$H_0 : \mu_1 = \mu_2$	t =	df =	p =	$H_0 \neq \mu_1 \neq \mu_2$	95% CI	
2011							Lower	Upper
	Spring	SE hillslope = SW hillslope	0.986	16	0.339		-0.063	0.173
	Spring	Hillslope = Channel	2.922	24	0.007	Significant	0.034	0.198
	Fall	SE hillslope = SW hillslope	-0.248	12	0.808		-0.096	0.076
	Fall	Hillslope = Channel	3.090	18	0.006	Significant	0.033	0.175
	Spring v. Fall	Hillslope = Hillslope	-1.118	19	0.278		-0.085	0.026
	Spring v. Fall	Channel = Channel	-1.870	9	0.094		-0.092	0.009
2012								
	Fall	SE hillslope = SW hillslope	0.254	18	0.803		-0.113	0.144
	Fall	Hillslope = Channel	2.889	20	0.009	Significant	0.039	0.240
	2011 v. 2012	Hillslope = Hillslope	4.322	19	0.000	Significant	0.091	0.261
	2011 v. 2012	Channel = Channel	5.207	9	0.001	Significant	0.094	0.239

Vegetation	Sample date	$H_0 : \mu_1 = \mu_2$	t =	df =	p =	$H_0 \neq \mu_1 \neq \mu_2$	95% CI	
2011							Lower	Upper
	Spring	SE hillslope = SW hillslope	-1.207	17	0.245		-0.166	0.045
	Spring	Hillslope = Channel	-1.684	17	0.111		-0.175	0.020
	Fall	SE hillslope = SW hillslope	-1.573	18	0.133		-0.200	0.029
	Fall	Hillslope = Channel	-0.924	13	0.373		-0.218	0.088
	Spring v. Fall	Hillslope = Hillslope	-3.807	19	0.001	Significant	-0.158	-0.046
	Spring v. Fall	Channel = Channel	-1.886	9	0.092		-0.196	0.018
2012								
	Fall	SE hillslope = SW hillslope	-2.153	18	0.045	Significant*	-0.142	-0.002
	Fall	Hillslope = Channel	-2.201	13	0.047	Significant	-0.195	-0.002
	2011 v. 2012	Right hillslope = Right hillslope	-3.036	9	0.014	Significant*	-0.230	-0.034
	2011 v. 2012	Left hillslope = Left hillslope	-5.324	9	0.000	Significant*	-0.207	-0.084
	2011 v. 2012	Channel = Channel	-4.044	9	0.003	Significant	-0.268	-0.076

Litter	Sample date	$H_0 : \mu_1 = \mu_2$	t =	df =	p =	$H_0 \neq \mu_1 \neq \mu_2$	95% CI	
2011							Lower	Upper
	Spring	SE hillslope = SW hillslope	-0.247	16	0.808		-0.134	0.106
	Spring	Hillslope = Channel	-3.328	28	0.002	Significant	-0.179	-0.043
	Fall	SE hillslope = SW hillslope	-1.712	16	0.106		-0.242	0.026
	Fall	Hillslope = Channel	0.404	28	0.689		-0.065	0.097
	Spring v. Fall	Hillslope = Hillslope	-0.587	19	0.565		-0.082	0.046
	Spring v. Fall	Channel = Channel	7.551	9	0.000	Significant	0.076	0.141
2012								
	Fall	SE hillslope = SW hillslope	-0.939	14	0.363		-0.097	0.038
	Fall	Hillslope = Channel	1.113	17	0.281		-0.028	0.091
	2011 v. 2012	Hillslope = Hillslope	-1.944	19	0.067		-0.146	0.005
	2011 v. 2012	Channel = Channel	-1.714	9	0.121		-0.127	0.018

Woody debris	Sample date	$H_0 : \mu_1 = \mu_2$	t =	df =	p =	$H_0 \neq \mu_1 \neq \mu_2$	95% CI	
2011							Lower	Upper
	Spring	SE hillslope = SW hillslope	0.164	18	0.872		-0.091	0.107
	Spring	Hillslope = Channel	0.207	16	0.839		-0.085	0.103
	Fall	SE hillslope = SW hillslope	1.250	18	0.227		-0.042	0.166
	Fall	Hillslope = Channel	0.150	18	0.882		-0.084	0.097
	Spring v. Fall	Hillslope = Hillslope	3.194	19	0.005	Significant	0.015	0.073
	Spring v. Fall	Channel = Channel	1.738	9	0.116		-0.013	0.095
2012								
	Fall	SE hillslope = SW hillslope	0.855	17	0.404		-0.058	0.138
	Fall	Hillslope = Channel	1.025	22	0.317		-0.037	0.108
	2011 v. 2012	Hillslope = Hillslope	0.341	19	0.737		-0.045	0.063
	2011 v. 2012	Channel = Channel	0.969	9	0.358		-0.051	0.128

Rock	Sample date	$H_0 : \mu_1 = \mu_2$	t =	df =	p =	$H_0 \neq \mu_1 \neq \mu_2$	95% CI	
2011							Lower	Upper
	Spring	SE hillslope = SW hillslope	0.015	15	0.988		-0.137	0.139
	Spring	Hillslope = Channel	-2.289	28	0.030	Significant	-0.168	-0.009
	Fall	SE hillslope = SW hillslope	1.777	18	0.092		-0.019	0.231
	Fall	Hillslope = Channel	-2.096	22	0.048	Significant	-0.196	-0.001
	Spring v. Fall	Hillslope = Hillslope	3.496	19	0.002	Significant	0.045	0.180
	Spring v. Fall	Channel = Channel	2.839	9	0.019	Significant	0.021	0.184
2012								
	Fall	SE hillslope = SW hillslope	1.297	16	0.213		-0.044	0.182
	Fall	Hillslope = Channel	-0.870	23	0.393		-0.119	0.048
	2011 v. 2012	Hillslope = Hillslope	-1.514	19	0.147		-0.132	0.021
	2011 v. 2012	Channel = Channel	0.632	9	0.543		-0.020	0.036

* SE hillslope and SW hillslope transects were significantly different; they were not grouped when tested between years for hillslope, but were grouped as one sample when tested against channel.

$H_0 : \mu_1 = \mu_2$ there is no significant difference between the two means.

$H_0 \neq \mu_1 \neq \mu_2$ the null hypothesis is rejected, there is a significant difference between the two means.

3.6 Channel cross-sections

Channel cross-sections measured channel stability or the resistance of the bed to scour or aggregation. Three to five channel cross-sections were spaced 12 to 30 m (39 to 98 ft) apart in each catchment, with spacing and count dependent upon channel length (Table 12). There was very little change in cross-sectional areas between the 26 Jul 2011 survey and 7 May 2012 survey and no trend in the difference in areas between the two surveys (Figure 24). The cross-sectional areas increased in six of the channels from 26 Jul 2011 to 7 May 2012. There was a mean decrease in three cross-sectional areas from 26 Jul 2011 to 7 May 2012 ranging from 0.03 to 0.40 m^2 (0.32 to 4.31 ft^2). Only one channel had no mean change between the two cross-section surveys. There is no significant difference t = 1.28 (df = 44, p = 0.206) (95% CI; lower = -0.003, upper = 0.015) in channel cross-sectional area between the two survey dates (Figure 25).

Table12. Catchment name and pair, number of cross-sections per catchment, mean spacing between cross-sections, mean cross-sectional area (m^2, ft^2) for 26 Jul 2011 and 7 May 2012 surveys, and difference between survey date means. Positive difference between surveys is attributed to channel scour, while negative difference between surveys is attributed to channel aggradation.

Catchment channel cross-sections	Cross-section per catchment	Average distance between channel cross-sections (m [ft])	26 Jul 2011 Area (m^2 [ft^2])	7 May 2012 Area (m^2 [ft^2])	Average difference in cross-sectional area (m^2 [ft])	Percentage of 2011 annual catchment sediment yield produced between survey dates (%)
A.1	4	25 [81]	7.88 [84.9]	7.76 [83.5]	0.12 [1.3]	59*
B.1	4	13 [42]	11.64 [125.3]	11.53 [124.1]	0.11 [1.2]	36*
C.2	4	17 [57]	3.14 [33.8]	3.18 [34.2]	-0.03 [-0.3]	--
D.2	3	12 [41]	19.19 [206.6]	19.60 [210.9]	-0.40 [-4.3]	43*
E.3	3	19 [62]	2.17 [23.4]	2.13 [22.9]	0.04 [0.5]	--
F.3	4	16 [52]	3.13 [33.7]	3.10 [33.4]	0.02 [0.3]	68*
G.4	4	30 [98]	5.51 [59.3]	5.54 [59.6]	-0.03 [-0.3]	44
H.4	5	30 [98]	6.05 [65.1]	5.98 [64.4]	0.07 [0.7]	48
I.5	5	30 [98]	6.90 [74.3]	6.85 [73.8]	0.05 [0.5]	41
J.5	4	30 [98]	7.53 [81.1]	7.54 [81.1]	0.00	89

* Percentages for reliable sediment yields from data of overwhelmed retention structures.

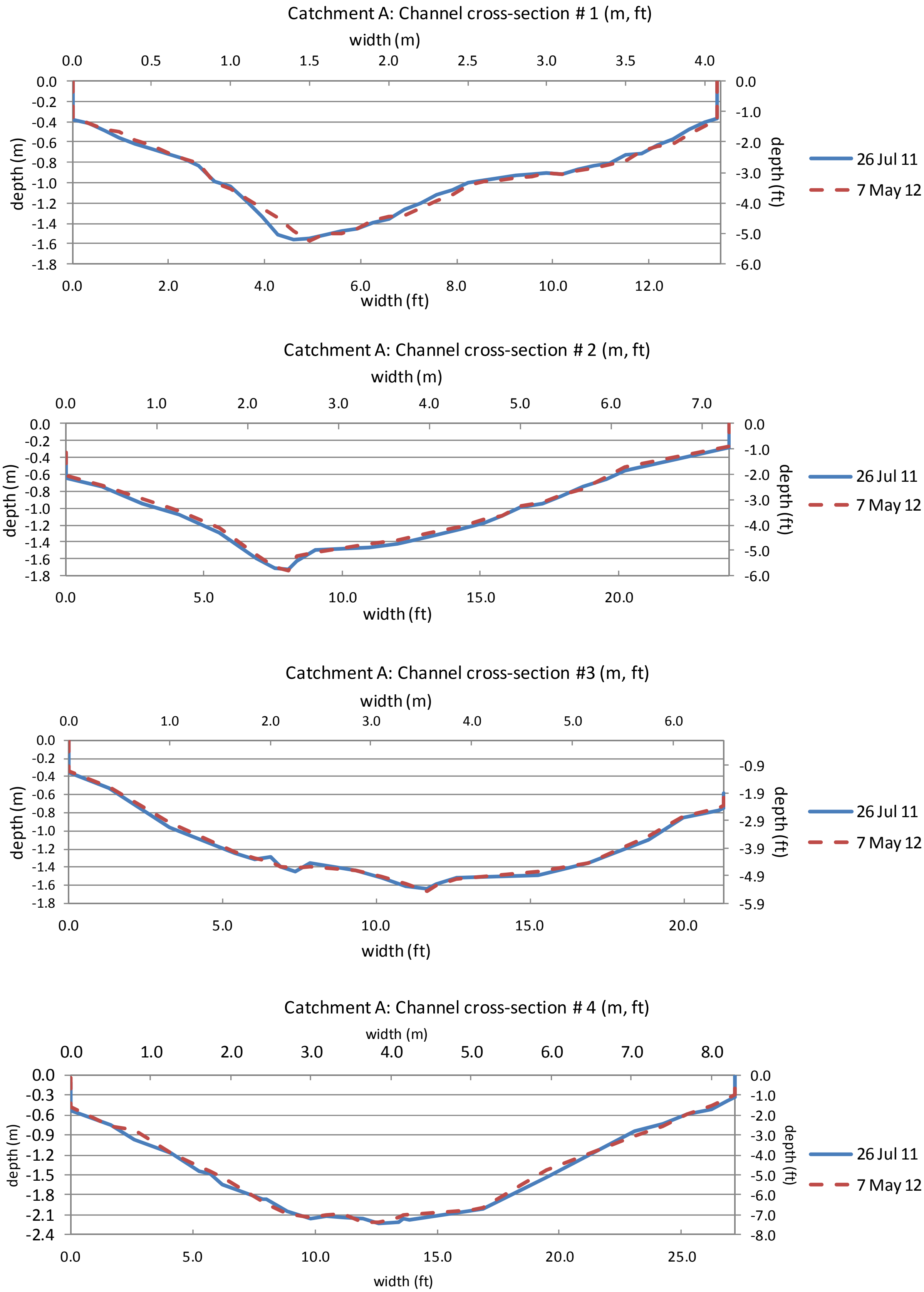

Figure 24. Four channel cross-sections in catchment A with #1 being the lowest channel cross-section up through #4 which is the highest channel cross-section in the catchment. Mean change in cross-sectional area in this catchment was 0.12 m^2 (1.3 ft^2)

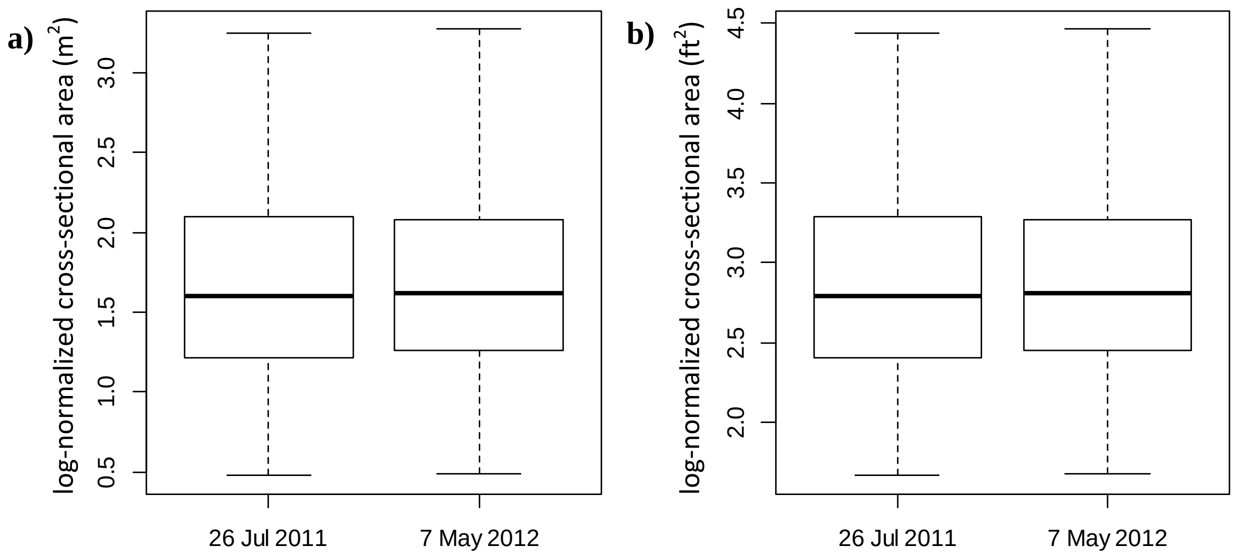

Figure 25. Box plot of log-normalized channel cross-section areas (**a)** m^2 **b)** ft^2) for the two survey dates.

3.7 Particle size analysis

There was relatively little change in mean D_{50} soil texture particle size during 2011 in Middle Canyon (Figure 26). There was no consistent trend in particle size distribution for hillslopes or channels on an event by event basis. Base of slope hillslope fences generally had the largest mean D_{50} soil texture particle size for each event. Hillslope D_{50} soil texture particle sizes ranged in sizes from ~0.22 to 0.54 mm (0.009 to 0.021 in) during 2011 and were generally larger than annual channel sediment yield D_{50} particle sizes, which ranged from 0.1 to 0.3 mm (0.004 to 0.012 in).

The soil texture of eroded sediment from hillslopes and from yields at catchments was relatively the same across the catchments in Middle Canyon during 2011. Hillslope and channel mean D_{50} values were log-normalized prior to statistical analysis due to large variation in soil texture among the samples (Table 13). Sediment samples from the five events in Middle Canyon during 2011 from upslope and base of hillslope fences were tested for a significant difference in mean log-D_{50} with the best fitting random intercept mixed model. There is no significant difference t = -0.247 (df = 1, p = 0.846) between log-D_{50}.

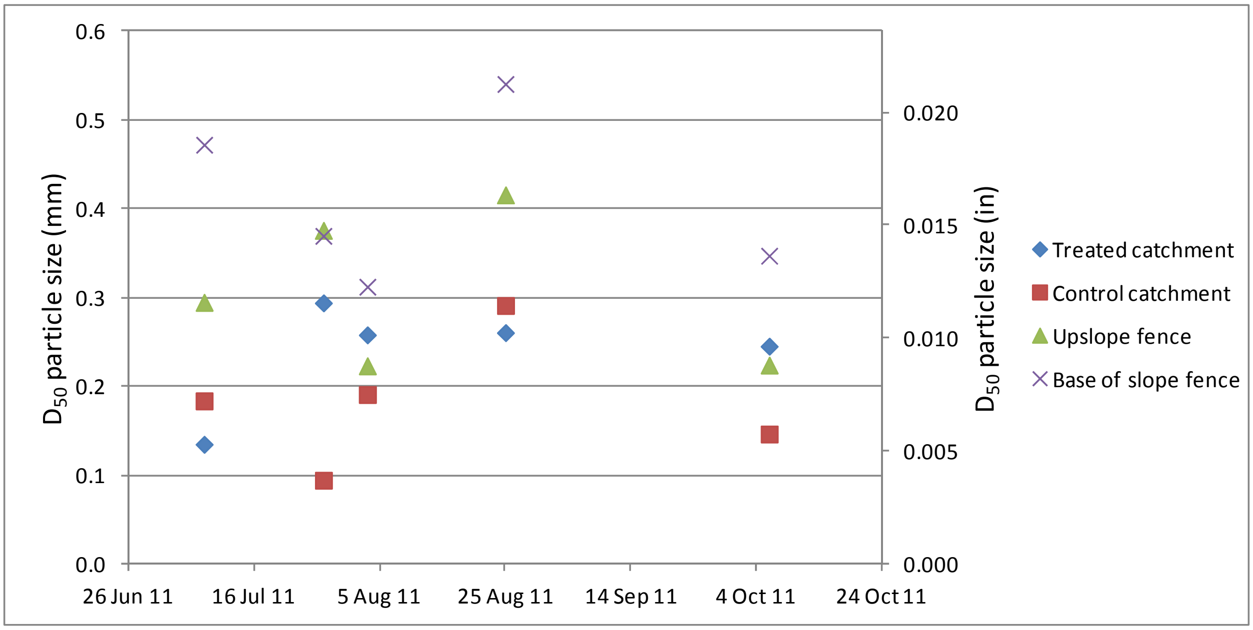

Figure 26. Mean D_{50} soil texture particle size for sediment yields from treated and control catchments, and sediment erosion in uplslope and base of hillslope fences by event date.

The soil texture at catchment outlets was similar for both treated and control catchments. Mean log-D_{50} was tested for a significant difference between Treated and Control catchment sediment yields from the five events during 2011, using a generalized least squares model with no random component. There is no significant difference t = 0.764 (df = 19, p = 0.456) in mean log-D_{50} between Treated and Control catchments. There is no significant difference t = 1.512 (df = 16, p = 0.154) in mean log-D_{50} between hillslopes erosion and catchment yields using a generalized least square model.

Table 13. Output of statistical models to determine if a significant difference exists, H_0: $\mu_1 = \mu_2$: (a.) log-normalized mean D_{50} for upslope fences = log-normalized mean D_{50} base of slope fences, (b.) log-normalized mean D_{50} in treated catchments = log-normalized mean D_{50} in control catchments, (c.) log-normalized mean D_{50} for hillslope fences = log-normalized mean D_{50} for channel catchment sediment.

a)

2011 Middle Canyon

H_0 = upslope fence log-D_{50} = base of slope fence log-D_{50}

Linear mixed-effects model

						95 % Confidence Intervals	
	Slope value	Std.Error	DF	t-value	p-value	lower	upper
Intercept	-0.887	0.596	13	-1.489	0.160	-2.174	0.400
pair	-0.282	0.690	1	-0.409	0.753	-9.046	8.481
fence: upper	-0.170	0.690	1	-0.247	0.846	-8.934	8.593

b)

2011 Middle Canyon

H_0 = treated catchment log-D_{50} = control catchment log-D_{50}

Generalized least squares fit model

					95 % Confidence Intervals	
	Slope value	Std.Error	t-value	p-value	lower	upper
Intercept	-1.494	1.064	-1.404	0.179	-3.750	0.762
pair	-0.053	0.231	-0.231	0.820	-0.542	0.436
treatment: Treated	0.176	0.231	0.764	0.456	-0.313	0.665

Degrees of freedom = 19

Residual standard error = 0.501

c)

2011 Middle Canyon

H_0 = hillslope log-D_{50} = channel log-D_{50}

Generalized least squares fit model

					95 % Confidence Intervals	
	Slope value	Std.Error	t-value	p-value	lower	upper
(Intercept)	-2.074	1.042	-1.991	0.068	-4.324	0.177
pair	0.186	0.247	0.752	0.465	-0.348	0.720
log-D_{50} hillslope	0.401	0.265	1.513	0.154	-0.171	0.973

Degrees of freedom = 16

Residual standard error = 0.457

Particle size distribution analyses have only been completed for the first three events in Middle Canyon for 2012, with only hillslope fence samples having a complete data set. Upslope and base of slope mean D_{50} particle sizes for 2012 ranged in size between the three events from

0.2 to 0.5 mm (0.009 to 0.019 in) (Figure 27), having a similar range to the mean D_{50} hillslope particle sizes in 2011. There is no consistent trend in particle size between the two fence locations.

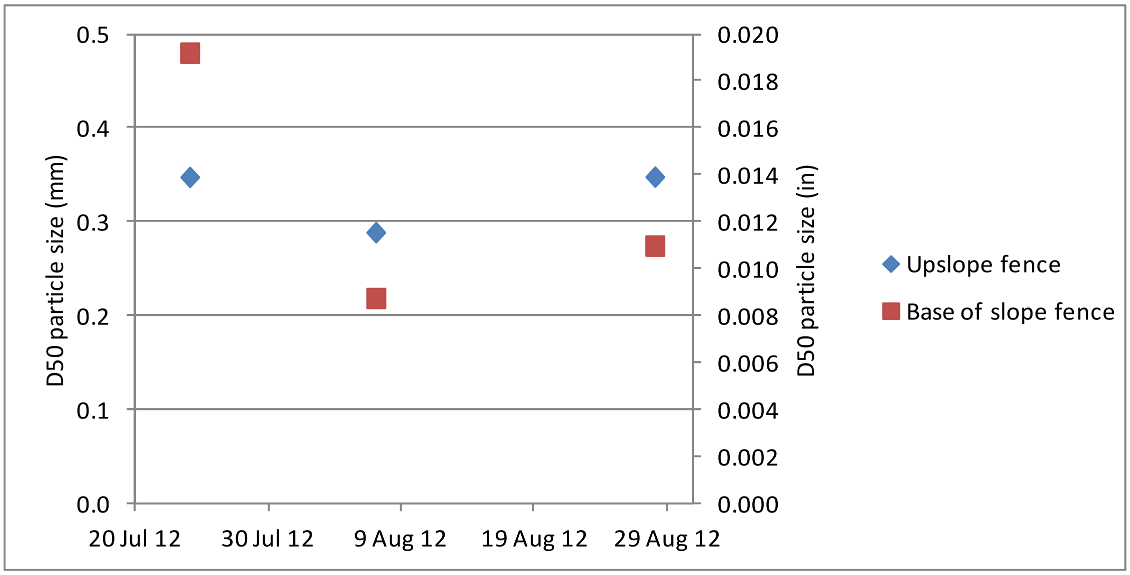

Figure 27. Mean D_{50} particle size for upslope and base of hillslope fence sediment erosion for the first three rain events during 2012.

3.8 Organic matter content

Channel sediment yields had higher organic matter content than sediment in hillslope fences in Middle Canyon during 2011 for all events (Figure 28). Organic matter content was roughly equal in hillslope fences for every event with a small range of 3.6 to 4.6 %. Channel sediment yields had a larger range of organic matter content from 5.3 to 9.9 %. Organic matter was content was higher in catchment sediment yields for the first two events, and decreased with additional events.

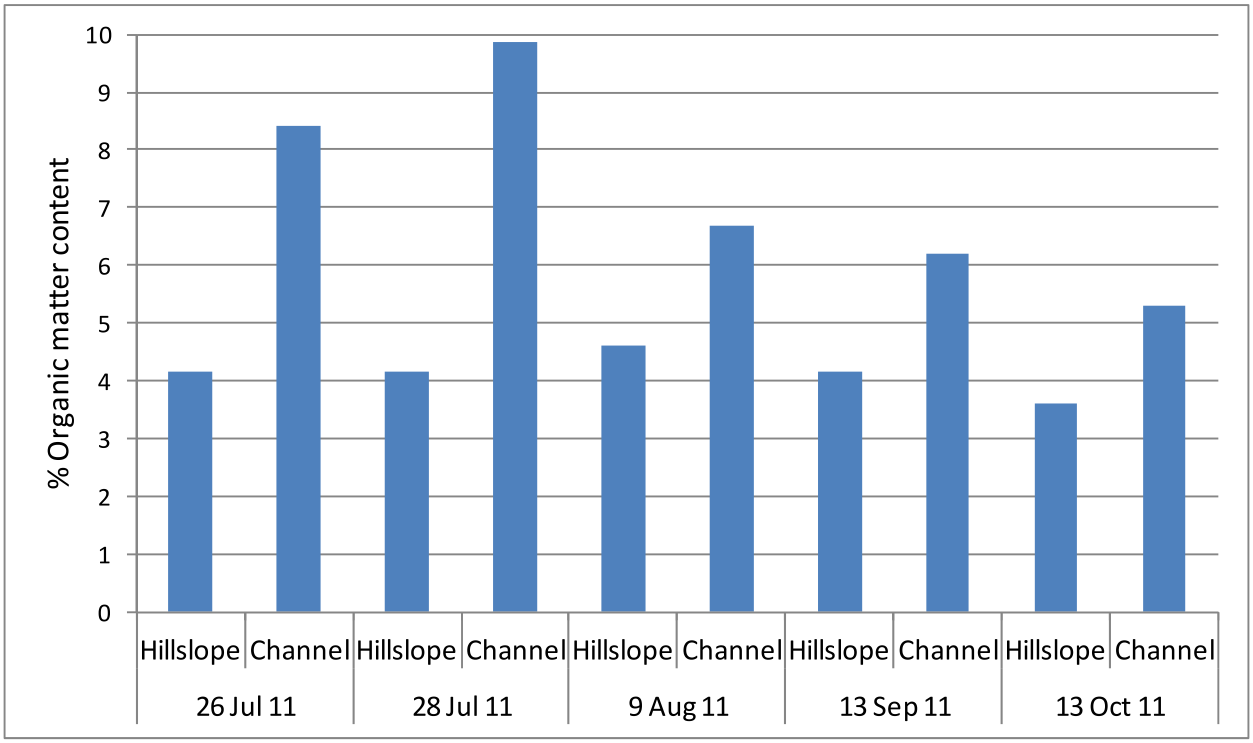

Figure 28. Organic matter content in sediment erosion from hillslopes and channel sediment yields show for each event.

Hillslope and channel organic matter in the sediment were log-normalized prior to analysis. A generalized least squares model found no significant difference t = 0.073 (df = 17, p = 0.942) in organic matter content between upslope and base of hillslope fence plots (Table 14). There is no significant difference t = 1.61 (df = 19, p = 0.128) in organic matter content between Treated and Control catchments using a generalized least squares model. Hillslope and channel organic matter content is not significantly different t = 0.925 (df = 16, p = 0.372) using a generalized least squares model. Soil samples from hillslopes and channel sediment yields in Middle Canyon were not been processed for organic matter content in 2012.

Table 14. Statistical model results determining significant difference of H_0: $\mu_1 = \mu_2$: **a)** log-normalized organic matter in upslope fences = log-normalized % organic matter in base of slope fences, **b)** log-normalized % organic matter in treated catchments = log-normalized % organic matter in control catchments, **c)** log-normalized % organic matter in hillslope fences = log-normalized % organic matter in catchment sediment retention structures.

a)

2011 Middle Canyon
H_0 = log-normalized upslope fence organics = log-normalized base of slope fence organics
Generalized least squares fit model

	Slope value	Std.Error	t-value	p-value	95 % Confidence Intervals lower	upper
Intercept	-2.450	0.501	-4.890	0.000	-3.524	-1.375
pair	-0.169	0.110	-1.532	0.148	-0.405	0.068
fence: upper	0.008	0.112	0.073	0.943	-0.232	0.248

Degrees of freedom = 17
Residual standard error = 0.205

b)

2011 Middle Canyon
H_0 = log-normalized treated catchment organics = log-normalized control catchment organics
Generalized least squares fit model

	Slope value	Std.Error	t-value	p-value	95 % Confidence Intervals lower	upper
Intercept	-3.125	0.901	-3.467	0.003	-5.036	-1.214
pair	0.051	0.195	0.259	0.799	-0.364	0.465
treatment: Treated	0.314	0.195	1.607	0.128	-0.100	0.728

Degrees of freedom = 16
Residual standard error = 0.424

c)

2011 Middle Canyon
H_0 = log-normalized hillslope organics = log-normalized channel organics
Generalized least squares fit model

	Slope value	Std.Error	t-value	p-value	95 % Confidence Intervals lower	upper
(Intercept)	-1.437	1.803	-0.797	0.440	-5.334	2.459
pair	0.095	0.255	0.373	0.715	-0.455	0.645
log-hilllslope organics	0.529	0.572	0.925	0.372	-0.706	1.765

Degrees of freedom = 16
Residual standard error = 0.478

4.0 Discussion

4.1 Treated catchment significance

We found the straw bale check dam channel treatment did little to reduce post-fire sedimentation rates. Straw bale check dams were analyzed to determine if they had a significant effect at reducing post-fire sediment erosion from ephemeral channels during the first and second post-fire years. In the first post fire-year there was no significant difference $t = -1.296$ ($df = 18$, $p = 0.216$) in catchment sediment yields between treated and control catchments. The treatment did little to mitigate sediment produced from small and commonly occurring rain events at the site that were equal to or less than a 1-year I_{30} intensity return periods. Instead, the straw bale check dams structures filled to sediment holding capacity during the first rain event with intensities equal to 1-year I_{30} (21 mm hr^{-1}, 0.8 in hr^{-1}) and 2-year I_{30} (28 mm hr^{-1}, 1.1 in hr^{-1}) return periods. In two treated catchments 56% of straw bale checks filled to sediment holding capacity during a rain event with less than a 1-year I_{30} intensity return period. The remaining empty or partially full structures in these catchments were filled to capacity during a second event with less than a 1-year I_{30} intensity. Given the straw bale check dams were already full at the beginning of 2012 there was no significant difference between treated and control catchment sediment yields.

Sedimentation rates varied greatly during the two year study. More often the treated catchments had lower sediment yields within paired catchments, even when straw bale check dams were already full, such as during the second post-fire year. The varying rate of sediment yields from paired catchments is most clearly seen in the paired catchment ratio. For instance the paired catchment ratio in 2012 ranged from 0.29:1 to 2.11:1 across the 5 paired catchments.

The catchment ratio for all pairs was assumed to be 1:1 as it was not possible to establish a pre-fire calibration period.

A number of environmental factors could have been influencing the large differences seen in paired catchment ratios that were not closer to a 1:1 ratio. Rainfall events may have had unequal rainfall intensities within an area smaller than a paired catchment. While it is assumed high intensity rain events are homogenous in intensity across the two adjacent catchments, the 1-year I_{10} intensity return period event in paired catchment E-F on 1 Aug 2012 produced 16.78 (±0.7) Mg ha^{-1} (7.49 [±0.3] t ac^{-1}) of sediment in catchment E and only 1.40 Mg ha^{-1} (0.62 t ac^{-1}) in catchment F. This was most likely due to unequal distribution of rainfall amount and intensity across the pair during the event. It may be possible to account for this in future studies by placing multiple rain gauges within each treated and control paired catchment.

Hillslope and/or channel processes may also move sediment incrementally out of catchments at different temporal and spatial rates. A change in the ratio of paired catchment sediment yields can be seen in Middle Canyon from 2011 to 2012. Pair G-H had a paired catchment ratio of 0.67:1 in 2011 change to 0.29:1 in 2012, and the paired catchment ratio in I-J of 0.36:1 in 2011 changed to 0.70:1 in 2012.

Another environmental factor potentially influencing the large difference in sediment yields could be soil properties within the catchments. Treated catchment F had reliable annual sediment yield of 25.71 Mg ha^{-1} (11.47 t ac^{-1}) in 2011 and maybe developed an efficient rill network that carried much of the loose or weakly held sediment for a 1-year I_{30} rain event from the soil surface. While in catchment E maybe the efficient drainage network had not developed due to a deeper soil horizon of weakly held aggregates and thus a 1-year I_{10} return period rain event eroded much larger sediment yields. Also, the number of channel heads and their locations and the catchment shape may affect how efficiently sediment is transported out of the catchment. The Control catchment B is a wide catchment that has one large primary and two small secondary channel heads with their channels joining together halfway down the catchment, whereas treated catchment A is a more narrow catchment with one channel head initiating very high in the catchment that drains into a long continuous channel (Table 1). The routing of hillslope runoff into one channel in catchment A may result in higher channel transport capacity rates compared to cumulative channel transport capacity rates for the three small channels in catchment B that split up the same amount of hillslope runoff. This may be one reason why the A:B catchment ratio during the second post-fire year is 2.11 (±0.16):1.

When sediment is detached and mobilized it is difficult to disrupt or significantly reduce sediment the sediment erosion process that occurs on hillslopes and in channels. While straw bale check dams did not significantly reduce sediment yields for rain events with an I_{30} intensity equal to or less than a 1-year return period, other treatments that have been tested to significantly reduce detached and mobilized sediment have found similar outcomes (Robichaud *et al*. 2008; Ruby, 1973). Robichaud *et al*. (2008) found log erosion barriers (LEBs) significantly reduced catchment sediment yields by as much as 65 % in treated catchments compared to control catchments, with a data set largely made up of rain events with less than 2-year I_{10} intensity return periods. However, no treatment effect was found for LEBs during rain events equal to or greater than a 2-year I_{10} intensity return period (Robichaud *et al*. 2008). When considering large scale erosion barriers, it was found there was no significant difference in sediment yields between canyons treated with concrete crib check dams in Southern California and canyons left as controls (Ruby, 1973). It was not possible to determine paired catchment treatment significance in Sevier Canyon due to sediment retention structure failures in 2011. The three treated catchments that received one to two rain events equal to or greater than 2-year I_{30} intensity return periods in the first year had reliable annual erosion rates that ranged from 19.53 to 25.71 Mg ha^{-1} (8.71 to 11.47 t ac^{-1}) . These erosion rates would probably not meet mitigation targets set by land managers who seek to reduce the effects of large post-fire sediment yields.

The finding of no significant difference between treated and control catchments runs contrary to the recommendation that straw bale check dams are effective at mitigating sediment yields produced from 2-year to 5-year I_{10} or I_{30} intensity return period rain events (Napper, 2006). The first factor directly influencing significance of treatment effect is treatment rate or number of straw bale check dams per catchment area. After taking into account failure rates, which were 0% in the current study, but can be expected to be around ~20% (Napper, 2006) and even as high as 50% (Colins and Johnston, 1995); it may be assumed installing additional structures in a treated channel increases the potential trapped sediment storage capacity, thus increasing the potential to significantly reduce sediment yields from treated catchments. Montgomery and Dietrich (1988) show a catchment's source area, the area from the channel head to the uppermost hydrologic divide, is inversely related to the channel gradient. Therefore, shallower channel gradients with larger source areas and shorter channel lengths may limit the number of straw bale check dams installed in the defined channel. This limitation may not allow for mitigation targets to be met if a large number of structures are called for. Drier climates that tend to have larger source areas (Montgomery and Dietrich, 1988) and shorter channel lengths may also limit factor the channel space available to accommodate for high treatment rates of straw bale check dams.

The point at which straw bale check dams significantly reduce sediment yields is difficult to discern from the limited literature. The lack of directly reporting treatment rates or the number of straw bale check dams per catchment area does not allow for temporal and spatial cross-comparison of straw bale check dam treatment effectiveness. One factor that may contribute to this absence is the failed or functioning rating given to individual structures and a tendency to mention cost per structure rather than cost per area (Miles *et al*. 1989; Collins and Johnston, 1995; Fox, 2009). Goldman (1986) emphasizes catchment area has a direct effect on the structural integrity of straw bale check dams, yet the number of structures per area is most often indirectly reported. The most accurate rate conversion is made from Fox (2009), where he identifies the catchment size and the number of channel treatments, in his case log debris dams (LDDs). The treatment rates in his study are equal to one log debris dam per two ha (~one LDD per five ac) and roughly one log debris dam per four ha (~one LDD per ten ac). A rough calculation of the treatment rate of straw bale check dams in California ranged from 8 to 11 straw bale check dams per hectare (3 to 5 SCDs ac^{-1}) (Collins and Johnston, 1995).

Treatment rates are often the starting place to estimate the predicted amount of sediment that will be mitigated from post-fire hillslopes, and treatment rate is commonly used in many post-fire treatment effectiveness studies and in management decisions. Ground cover treatments of seeding, straw mulches, and wood shreds are applied at mass per area (Robichaud, 2000; Groen and Woods, 2008, Cerdá, 2009). Contour-felled log erosion barriers are reported by Robichaud *et al*. (2008) in densities (no. ha^{-1}, no ac^{-1}), and length per unit area (m ha^{-1}, ft ac^{-1}), or essentially a number count of felled-logs per area given an average tree length. Suggested treatment rates of no less than one straw bale check dam per 0.4 hectare (1 ac^{-1}) (Goldman, 1986) or sediment trapped in a lower straw bale check dam should extend to the base the straw bale check dam located directly above in the channel (Napper, 2006) address structural function aimed at reducing failure rates rather than measuring the treatment effectiveness at reducing sediment yields. It is important to standardize reporting methods of straw bale check dam treatment rate for many reasons including cross-comparison between quantitative studies and qualitative assessment by land managers.

A proposed standardized treatment rate is the number of straw bale check dams per area to allow for the comparison of the treatments effect on sediment yields from catchment outlets. This treatment rate can be compared with future studies having similar designs to determine the most effective straw bale check dam treatment rate (or channel treatment rate) to meet mitigation targets. Treatment rate per area is the preferred standardization as opposed to a treatment rate of straw bale check dams per channel length. Moody and Martin (2009) recognize "sediment erosion is not uniformly distributed across the landscape", however, they chose mass per area (Mg ha^{-1}, t ac^{-1}) erosion rate as the most appropriate means for comparing erosion rates at the point, hillslope, and channel scales. Given straw bale check dams are designed for channels it seems reasonable to choose a treatment rate of the number of straw bale check dams per length of channel. There are benefits to relating treatment to channel length including ease in measuring from the lowest placed structure in the channel to the channel head with a cloth tape measure, rather than walking the perimeter of the catchment with a Global Positioning System device (GPS) to determine the area. However, it is important the proposed standardized treatment applies to all post-fire case studies and applications.

The major drawback to treatment rate per channel length is a defined channel may not exist in the proposed treated catchment. Germanoski and Miller (2004) classify upland basins into four groups, flood-dominated, deeply incised channels, fan-dominated, and pseudo-stable channels, based on a channels sensitivity to incision. Miller *et al*. (2012) shows bedrock lithology or rock types and weathering pattern also influences the absence or presence of surficial channels and categorizes the previous four groups into 13 process zones. Of the 13 process zones, it may be appropriate to treat five of these zones (bedrock hollow, incised hollow, unincised hollow, unfilled valley, bedrock valley) with straw bale check dams if high sediment yields are predicted to occur from these channels following wildfire. A defined V-shaped channel exists in only one of these zones while the other channel are unincised and U-shaped making it difficult to accurately measure a channel length. This makes standardizing the treatment rate of straw bale check dam per catchment area the most universal across these catchment channel types.

4.2 Straw bale check dam function

A properly functioning straw bale check dam captures only a fixed amount of sediment. Our second objective determined the mean storage capacity of a straw bale check dam is 1.27 Mg (1.00 m^3) [1.40 t, 35.2 ft^3], with a median of 1.00 Mg (0.90 m^3) [1.11 t, 31.8 ft^3]. These values reflect straw bale check dam sediment storage capacities found by Miles *et al.* (1989), who determined the average storage capacity to be 1.1 m^3 (41 ft^3) . At the treatment rate of four straw bale check dams ha^{-1} [two SCDs ac^{-1}] straw bale check dams trapped a mean mass of 5.87 Mg ha^{-1} (4.4 m^3 ha^{-1}) [2.62 t ac^{-1}, 157 ft^3 ac^{-1}]. Log debris dams treated at a rate of one log debris dam per four hectares stored 0.29 m^3 (0.38 yr^3) of sediment ha^{-1} (Fox, 2009).

The channel gradient did not have significant influence $t = 1.177$ ($df = 11$, $p = 0.262$) on the mass of sediment trapped behind straw bale check dams. However, the amount of mass trapped by straw bale check dams tended to decrease with the increasing channel gradient, and given a larger sample size gradient may be found to have a significant effect. In the treated catchments A and F, large woody debris (30 cm long x 10 cm diam.) and cobbles (> 10 cm diam.) mobilized by overland flow were trapped by the wooden stakes securing the straw bales to the ground (Figure 29). The debris trapped in the 'trash rack' increased the spillway height at the center spillway of the U-shaped structure and increased the straw bale check dam trap volumes. However, the increased spillway height shifted the flow path to the new low point of the structure which was around the bottoms of the end straw bales causing flow to scour into the channel banks. An effect opposite of the trash rack happened to log debris dam structures, where the trapped sediment height was half the structural height due to gaps within the structures reducing the sediment storage capacity. It is important to tightly abut straw bale check dams together and fill voids between the bales with sticks, excess straw, and/or rocks to reduce the chance of flow between the straw bales.

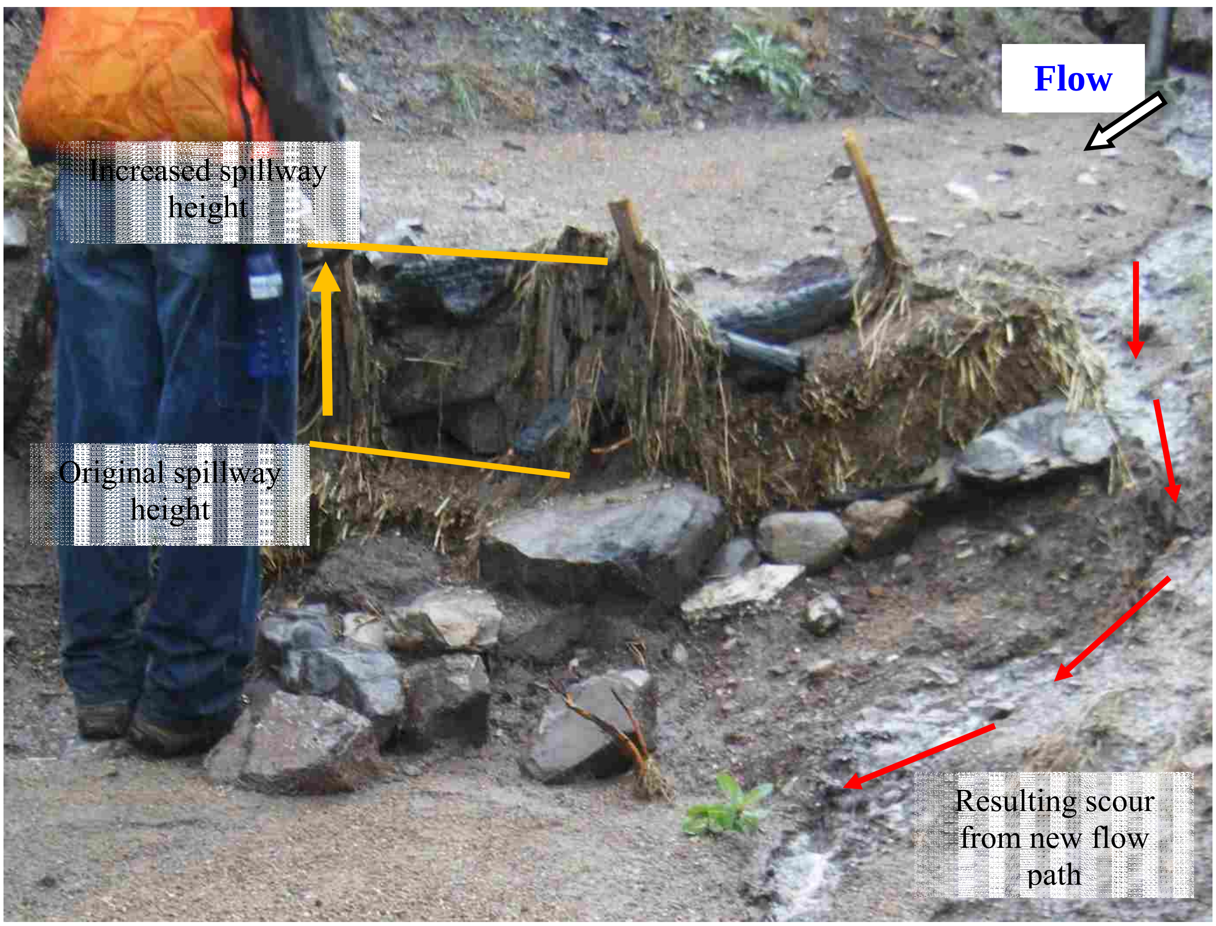

Figure 29. 'Trash-rack' effect was caused by mobilized cobble and large woody debris being trapped by the stakes securing the straw bale check dams to the channel bed.

Straw bale check dams filled with sediment are stable and change little in appearance as sediment is transported unmitigated over the structures and out the catchments. The majority of straw bale check dams filled to maximum sediment holding capacity after the first (8 Jul 2011) event, but they changed very little in physical appearance as if no additional events had flowed through the channels. However 43 to 68 % of reliable sediment yields measurements for the first post-fire year passed over the structures un-mitigated. Structures held in place with no failures or major loss of trapped sediment by washing out during the first or second post-fire years. Inspection of straw bales in early May 2012 after the winter revealed minor decomposition of straw, and mostly intact. Damage to roughly 3 structures occurred by wildlife (deer or elk) movement up and/or down the ephemeral channel corridor during 2011-2012 winter or 2012 spring.

4.3 Straw bale check dam treatment effectiveness

Straw bale check dam efficiency was low at the site because of the very large post-fire sediment yields. We determined with the third objective the catchment scale trap efficiency of straw bale check dams by relating total sediment trapped by straw bale check dams to total annual catchment sediment yield. The trap efficiency of straw bale check dams is a function of the annual sediment yields and treatment rate, and is the reason why there is a large range (14 to 50 %) of trap efficiencies in treated catchments in 2011 as compared to 2012. Since the treatment rate was kept constant across the site, the potential mass of sediment trapped per area was relatively equal between all treated catchments. When low annual sediment yields occur as in Middle Canyon, there is little excess sediment available to be transported down channel once the straw bale check dams have filled to their sediment holding capacity, thus the trap efficiency was as high as 50%. With high annual sediment yield rates there is a large amount of excess sediment transported out of the catchment once straw bale check dams filled to their sediment holding capacity. Sevier Canyon which had very high annual sediment yields in 2011 had straw bale check dam efficiencies as low as 14%.

While trap efficiencies were low at this study site, I would expect straw bale check dams to have higher trap efficiencies in areas of the Western U.S. with low post-fire sediment yields from channels. Trap efficiencies would probably be the highest in the Pacific and Sub-Pacific regions as described by Moody and Martin (2009). The low to medium rainfall intensity regimes in these regions account for the lowest channel sediment yield volumes in the West (Moody and Martin, 2009). In contrast trap efficiencies would be expected to be the lowest at this study area and in the Arizona rainfall regime that has the highest rainfall intensity events of the four major Western rainfall regimes. The Arizona rainfall regime has the highest post-fire channel sediment yield volumes in the West (Moody and Martin, 2009).

The range in trap efficiencies is seen in a channel treatment in Spain that has low post-fire sediment yield. While there was a low trap efficiency of 13% for log debris dams, they were treated at a very low rate of 1 per 4 ha (Fox, 2009). Since the trap efficiency was not given by the author, I had to find this trap efficiency by applying values given within the paper to Equation 1. I multiplied the median trap volume (1.28 m^3, 45 ft^3) by the number of structures in the treated catchment (eight) to find the total volume trapped per treated catchment. I found potential catchment sediment yield by adding the total volume of sediment trapped by log debris dams per catchment to the volume of sediment trapped in the sediment basin at the watershed outlet. I then divided the total volume of sediment trapped per treated catchment by the potential catchment sediment yield to determine the trap efficiency of the log debris dams. Even though the treatment rate for this study was 17.5 times greater the treatment rate of Fox (2009), the trap efficiencies are similar because the relationship of treatment rate to sediment yield rates were roughly equal at both the sites.

4.4 Channel response to straw bale check dams

The sediment mobilized off hillslopes and through channels to catchment outlets had very little effect on the landscape function. We determined that straw bale check dams did not reduce knickpoint migration because it was not present at the site. While this is one of the two primary objectives of these structures (Tracy and Ruby, 1994), grade control was not necessary because of the stability of the channels. Cross-sectional areas changed little suggesting channel beds were resistant to scour by flow and also had little aggregation. Turowski *et al.* (2008) classified bedrock channels as being unable to widen, scour (or lower in elevation), or shift the bed unless the bedrock is eroded. If the channels at the site were to fall into this classification, 'tools' or rocks introduced to the channel hillslopes or plucked from the channel bed would need to be transported by bouncing and sliding to erode enough bedrock to substantially alter the channel (Sklar and Dietrich, 2001). Rocks present in sediment yields up to ~10 cm (4 in) along the B-axis or the middle-length between the x-y-z axis of an oblong object, were captured in the sediment retention basins. However, flow duration allowing the 'tools' to alter the bed probably did not last long enough to have any effect on altering the bed.

The thick bedrock unit at the site stabilizes the landscape making the ephemeral channels resistant to change. The stable channels at the site are likely influenced by the characteristics of the Sevier River Formation rock unit, which appeared to be resistant to knick point migration. Knick point migration has been shown to be dependent on bed thickness with channel incision progressing in the direction of dip (Miller, 1991). Channels in this study may be more resistant to knick points because they exist entirely within the Sevier River Formation, which is a massive rock unit 100 to 300 m (~300 to 1000 ft) thick with little to no bedding plane throughout its unit thickness. In addition all channels run roughly perpendicular to the dip of the unit probably hindering channel incision. Using Miller *et al*. (2012) 13 process zones, this study channels fall into the unfilled valley category with a channel bed composed of bedrock as opposed to fill from surrounding hillslopes. Straw bale check dams in stable ephemeral channels are resistant to failure and releasing stored sediment. This allows for multi-year storage of trapped sediment for as long as the structural integrity of the straw within the bales allows.

4.5 Ground cover

The rate of sedimentation across the site is a function of the limited vegetation cover across the hillslopes and in the channels. Ground cover was reduced by combustion during the Twitchell Canyon Fire. The reduction in live vegetation, litter such as leaves or dead grasses, and other organics that mitigated overland flow and soil erosion during high intensity rain events changed the hydrologic response of not only the studied catchments, but across the burned landscape. The area of mineral soil exposed to raindrop impact and overland flow is the most critical to reduce to bring the landscape back to pre-fire conditions. Mineral soil exposed to overland flow and raindrop impact was reduced from 2011 to 2012 by regrowth of vegetation by 17 % on hillslopes. The most noticeable regrowth was gamble oak shrub (*Quercus gambelii*) that had grown as much as a 30 cm (1 ft) in some patches by the fall of 2011 and by 60 to 90 cm (2 to 3 ft) by 2012. The gamble oak shrub was much denser on north aspect hillslopes than on south aspect hillslopes. Gamble oak reduced the surface area of exposed mineral soil primarily by quick regrowth of vegetation. Grasses had a similar effect at reducing the surface area of exposed mineral soil. The vegetative regrowth from annual grasses and gamble oak shrub were to two primary factors that increased vegetation cover in the first two post-fire years (18 to 30%).

Robichaud (2005) has shown exposed area of mineral soil needs to be ~25% or less before vegetation and litter have mitigative effects on the hydrologic response. While there is a significant difference in area of mineral soil reduced from fall of 2011 to fall of 2012, soil exposure needs to decrease by 15 to 20 % more before it is a low enough value before there is a noticeable reduction in erosion rates by raindrop impact and overland flow. This may take a few more years depending on available rainfall for plant growth and seed availability to increase vegetation and litter cover.

4.6 Particle size analysis and organic matter

Sedimentation rates from hillslopes and through channels were so great that the soil texture changed very little while being transported through the system. There was little change in texture of eroded soil at both the hillslope scales and in between the treated and control catchments. This may be from the high hillslope erosion rates and catchment sediment yields. During the brief period of high runoff rates and high erosion rates caused by large rain storms the catchments may have had increased connectivity between zones (Miller *et al*. 2012) or the hillslopes and channels, essentially homogenizing the soil texture throughout the catchment. There may have been little difference in the particle size distribution content because the thick bedrock unit has produced a constant soil texture from the base of the catchments to the tops of the ridges. This would make a sample of soil texture that only moved 50 cm (~1.6 ft) the same as a sample of soil texture that been transported the length of the watershed. Also, the soil type may not have strong aggregates because of the high sand content (~70 to 80 %) or mostly weak frictional forces holding sand grains together as opposed to strong electrostatic forces between clay particles. This would break the weak soil aggregates down into primary particles more readily when exposed to raindrop impact and/or during transportation, thus making a more homogenous soil texture.

The organic matter was not significantly different between the upslope and base of hillslope fences as well as between treated and control catchments. Organic matter was probably evenly distributed throughout catchments prior to the fire, due to the relatively homogeneous mixture on pinion pines and junipers interspersed with mountain big sage brush prior to the burn, seen on unburned surrounding areas.

5.0 Conclusions

Sediment yields across the site were extremely high causing straw bale check dams to have little effect on reducing rates. Catchments in Middle Canyon treated at a rate of four straw bale check dams ha^{-1} (two SCDs ac^{-1}) did not significantly reduce sediment yields compared to paired control catchments during low intensity events with I_{30} intensities equal to or less than 21 mm hr^{-1} (0.8 in hr^{-1}). Given all straw bale check dams were filled to sediment holding capacity and non-functioning at the beginning of the second post-fire year there was no significant difference in sediment yields between treated and control catchments during the second post-fire year. Increasing the current treatment rate to significantly reduce or meet sediment yield mitigation targets may not be feasible if the defined ephemeral channel is too short to accommodate for high treatment rates.

Straw bale check dams filled to sediment holding capacity during the first and second sediment yield event and allowed large sediment yields to pass over the straw bale check dams. In Sevier Canyon, straw bale check dams were filled to sediment holding capacity during a 1-year I_{30} (21 mm hr^{-1}, 0.8 in hr^{-1}) return period event in two catchments and by both a 2-year I_{30} (28 mm hr^{-1}, 1.1 mm hr^{-1}) and 1-year I_{30} (20 mm hr^{-1}, 0.8 in hr^{-1}) return period event in the third catchment. The reliable annual sediment yields from first post-fire year Sevier Canyon treated catchments show 19.53 to 25.71 Mg ha^{-1} (8.71 to 11.47 t ac^{-1}) of sediment was transported past the straw bale check dams. In Middle Canyon, 56 % of the empty straw bale check dams filled to sediment holding capacity by a rain event with less than a 1-year I_{30} (13 mm hr^{-1}, 0.5 in hr^{-1}) intensity return period. The remaining empty or partially full straw bale check dams were filled by a second event that had an I_{30} intensity less than a 1-year return period. The annual sediment yield transported past straw bale check dams in Middle Canyon during the first post-year was 3.54 to 4.33 (±0.1) Mg ha^{-1} [1.58 to 1.93 (±0.1) t ac^{-1}].

The landscape of the study area was resistant to change despite the wildfire, allowing straw bale check dams fill to capacity and ephemeral channels to change little over the course of the study. There were no failures of straw bale check dams during the two years of monitoring. The mean mass of sediment trapped by straw bale check dams filled to capacity was 1.27 Mg (1.40 t) per structure. The mean mass of sediment trapped per catchment area at a treatment rate of four straw bale check dams ha^{-1} (2 SCDs ac^{-1}) was 5.87 Mg ha^{-1} (2.62 t ac^{-1}). It is important to standardize treatment rate to the number of straw bale check dams per catchment area. The mean amount of sediment scoured below the spillway of straw bale check dams was 0.06 Mg (0.07 t). The straw bale check dams were installed in stable channels resistant to scour, which helped to prevent structural failures from spillway scour undermining the structure on the down-stream side. Straw bale check dam treatment was not need to stop or slowing knick point migration because the channels were stable and resistant to scour.

References

Badía D, Marti C (2008) Fire and rainfall energy effects on soil erosion and runoff generation in semi-arid forested lands. *Arid Land Research and Management* **22**(2), 93-108.

Baker WL (2009) 'Fire Ecology in Rocky Mountain Landscapes.' (Island Press: Washington DC), 356-414.

Benavides-Solorio J, MacDonald LH (2005) Measurement and prediction of post-fire erosion at the hillslope scale, colorado front range. *International Journal of Wildland Fire* **14**(4), 457-74.

Bonnin GM, Martin D, Lin B, Parzybok T, Yekta M, Riley D (2006) 'Precipitation–Frequency Atlas of the United States,' NOAA Atlas 14, Volume 1, Version 5. NOAA–National Weather Service, Silver Spring, Maryland

Brooks KN, Ffolliott PF, Magner JA (2003) 'Hydrology and the management of watersheds.' 3rd ed. (Wiley-Blackwell: Ames, Iowa), 34-37.

Cambardella CA, Moorman TB, Parkin TB, Karlen DL, Novak JM, Turco RF, Konopka AE. (1994) Field-scale variability of soil properties in central Iowa soils. *Soil Science Society of America Journal* **58**(5), 1501-11.

Canfield HE, Wilson CJ, Lane LJ, Crowell KJ, Thomas WA (2005) Modeling scour and deposition in ephemeral channels after wildfire. *Catena* **61**(2), 273-91.

Cerdá A, Robichaud PR (2009) 'Fire Effects on Soils and Restoration Strategies'. (Science Publishers; Enfield, NH), 353-4.

Ciach GJ (2003) Local random errors in tipping-bucket rain gauge measurements. *Journal of Atmospheric and Oceanic Technology* **20**(5), 752-9.

Collins LM, Johnston CE (1995) Effectiveness of straw bale dams for erosion control in the Oakland hills following the fire of 1991. *International Association of Wildland Fire* Brushfires in California wildlands: ecology and resource management. Fairfield WA, 171-83.

Cunningham CG, Steven TA (1979) 'Mount Belknap and Red Hills calderas and associated rocks, Marysvale volcanic field, west-central Utah.' US Geological Survey (Washington: U.S. Govt. Print. Off.)

DeBano LF (2000) The role of fire and soil heating on water repellency in wildland environments: A review. *Journal of Hydrology* **231**, 195-206.

Dekker LW, Ritsema CJ (1994) How water moves in a water repellent sandy soil: 1. potential and actual water repellency. *Water Resources Research* **30**(9), 2507-17.

Dingman SL (2009) 'Fluvial Hydraulics.' (Oxford University Press, Inc.: New York, New York) 117.

Doerr SH, Woods SW, Martin DA, Casimiro M (2009) 'Natural background' soil water repellency in conifer forests of the north-western USA: Its prediction and relationship to wildfire occurrence. *Journal of Hydrology* **371**(1), 12-21.

Foltz RB, Robichaud PR, Rhee H (2009) A synthesis of post-fire road treatments for BAER teams: Methods, treatment effectiveness, and decision making tools for rehabilitation. USDA Forest Service, Rocky Mountain Research Station. Fort Collins, CO General Technical Report RMRS-GTR-228. 44-65. (Unpublished database)

Fox DM (2011) Evaluation of the efficiency of some sediment trapping methods after a Mediterranean forest fire. *Journal of Environmental Management* **92**(2), 258-65.

Gabet EJ, Bookter A (2008) A morphometric analysis of gullies scoured by post-fire progressively bulked debris flows in southwest Montana, USA. *Geomorphology* **96**(3), 298-309.

Gallup RM (1975) Concrete crib check dams. USDA Forest Service, Region 5 San Dimas Equipment Development Center, *Engineering Field Notes* **7**(6), 1-12.

Gee GW, Bauder JW (1986) Particle-size analysis. In: *Methods of Soil Analysis: Part 1*, Klute A (ed.). (American Society of Agronomy: Madison, WI), 383–411.

Germanoski D, Miller JR (2004) Basin sensitivity to channel incision in response to natural and anthropogenic disturbance. *Great Basin Riparian Ecosystems-Ecology*, (Management and Restoration.Island Press: Covelo, CA), 88-123.

Goldman SJ, Jackson K, Bursztynsky TA (1986) 'Erosion and Sediment Control Handbook.' (McGraw-Hill: New York) 8.49-8.53

Groen AH, Woods SW (2008) Effectiveness of aerial seeding and straw mulch for reducing post-wildfire erosion, north-western Montana, USA. *International Journal of Wildland Fire* **17**(5), 559-71.

Harrelson CC, Rawlins CL, Potyondy JP (1994) 'Stream channel reference sites: An illustrated guide to field technique.' USDA Forest Service, Rocky Mountain Forest and Range Experiment Station, Fort Collins, CO General Technical Report RMRS-RM-245. 1-61.

Hausenbuiller RL (1972) 'Soil Science: Principles and Practices.' (W.C. Brown Co.: Dubuque, Iowa). 226-34.

Higgins, RW, Mo KC, Yao Y (1998) Interannual variability of the US summer precipitation regime with emphasis on the southwestern monsoon. *Journal of Climate* **11**(10), 2582-2606.

Higgins R, Yao Y, Wang X (1997) Influence of the North American monsoon system on the US summer precipitation regime. *Journal of Climate* **10**(10), 2600-22.

Inbar M, Tamir M, Wittenberg L (1998) Runoff and erosion processes after a forest fire in Mount Carmel, a Mediterranean area. *Geomorphology* **24**(1), 17-33.

Jackson M, Roering JJ (2009) Post-fire geomorphic response in steep, forested landscapes: Oregon coast range, USA. *Quaternary Science Reviews* **28**(11), 1131-46.

Janusz N (1986) The dynamic calibration of tipping-bucket rain gauges. *Nordic Hydrology* **17**(3), 203-14.

Johansen MP, Hakonson TE, Breshears DD (2001) Post-fire runoff and erosion from rainfall simulation: Contrasting forests with shrublands and grasslands. *Hydrological Processes* **15**(15), 2953-65.

Kean JW, Staley DM, Cannon SH (2011) In situ measurements of post-fire debris flows in southern California: Comparisons of the timing and magnitude of 24 debris-flow events with rainfall and soil moisture conditions. *Journal of Geophysical Research-Earth Surface* **116**, F04019.

Keller EA, Valentine DW, Gibbs DR (1997) Hydrological response of small watersheds following the southern California painted cave fire of June 1990. *Hydrological Processes* **11**(4), 401-14.

Knapen A, Poesen J (2010) Soil erosion resistance effects on rill and gully initiation points and dimensions. *Earth Surface Processes and Landforms* **35**(2), 217-28.

Koestner K, Youberg A, Neary DG (2011) Field trip guide to the 2010 Schultz Fire Burn Area Arizona. Hydrological Society Annual Symposium; Flagstaff, Arizona; September 18, 2011. Flagstaff, AZ: Northern Arizona University, 4-5.

Legleiter CJ, Lawrence RL, Fonstad MA, Andrew Marcus W, Aspinall R (2003) Fluvial response a decade after wildfire in the northern Yellowstone ecosystem: A spatially explicit analysis. *Geomorphology* **54**(3), 119-36.

Lentile LB, Holden ZA, Smith AM, Falkowski MJ, Hudak AT, Morgan P, Lewis SA, Gessler PE, Benson NC (2006) Remote sensing techniques to assess active fire characteristics and post-fire effects. *International Journal of Wildland Fire* **15**(3), 319-45.

Lloret F (1998) Fire, canopy cover and seedling dynamics in Mediterranean shrubland of northeastern Spain. *Journal of Vegetation Science* **9**(3), 417-30.

Malvar MC, Prats SA, Nunes JP, Keizer JJ (2011) Post-fire overland flow generation and inter-rill erosion under simulated rainfall in two eucalypt stands in north-central Portugal. *Environmental Research* **111**(2), 222-36.

Meyer GA, Wells SG (1997) Fire-related sedimentation events on alluvial fans, Yellowstone National Park, USA. *Journal of Sedimentary Research* **67**(5), 776-791.

Meyer LD, Line DE, Harmon WC (1992) Size characteristics of sediment from agricultural soils. *Journal of Soil and Water Conservation* **47**(1), 107-11.

Miles SR, Haskins DM, Ranken DW (1989) Emergency burn rehabilitation: Cost, risk, and effectiveness. In: Berg NH, tech. coord. Proceedings of the symposium on fire and watershed management, 26-28 Oct 1988, Sacramento, California. Berkeley, CA: USDA Forest Service, Pacific Southwest Forest and Range Experiment Station, General Technical Report PSW-109, 97-102.

Miller JR (1991) The influence of bedrock geology on knickpoint development and channel-bed degradation along downcutting streams in south-central indiana. *The Journal of Geology* **99**(4), 591-605.

Miller JR, Lord ML, Villarroel LF, Germanoski D, Chambers JC (2012) Structural organization of process zones in upland watersheds of central Nevada and its influence on basin connectivity, dynamics, and wet meadow complexes. *Geomorphology* **139**, 384-402.

Montgomery DR, Dietrich WE (1988) Where do channels begin? *Nature* **336**(17), 232-4.

Moody JA, Smith JD, Ragan B (2005) Critical shear stress for erosion of cohesive soils subjected to temperatures typical of wildfires. *Journal of Geophysical Research: Earth Surface* **110**, 1-13.

Moody JA, Martin DA (2009) Synthesis of sediment yields after wildland fire in different rainfall regimes in the western united states. *International Journal of Wildland Fire* **18**(1), 96-115.

Moody JA, Martin DA (2001) Post-fire, rainfall intensity peak discharge relations for three mountainous watersheds in the western USA. *Hydrological Processes* **15**(15), 2981-93.

Morgan P, Heyerdahl EK, Gibson CE (2008) Multi-season climate synchronized forest fires throughout the 20th century, northern Rockies, USA. *Ecology* **89**(3), 717-28.

Napper C, (2006) Burned area emergency response treatments catalog. USDA Forest Service, National Technology and Development Program, San Dimas, CA. 0625 1801-SDTDC. 81-91.

Neary DG, Klopatek CC, DeBano LF, Ffolliott PF (1999) Fire effects on belowground sustainability: A review and synthesis. *Forest Ecology and Management* **122**(1), 51-71.

NWCG (2006) Glossary of wildland fire terminology. National Wildfire Coordinating Group, Incident Operations Standards Working Team. Available at http://nwcg.gov/pms/pubs/glossary/b.htm [Verified 22 October 2012]

Pierson FB, Robichaud PR, Moffet CA, Spaeth KE, Hardegree SP, Clark PE, Williams CJ (2008) Fire effects on rangeland hydrology and erosion in a steep sagebrush-dominated landscape. *Hydrological Processes* **22**(16), 2916-29.

Prosser IP, Slade CJ (1994) Gully formation and the role of valley-floor vegetation, southeastern Australia. *Geology* **22**(12), 1127-30.

R Core Team (2012) R: A language and environment for statistical computing. In: R Foundation for Statistical Computing [database online]. Vienna, Austria, Available from http://www.R-project.org. [Verified 10 March 2013]

Ramsey FL, Schafer DW (2012) 'The Statistical Sleuth: A Course in Methods of Data Analysis.' (Brooks/Cole: Belmont, CA) 466-471.

Robichaud PR, Beyers JL, Neary DG (2000) ‘Evaluating the effectiveness of postfire rehabilitation treatments.’ USDA Forest Service, Rocky Mountain Research Station, Fort Collins, CO General Technical Report RMRS-GTR-63, 20-21

Robichaud PR, Brown RE (2002) 'Silt fences: An economical technique for measuring hillslope soil erosion.' USDA Forest Service, Rocky Mountain Research Station, Fort Collins, CO General Technical Report RMRS-GTR-94, 1-8.

Robichaud PR, Brown RE (2005) Postfire rehabilitation treatments: are we learning what works. *Managing Watershed for Human and Natural Impacts: Engineering, Ecological, and Economic Challenges.* Proceedings of the 2005Watershed Management Conference. American Society of Civil Engineers, Williamsburg, VA

Robichaud PR, Wagenbrenner JW, Brown RE (2010) Rill erosion in natural and disturbed forests: 1. measurements. *Water Resources Research* **46**(10), W10506.

Robichaud PR, Wagenbrenner JW, Brown RE, Wohlgemuth PM, Beyers JL (2008) Evaluating the effectiveness of contour-felled log erosion barriers as a post-fire runoff and erosion mitigation treatment in the western united states. *International Journal of Wildland Fire* **17**(2), 255-73.

Rowley P, Cunningham D, Steven CG, Workman TA, Anderson JB, John J, Theissen KM (2002) Geologic Map of the Central Marysvale Volcanic Field, Southwestern Utah: U.S. Geological Survey Geologic Investigations Series I-2645-A, Denver, CO

Ruby EC (1973) 'Evaluation of check dams for sediment control’ Los Angeles River Watershed, Angeles National Forest, Region 5, San Francisco, CA

Ruby EC (1997) ‘Notes on burned-area emergency rehabilitation’ *BAER Treatments* Available at USDA Forest Service, Rocky Mountain Research Station, Moscow, ID

Scott DF, Versfeld D, Lesch W (1998) Erosion and sediment yield in relation to afforestation and fire in the mountains of the western cape province, South Africa. *South African Geographical Journal* **80**(1), 52-9.

Shakesby R, Doerr S (2006) Wildfire as a hydrological and geomorphological agent. *Earth-Science Reviews* **74**(3), 269-307.

Shakesby R, Doerr S, Walsh R (2000) The erosional impact of soil hydrophobicity: Current problems and future research directions. *Journal of Hydrology* **231**, 178-91.

Shakesby RA, Coelho C, Ferreira AD, Terry JP, Walsh R (1993) Wildfire impacts on soil-erosion and hydrology in wet Mediterranean forest, Portugal. *International Journal of Wildland Fire* **3**(2), 95-110.

Sklar LS, Dietrich WE (2001) Sediment and rock strength controls on river incision into bedrock. *Geology* **29**(12), 1087-90

Smith DM (1994) The forests of the United States. In 'Regional Silviculture of the United States', 3rd ed. (Ed. JW Barrett) (Wiley: New York), 1-10.

Smith H, Dragovich D (2008) Post-fire hillslope erosion response in a sub-alpine environment, south-eastern Australia. *Catena* **73**(3), 274-85.

Splitter TE (1995) Fire and the debris flow potential of winter storms. *Brushfires in California: Ecology and Resource Management*, 113-20

Terry JP, Shakesby RA (1993) Soil hydrophobicity effects on rainsplash: Simulated rainfall and photographic evidence. *Earth Surface Processes and Landforms* **18**(6), 519-25.

Tracy R, Ruby E (1994) Burned area emergency rehabilitation; structural treatment, site selection criteria, and project requirements. USDA Forest Service, Burned Area Emergency Response training course (1998), Region 5, San Francisco, CA

Turowski JM, Hovius N, Wilson A, Horng M (2008) Hydraulic geometry, river sediment and the definition of bedrock channels. *Geomorphology* **99**(1), 26-38.

UT-FIF BAER Report (2010) Twitchell Canyon Fire Burned Area Report. USDA Forest Service, FS-2500-8, Fishlake National Forest, Richfield, UT.

Vaillant NM, Fites-Kaufman JA, Stephens SL (2009) Effectiveness of prescribed fire as a fuel treatment in Californian coniferous forests. *International Journal of Wildland Fire* **18**(2), 165-75.

Wessel A (1988) On using the effective contact angle and the water drop penetration time for classification of water repellency in dune soils. *Earth Surface Processes and Landforms* **13**(6), 555-61.

West B, Welch K, Galecki A (2007) 'Linear Mixed Models: A Practical Guide Using Statistical Software'. (Chapman & Hall/CRC: Boca, Raton) 9.

Westerling AL, Hidalgo HG, Cayan DR, Swetnam TW (2006) Warming and earlier spring increase western U.S. forest wildfire activity. *Science* **313**(5789), 940-3.

Willgoose G, Bras RL, Rodriguez-Iturbe I (1992) The relationship between catchment and hillslope properties: Implications of a catchment evolution model. *Geomorphology* **5**(1), 21-37.

Wilson CC, Dell JD (1971) The fuels buildup in American forests: A plan of action and research. *Journal of Forestry* **69**(8), 471-5.

Wondzell SM, King JG (2003) Postfire erosional processes in the Pacific Northwest and Rocky Mountain regions. *Forest Ecology and Management* **178**(1), 1-12.

Woods SW, Birkas A, Ahl R (2007) Spatial variability of soil hydrophobicity after wildfires in Montana and Colorado. *Geomorphology* **86**(3), 465-79.

Zuur AF (2009) 'Mixed Effects Models and Extensions in Ecology with R.' Statistics for Biology and Health, (Springer Science+Business Media: New York, New York), 101-142.

Appendix

The data for this thesis is stored electronically on file at the USDA Forest Service, Rocky Mountain Research Station, in Moscow, Idaho 83843 under Dr. Peter R. Robichaud. The file structure with a description of folder and file contents is as follows:

Master folder: ‘’ delineates folder

- ‘Twitchell’*
  - ‘Cover’
    - ‘2011’
      - Summer 2011 ground cover survey data and Fall 2011 ground cover survey data
    - ‘2012’
      - Fall 2012 ground cover survey data
  - ‘CR10’
    - Ultra sonic data for 2011 and 2012 that tells the depth behind the upper sediment retention structure in catchment H (TWHWD2)
  - ‘Cross Sections’ - Cross-section data spread sheets
  - ‘Field notebooks’
    - Scanned copies of field notebooks with 2011 data from the Twitchell site
    - Copies of 2012 field data is found in the master Twitchell Canyon fire three ringed binder
  - ‘Maps’ –
    - .pfd maps of Middle and Sevier Canyons
    - ‘Garmin’ – all GPS data including catchment and hillslope perimeters, raingauge locations, hillslope fence locations.
  - ‘Moisture_Bulk density’ – bulk density samples taken in sediment deposits
  - ‘Photos’ – all photos from the site for 2011 through 2012, the file “Watershed areas__Photo numbers.xlsx” in ‘Twitchell’ gives information associated with each photo
  - ‘PSA and organics’ – PSA and organic matter data from Middle Canyon samples for 2011
  - ‘Rain_data’ – ‘2011’ and ‘2012’ rain data organized by rain gauge with total rainfall, I_{10}, and I_{30} intensities calculated for each event
  - ‘Sediment yields’ –
    - ‘2011’
      - catchment sediment yields and hillslope sediment yields: event by event basis
      - the master file with the yearly sediment yield data
      - all straw bale check dam data is found in: “2011__Sediment_yields_Feb-26_2013.xlsx”
      - ‘2012’ catchment sediment yields and hillslope sediment yields: event by event basis, compiled yearly data
      - Master data spread sheet for statistical analysis
- Trimble Geomatics Office Software on Bob Browns Dell laptop
  - Twtichell fire: Survey data of the Twitchell field site

* ‘’ delineates folder from a file